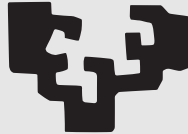


eman ta zabal zazu



Universidad
del País Vasco Euskal Herriko
Unibertsitatea

Master in Quantum Science and Technology

DYNAMICS FOR 2-VERTEX MODELS IN LOOP QUANTUM GRAVITY

Eneko Aranguren Ruiz

September 7, 2021

Director

Iñaki Garay Elizondo

Contents

1	Introduction	5
1.1	Quantum Gravity	6
1.2	Loop Quantum Gravity	7
1.2.1	Hamiltonian Formalism and Loop Representation	7
1.2.2	Spinorial and $U(N)$ Formalisms	7
1.3	State of the Art of LQG	8
1.4	Outlook	9
2	Fundamental Aspects of General Relativity	11
2.1	Differentiable Manifold	11
2.1.1	Tensors	12
2.1.2	Diffeomorphism Invariance	12
2.2	Covariant Derivative	13
2.2.1	Intrinsic Curvature	14
2.3	Lie Derivative	15
2.3.1	Extrinsic Curvature	15
3	Hamiltonian Formulation of General Relativity and Ashtekar Variables	17
3.1	3+1 Decomposition	17
3.2	ADM Formalism	21
3.2.1	Quantization	23
3.3	Ashtekar Variables	23
3.3.1	Triads	24
3.3.2	Connection	24
3.3.3	Hamiltonian Formulation	25
4	Loop Representation for Quantum Gravity	27
4.1	Holonomies	28
4.2	Spin Networks	29
4.2.1	Inner product	30
4.3	Geometric Operators	31
4.3.1	Area Operator	31
4.3.2	Volume Operator	32

5 Spinorial Techniques and $U(N)$ Formalism	33
5.1 Spinorial Classical Framework	33
5.2 $U(N)$ Formalism	37
6 Dynamics for 2-Vertex Models	39
6.1 Reduced Sector in 2-Vertex Models	39
6.2 Proposal for the Dynamics	40
6.2.1 Simplest non-Trivial Hamiltonian	40
6.2.2 Generalized Lattice Gauge Hamiltonian	42
6.2.3 Intermediate Normalization Hamiltonian	43
6.3 Dynamics for H_{LQG}	43
6.3.1 2 Edges	43
6.3.2 4 Edges	48
6.3.2.1 Generalization of the Bivalent Model	48
6.3.2.2 Non-Zero Volume Tetrahedron	53
6.3.3 Arbitrary Number of Edges	57
6.3.3.1 2N Edges	57
6.3.3.2 N+1 Edges	59
6.4 Quantization	61
7 Conclusion	63
Bibliography	66

Chapter 1

Introduction

From the beginning, humanity has attempted to explain different phenomena of nature and the surrounding world. However, due to the enormous complexity of the Cosmos, scientists have repeatedly stumbled upon different situations they could not comprehend. These standstills were overcome when new theories tried to give a suitable explanation. Such theories were more generic and abstract since they had to embrace previously accepted interpretations. One example of this would be the theory of gravitation which, after the legacy of Newton, acquired a more precise formulation with the arrival of A. Einstein's theory of General Relativity in 1915.

Einstein's Theory of Relativity, which was a breakthrough in its own right, called the standard Newtonian picture of gravitation into question in pursuit of a theory with an emphatic statement: gravity emerges as a consequence of the curvature of spacetime. This theory explained numerous phenomena that had been inexplicable until then, such as the full precession of Mercury's perihelion [1].

General Relativity serves as an excellent tool to describe dynamical systems, but it fails at scales below the Planck length¹ $\ell_P \sim 10^{-35}$ m, where even the notions of space and time lose their classical sense. Black holes and initial-time singularities (such as the Big Bang) are scenarios where the quantum effects of gravity become significant, and thus, a quantum theory of gravity to describe them is required.

While Einstein was developing his Theories of Relativity, another breakthrough was flourishing gradually by various outstanding physicists, such as M. Planck, N. Bohr, and E. Schrödinger—even Einstein himself contributed to such development with the photoelectric effect. This breakthrough would then take the name of Quantum Mechanics as it conceived light and other energy sources to be discretized in small portions or quanta. Quantum Mechanics was full of phenomena that were inconceivable from that epoch's classical point of view (probabilistic outcomes or the uncertainty principle, for example), but it was capable of explaining the behavior of the microscopic world. The physical (and often

¹To get an overall idea of the actual magnitude of this scale, we recall that the length scales reached by the Large Hadron Collider are $\sim 10^{-19}$ m; 16 orders of magnitude greater than the Planck length [2].

philosophical) interpretations of Quantum Mechanics were not devoid of controversy either, since numerous interpretations were considered, such as the *many-worlds interpretation* [3] proposed by H. Everett in 1957.

1.1 Quantum Gravity

When we search for a relativistic quantum theory, we obtain Quantum Field Theory, which has proven excellent results with the development of the standard model of particle physics. This model describes the fundamental structure of matter and vacuum by considering elementary particles whose interactions are accounted for via three of the four fundamental forces—leaving gravity apart, which has not been successfully incorporated yet.

Accordingly, it is reasonable to try to provide a quantum description of the gravitational interaction, thus searching for a model that could shed light on the understanding of the Universe in the limits where our current theories break down. We can classify the different attempts to quantize General Relativity into two groups: the perturbative and the non-perturbative approaches.

At the summit of the perturbative approaches, we have the String Theory, whose central idea is to replace the concept of point-particles in standard Quantum Field Theories with one-dimensional (non-classical) extended objects called strings, living in a 10-dimensional spacetime. These strings are all identical, being their vibrational modes the only feature characterizing them. According to this theory, a specific vibration of the strings will correspond to a graviton, the gauge boson of the gravitational force. In the mid-1990s, it was conjectured that five versions of String Theory could be unified into an 11-dimensional theory, called M-Theory [4–6].

On the other hand, we have the non-perturbative approaches, led by Loop Quantum Gravity (LQG) [7–9]. Based on the parametrization of the phase space of General Relativity in terms of the Ashtekar (connection) variables, LQG is a theory constructed in terms of holonomies and fluxes, which are related to the connection variables and their conjugate momenta, respectively. To give a quantum description of the theory, a suitable basis was introduced, whose elements are known as spin networks. In this basis, we obtain one of the most desirable results of any theory of quantum gravity; the granular structure of space. In LQG this is achieved via the area and volume operators [10–12]. A spin network can be represented pictorially as a graph dressed with a spin j at each edge, labeling the irreducible representations of the $SU(2)$ holonomies; and intertwiners at the vertices, which are $SU(2)$ invariant tensors. As a result, this theory provides a discretized notion of space with quanta of area associated with the edges and chunks of volume associated with the intertwiners.

Both approaches to quantum gravity² entail outstanding developments that help us gain

²Even though we have simply mentioned the two most prominent research programs in quantum gravity, several other directions are also being considered, such as the Simplicial Quantum Gravity [13, 14] or the Null Surface Formulation [15–17].

intuition into the behavior of the Universe. However, these theories contain difficulties that have not yet been untangled. In this project, we will focus on the non-perturbative approach by exploring one of the main open problems of LQG; the implementation of the dynamics.

1.2 Loop Quantum Gravity

In this section we will briefly review the steps in order to construct the theory of LQG. On the other hand, we will introduce the new perspective given by the spinorial and $U(N)$ formalisms.

1.2.1 Hamiltonian Formalism and Loop Representation

Although the first steps towards the construction of a quantum theory of gravity (see [18, 19]) can be traced back to the early 1930s, when L. Rosenfeld wrote the first technical papers on quantum gravity [20], the origin of the canonical non-perturbative formulation can be dated to 1961, when R. Arnowitt, S. Deser, and C. W. Misner completed the Hamiltonian formulation of General Relativity [21]. This development was then used by J. Wheeler [22] and B. DeWitt [23] to construct a canonical quantization of the theory with the Wheeler-DeWitt equation describing the wave-functional of the Universe, which would specify the geometry at every point of the 3-dimensional space.

Nevertheless, due to the problems of mathematical nature that such equation presented, it was desirable to seek a new set of variables to describe General Relativity, which could make the quantization more tractable. These new variables [24, 25] were introduced by A. Ashtekar in 1986 and facilitated the development of the theory, laying the groundwork for the forthcoming loop representation of quantum gravity.

Soon after A. Ashtekar introduced his new variables, T. Jacobson and L. Smolin [26] realized that the Wheeler-DeWitt equation admitted a simple class of solutions, given by the traces of the holonomies (parallel transports of the connection) along smooth non-self interacting loops. This discovery prompted C. Rovelli and L. Smolin to change the basis of quantum gravity in favor of Wilson loops [27, 28], where quantum states could be expanded. However, this basis was overcomplete, meaning that its elements were not independent of each other. This was tackled by giving one step further and presenting the spin network basis, developed by C. Rovelli and L. Smolin [29], whose motivation came from the work done by R. Penrose 25 years before [30]. This new basis allowed the computation of quantum operators for the area and volume, providing the space with a granular structure.

1.2.2 Spinorial and $U(N)$ Formalisms

Following the discretized notion of space given by the spin networks (with the area and volume operators), we can construct the spinorial formalism [31]; a classical framework

whose quantization will give us the kinematical Hilbert space of LQG. To build this formalism, we can consider a simple graph and dress it with a pair of classical spinors ($|z_i^s\rangle, |z_i^t\rangle$) living at the beginning (source) and at the end (target) of the edge i , respectively. From an old theorem by H. Minkowski [32], it was realized that if the spinors at a given vertex satisfy a closure constraint, then we can uniquely define (up to translations) a polyhedron to that vertex, with as many faces as edges are linked to it. Furthermore, we can impose these polyhedrons to be glued by faces of equal area—but not necessarily equal shape—via the area matching constraint, where (twice) the area of each face will be given by the modulus of the spinor associated with it. This construction is known as the twisted geometries [33–35].

On the other hand, the $U(N)$ formalism presented in [36–39] studies the Hilbert space associated with the intertwiners. Using the Schwinger representation of the $SU(2)$ group [40], this formulation defines certain $SU(2)$ invariant operators acting on the vertices, which reduce/increase the areas of the individual surfaces.

1.3 State of the Art of LQG

The representation in the spin network basis grants the theory with an implicit way of implementing two of the three constraints of LQG, namely the diffeomorphism constraint and the Gauss' law. However, the implementation of the Hamiltonian (or scalar) constraint has not been successfully treated yet. In fact, the inability to handle this constraint is one of the major obstacles of the theory, which prevents the computation of the dynamics—the construction of the theory is purely kinematical. Nevertheless, numerous strategies have been presented to untangle this issue. On the one hand, we have the spinfoam formalism, first derived in [41, 42] by M. P. Reisenberg and C. Rovelli. This proposal attempts to implement the evolution of the spin networks using Feynman functional integrals. On the other hand, the construction of a master constraint [43–45] could be an alternative method to overcome the problem of the dynamics. Nevertheless, a complete and successful implementation of the dynamics has not been achieved yet, and remains one open problem of the theory.

An additional problem concerns the semiclassical limit of the theory. The discreteness of the spatial geometry corresponds to the ultra-high energy regime, where the notion of a continuous spacetime no longer holds. However, in the low energy limit, we expect a suitable theory of quantum gravity to recover the predictions provided by General Relativity, where the spacetime is taken to be continuous and smooth. However, the relationship between a semiclassical limit of LQG and General Relativity is still unclear [46, 47].

Notwithstanding these difficulties, LQG has obtained successful accomplishments. During the late 1990s, a key result of the theory was achieved. C. Rovelli and L. Smolin [12], together with A. Ashtekar and J. Lewandowski [10, 11], obtained the eigenvalues for the area and volume operators. The discreteness of geometry is something that one expects from a quantum theory of gravity and thus, obtaining the spectrum for geometric operators

makes LQG an appealing formulation. Furthermore, a derivation of the Bekenstein-Hawking black hole entropy was also computed within LQG in [48–53].

Additional advances have also been achieved in the cosmological variant of LQG, named Loop Quantum Cosmology (LQC) [54–56]. This formulation is a quantization of the homogeneous and isotropic solutions of General Relativity using the techniques of LQG. However, symmetry reduction and quantization processes do not generally commute [57], so LQC is not considered part of LQG. Nevertheless, the results obtained by this approach must still be taken into consideration since they serve as a sample to future research lines on the LQG framework. In fact, it was shown in [58] that within the LQC scenario, the Big Bang is replaced by a *Big Bounce*, thus eliminating the initial-time singularity, which represents one of the biggest challenges of Relativistic Cosmology. These accomplishments serve as an incentive to keep developing the theory of LQG as a quantum description of the gravitational interaction.

In order to tackle the problems with the implementation of the dynamics, it is useful to consider truncated models within the theory—consider only a finite number of degrees of freedom. Furthermore, we can reduce the degrees of freedom of these models by imposing homogeneity and isotropy, as done in [38, 39]. Such works found analogies between the Hamiltonian of these reduced models and the Hamiltonian proposed in LQC, and discussed about the possibility of a cosmological sector within the LQG framework.

1.4 Outlook

The document at hand proposes a suitable implementation of the dynamics for general 2-vertex models in the spinorial formulation of LQG.

Once a brief introduction to differential geometry has been presented in chapter 2, chapter 3 will develop the ADM formalism and the description of General Relativity in terms of the Ashtekar variables. The constraints revealed within these developments will give us insight into the symmetries of the formalism, which will vertebrate the entire project.

Afterward, the difficulties encountered when quantizing these formulations will lead us to an alternative (loop) representation, introduced in chapter 4. Then, a change of basis in terms of spin networks will provide a lattice-like structure to space using dressed graphs. These states will diagonalize the area and volume operators, which are associated with the edges and the vertices of the graph, respectively.

In chapter 5, based on the spinorial formalism, we will promote this discrete notion to a more geometrical level by equipping a graph with a pair of classical spinors living at the beginning and at the end of every edge. Then, we will impose the closure constraint, and thus we will associate a closed polyhedron with each vertex of the graph. Requiring an additional constraint, namely the area-matching constraint, we will construct the space of twisted geometries.

Finally, in chapter 6, we will study the dynamics of various two-vertex models by truncating the formalism. For that, we will generalize the work done in [38, 39] by moving out of the homogeneous and isotropic sector. We will solve numerically the equations of motion defining the time evolution of different systems by resorting to computational techniques. In particular, we will pay special attention to the tetrahedron—dual to a four-valent vertex—since it represents the simplest non-trivial quanta of space. Then, we will discuss the results and compare them with the ones obtained previously for the reduced sector. Diving into the dynamics of these 2-vertex models, we will also recognize in this case a possible cosmological regime within the LQG framework.

Chapter 2

Fundamental Aspects of General Relativity

Before going deep into LQG, we will review some fundamental aspects of differential geometry and General Relativity, setting thus the basis for the forthcoming calculations.

2.1 Differentiable Manifold

The fundamental object in the field of differential geometry will be differentiable manifolds. In general terms, a differentiable manifold is a set made of pieces that locally look like open subsets (patches) of \mathbb{R}^n , where the functions that sew these patches together have an inverse and are differentiable¹. Any smooth surface (flat, spherical, ...) would be a differentiable manifold. On the contrary, the surface of a cone would not correspond to a differentiable manifold since its tip would make it non-differentiable at that point [59].

Once we have presented the concept of a differentiable manifold, we may now introduce various kinds of structures on them. We begin with the tangent space and vectors.

The tangent space of the manifold \mathcal{M} at the point $p \in \mathcal{M}$, $T_p\mathcal{M}$, is the vector space of vectors which are tangent to all the curves γ going through p . This space has the same dimensionality as \mathcal{M} and can be identified with the space of directional derivatives. The partial derivatives $\{\partial_\mu\}$ constitute a suitable basis for such space.

The transformation law under changes of coordinates is immediate; the elements of the basis in a new coordinate system x'^μ are given by the chain rule:

$$\partial'_\mu = \frac{\partial x^\nu}{\partial x'^\mu} \partial_\nu. \quad (2.1)$$

Equivalently, the components of a vector transform as,

$$V'^\mu = \frac{\partial x'^\mu}{\partial x^\nu} V^\nu. \quad (2.2)$$

¹This set of patches is called an *atlas*.

The cotangent space of the manifold \mathcal{M} , $T_p^*\mathcal{M}$, is defined as the dual of the tangent space $T_p\mathcal{M}$, and its elements are linear maps f that operate on the tangent space as $f : T_p\mathcal{M} \rightarrow \mathbb{R}$. The differentials $\{dx^\mu\}$ constitute the basis of the cotangent space.

We can write an arbitrary vector in terms of the elements of the tangent space as $V = V^\mu \partial_\mu$, whereas for a general 1-form (an element of the cotangent space) we have $\omega = \omega_\mu dx^\mu$. The elements of the tangent space are called *contravariant* elements, and those of the cotangent space are known as *covariant*.

2.1.1 Tensors

A tensor T of rank (k, l) is a multilinear map of a collection of k dual vectors and l vectors to \mathbb{R} , that can be expanded in the basis of the tangent and cotangent spaces $\{\partial_{\mu_1} \otimes \cdots \otimes \partial_{\mu_k} \otimes dx^{\nu_1} \otimes \cdots \otimes dx^{\nu_l}\}$ in the following way [59]:

$$T = T^{\mu_1 \cdots \mu_k}_{\nu_1 \cdots \nu_l} \partial_{\mu_1} \otimes \cdots \otimes \partial_{\mu_k} \otimes dx^{\nu_1} \otimes \cdots \otimes dx^{\nu_l}, \quad (2.3)$$

where $T^{\mu_1 \cdots \mu_k}_{\nu_1 \cdots \nu_l}$ are the components of the tensor T in that basis. The transformation law for a general tensor is given by:

$$T'^{\mu_1 \cdots \mu_k}_{\nu_1 \cdots \nu_l} = \frac{\partial x'^{\mu_1}}{\partial x^{\rho_1}} \cdots \frac{\partial x'^{\mu_k}}{\partial x^{\rho_k}} \frac{\partial x^{\eta_1}}{\partial x'^{\nu_1}} \cdots \frac{\partial x^{\eta_l}}{\partial x'^{\nu_l}} T^{\rho_1 \cdots \rho_k}_{\eta_1 \cdots \eta_l}. \quad (2.4)$$

The metric tensor $g_{\mu\nu}$ is a $(0, 2)$ symmetric tensor which plays a crucial role in the mathematical field of differentiable manifolds and General Relativity. It serves to calculate metric concepts such as distances, angles and volumes. Moreover, it provides us with the notion of past and future, and it can be used to describe the causal relations of different events. The line element is defined via the metric as,

$$ds^2 = g_{\mu\nu} dx^\mu dx^\nu. \quad (2.5)$$

2.1.2 Diffeomorphism Invariance

General Relativity is constructed in a coordinate-independent way thanks to the principle of general covariance [60], according to which any physical theory can be expressed in the same form regardless of the coordinate basis. This reflects the absence of a predetermined background structure for all physical theories. Therefore, Einstein's General Relativity can be seen as a gauge theory where the gauge symmetry is the diffeomorphism invariance or invariance under general changes of coordinates.

Given two sets \mathcal{M} and \mathcal{N} , a diffeomorphism ϕ is a one-to-one, onto, and C^∞ (infinitely differentiable) map $\phi : \mathcal{M} \rightarrow \mathcal{N}$ with the inverse $\phi^{-1} : \mathcal{N} \rightarrow \mathcal{M}$ being also C^∞ . If there exists a diffeomorphism mapping both sets, then they have the same manifold structure [61].

2.2 Covariant Derivative

Algebraic operations that are tensorial convert tensors into tensors; for example, addition, subtraction, and contraction. However, some operations are not tensorial, such as the partial derivative. If we calculate the transformation of a partial derivative acting on a general tensor, we find

$$\partial'_\mu X^{\nu} = \frac{\partial x^\nu}{\partial x^\eta} \frac{\partial x^\sigma}{\partial x'^\mu} \partial_\sigma X^\eta + \frac{\partial^2 x^\nu}{\partial x^\eta \partial x^\sigma} \frac{\partial x^\sigma}{\partial x'^\mu} X^\eta. \quad (2.6)$$

If the second term on the right-hand side were not present, this would be the usual tensor transformation law of equation 2.4. However, this second term prevents the partial derivative from transforming like a tensor.

To understand why this happens, we need to recall that the process of differentiation involves comparing quantities evaluated at neighboring points of the manifold, divided by a parameter that determines the separation between them. As a result, we will have transformation matrices living at different points, making the partial derivative not behave as a tensor. In order to obtain a tensorial derivative operator, we need to define a structure that will let us connect two points belonging to different tangent spaces [62].

The covariant derivative ∇_μ of a tensor along a direction is a derivative operator which transforms like a tensor, so it can be seen as a tensorial alternative to ∂_μ . There is a lot of freedom in choosing a suitable covariant derivative, but in General Relativity (and thus in this project) we use the metric-compatible one,

$$\nabla_\mu g_{\nu\sigma} = 0, \quad (2.7)$$

because it provides a parallel transport operation preserving angles and lengths.

The covariant derivative acting on a covariant and a contravariant vector, respectively, reads as follows:

$$\nabla_\mu \omega_\nu = \partial_\mu \omega_\nu - \Gamma_{\mu\nu}^\sigma \omega_\sigma, \quad (2.8)$$

$$\nabla_\mu V^\nu = \partial_\mu V^\nu + \Gamma_{\mu\sigma}^\nu V^\sigma, \quad (2.9)$$

where $\Gamma_{\mu\nu}^\sigma$ is the *Christoffel symbol* or connection. This symbol—which is not a tensor—is a tool that tells us how to link neighboring vectors living on different tangent spaces of a manifold. Its expression is given by:

$$\Gamma_{\mu\nu}^\sigma = \frac{1}{2} g^{\sigma\lambda} (\partial_\mu g_{\nu\lambda} + \partial_\nu g_{\lambda\mu} - \partial_\lambda g_{\mu\nu}). \quad (2.10)$$

For a general tensor of rank (k, l) , the covariant derivative acts as,

$$\begin{aligned} \nabla_\mu T^{\nu_1 \dots \nu_k}_{\sigma_1 \dots \sigma_l} &= \partial_\mu T^{\nu_1 \dots \nu_k}_{\sigma_1 \dots \sigma_l} \\ &+ \sum_i \Gamma_{\mu\nu_i}^\lambda T^{\nu_1 \dots \lambda \dots \nu_k}_{\sigma_1 \dots \sigma_l} - \sum_j \Gamma_{\mu\sigma_j}^\lambda T^{\nu_1 \dots \nu_k}_{\sigma_1 \dots \lambda \dots \sigma_l}. \end{aligned} \quad (2.11)$$

Once we have defined the covariant derivative operator, we can now introduce the notion of parallel transport. A tensor is said to be parallel transported along a curve γ with tangent vector t^μ if the following relation is satisfied [61]:

$$t^\mu \nabla_\mu T_{\nu\cdots}^\sigma = 0. \quad (2.12)$$

If we parallel transport a vector along a closed curve, the vector we end up with might be rotated with respect to the one we had initially. This discrepancy between the initial and final vectors will depend on the curve chosen and the curvature of the manifold itself. We can thus use the path dependence of the parallel transport to define the notion of (intrinsic) curvature, which will be done in the next section.

2.2.1 Intrinsic Curvature

The inability of a vector to return to the initial state when parallel transported along a closed curve is translated as the lack of commutability of the covariant derivatives, which uniquely defines the Riemann tensor characterizing the *intrinsic curvature* of the manifold. We can express this in terms of a 1-form as:

$$[\nabla_\mu, \nabla_\nu] \omega_\sigma = R_{\mu\nu\sigma}^\lambda \omega_\lambda, \quad (2.13)$$

where $R_{\mu\nu\sigma}^\lambda$ is the Riemann curvature tensor. This tensor can be expanded as:

$$R_{\mu\nu\sigma}^\rho = \partial_\nu \Gamma_{\mu\sigma}^\rho - \partial_\mu \Gamma_{\nu\sigma}^\rho + \Gamma_{\mu\sigma}^\lambda \Gamma_{\lambda\nu}^\rho - \Gamma_{\nu\sigma}^\lambda \Gamma_{\lambda\mu}^\rho, \quad (2.14)$$

with the following symmetries and identities:

$$R_{\mu\nu\sigma\rho} = -R_{\mu\nu\rho\sigma} = -R_{\nu\mu\sigma\rho} = R_{\sigma\rho\mu\nu}, \quad (2.15)$$

$$R_{\mu\nu\sigma\rho} + R_{\mu\rho\nu\sigma} + R_{\mu\sigma\rho\nu} = 0, \quad (2.16)$$

$$\nabla_\mu R_{\rho\lambda\nu\sigma} + \nabla_\sigma R_{\rho\lambda\mu\nu} + \nabla_\nu R_{\rho\lambda\sigma\mu} = 0, \quad (2.17)$$

where equations 2.16 and 2.17 are known as the first (algebraic) and second (differential) Bianchi identities, respectively. As a matter of fact, a necessary and sufficient condition for the metric to be flat is that the Riemann tensor vanishes [62].

Contracting the Riemann tensor gives us the Ricci tensor which, using the Christoffel symbol defined above, is automatically symmetric:

$$R_{\mu\nu} = R_{\mu\lambda\nu}^\lambda. \quad (2.18)$$

Equivalently, the scalar curvature is given by contracting the Ricci tensor:

$$R = R_\mu^\mu = g^{\mu\nu} R_{\mu\nu}. \quad (2.19)$$

2.3 Lie Derivative

The Lie derivative $\mathcal{L}_X T_{\nu\dots}^{\mu\dots}$ is a differential operator that evaluates the variation of a tensor field $T_{\nu\dots}^{\mu\dots}$ along the flow of a vector field X , given by:

$$\mathcal{L}_X T_{\nu\dots}^{\mu\dots} = X^\sigma \partial_\sigma T_{\nu\dots}^{\mu\dots} - T_{\nu\dots}^{\sigma\dots} \partial_\sigma X^\mu - \dots + T_{\sigma\dots}^{\mu\dots} \partial_\nu X^\sigma + \dots \quad (2.20)$$

In particular, for covariant and contravariant vectors we have, respectively:

$$\mathcal{L}_X \omega_\mu = X^\nu \partial_\nu \omega_\mu + \omega_\nu \partial_\mu X^\nu, \quad (2.21)$$

$$\mathcal{L}_X V^\mu = X^\nu \partial_\nu V^\mu - V^\nu \partial_\nu X^\mu. \quad (2.22)$$

Nevertheless, since \mathcal{L}_X does not depend on the connection, we can substitute the partial derivative ∂_μ on equation 2.20 with the covariant derivative ∇_μ .

2.3.1 Extrinsic Curvature

In section 2.2.1 we introduced the concept of intrinsic curvature, and we explained that it is related to the parallel transport of a tensor along a curve γ . Indeed, this curvature is an intrinsic magnitude of the manifold, and thus it can be measured directly with information from the manifold itself.

Nonetheless, there is a different type of curvature known as *extrinsic curvature*, which describes how a surface is embedded in a higher-dimensional space. This extrinsic curvature $K_{\mu\nu}$ is directly related to the Lie derivative of the metric,

$$K_{\mu\nu} = \frac{1}{2} \mathcal{L}_n g_{\mu\nu}, \quad (2.23)$$

where the Lie derivative acts along the unit vector field n^μ normal to a hypersurface Σ . As we will see later in this project, this new concept will be crucial for developing the Hamiltonian formulation of General Relativity, which will be done in the following chapter.

Chapter 3

Hamiltonian Formulation of General Relativity and Ashtekar Variables

Once we have set the mathematical basis of differentiable manifolds, we are now ready to introduce the Hamiltonian formulation of General Relativity, a step towards developing the theory of LQG.

The procedure that we will carry out in what follows seems dangerous in a generically covariant theory; we will break up the spacetime manifold into space and time¹. This is necessary if we want to define velocities and conjugate momenta.

3.1 3+1 Decomposition

In other theories of classical physics, we are given a background structure (spacetime) and we attempt to determine the time evolution of certain quantities based on their initial values and time derivatives. However, in General Relativity the quantity we want to evolve is the spacetime itself (the background), so its Hamiltonian formulation will have some subtleties that other theories miss. This is the idea behind the 3+1 decomposition; to interpret the spacetime as a 3-dimensional object which *evolves* according to a particular notion of global time [63].

To raise the action to its canonical form, one has to assume that the topology of \mathcal{M} with coordinates X^μ ($\mu = 0, 1, 2, 3$) is $\mathcal{M} \cong \mathbb{R} \times \widehat{\Sigma}$, where $\widehat{\Sigma}$ is a 3-dimensional Cauchy surface of arbitrary topology. This can be done for any globally hyperbolic spacetime $(\mathcal{M}, g_{\mu\nu})$ [61]. Then, \mathcal{M} can be foliated into hypersurfaces $\Sigma_t \equiv \Phi_t(\widehat{\Sigma})$; that is, for the time-like function $t \in \mathbb{R}$ parametrizing the Cauchy surface, we have an embedding $\Phi_t : \widehat{\Sigma} \longrightarrow \mathcal{M}$ (see figure 3.1) defined by $\Phi_t(x) \equiv \Phi(t, x)$, where x^a ($a = 1, 2, 3$) are the local coordinates of $\widehat{\Sigma}$ [64].

¹This procedure is known as the 3+1 decomposition, and even if in the literature the 3+1 decomposition and the ADM formalism (the Hamiltonian formulation of General Relativity) are sometimes treated equally, we will use them separately. First, we will decompose the spacetime into space and time and then we will develop the ADM formalism.

Embedding means that $\Phi : \widehat{\Sigma} \longrightarrow \Sigma$ is a homeomorphism, i.e. a one-to-one mapping with Φ and Φ^{-1} continuous. To understand better the idea behind the 3+1 decomposition, we will assume that the hypersurface Σ is parametrized on \mathcal{M} by taking $t = 0$ with cartesian coordinates. In this case [65],

$$\begin{aligned}\Phi : \quad \widehat{\Sigma} \quad &\longrightarrow \quad \mathcal{M} \\ (x, y, z) \quad &\longmapsto \quad (0, x, y, z).\end{aligned}\tag{3.1}$$

If we want to transport elements from the tangent space of a point $p \in \widehat{\Sigma}$, then we need the mapping Φ^* called *push forward*,

$$\begin{aligned}\Phi^* : \quad \mathcal{T}_p(\widehat{\Sigma}) \quad &\longrightarrow \quad \mathcal{T}_p(\mathcal{M}) \\ \mathbf{v} = (v^x, v^y, v^z) \quad &\longmapsto \quad \Phi^*\mathbf{v} = (0, v^x, v^y, v^z).\end{aligned}\tag{3.2}$$

Similarly, the elements of the cotangent space of \mathcal{M} will be mapped via the following *pull back* Φ_* ,

$$\begin{aligned}\Phi_* : \quad \mathcal{T}_p^*(\mathcal{M}) \quad &\longrightarrow \quad \mathcal{T}_p^*(\widehat{\Sigma}) \\ \boldsymbol{\omega} = (\omega_t, \omega_x, \omega_y, \omega_z) \quad &\longmapsto \quad \Phi_*\boldsymbol{\omega} = (\omega_x, \omega_y, \omega_z).\end{aligned}\tag{3.3}$$

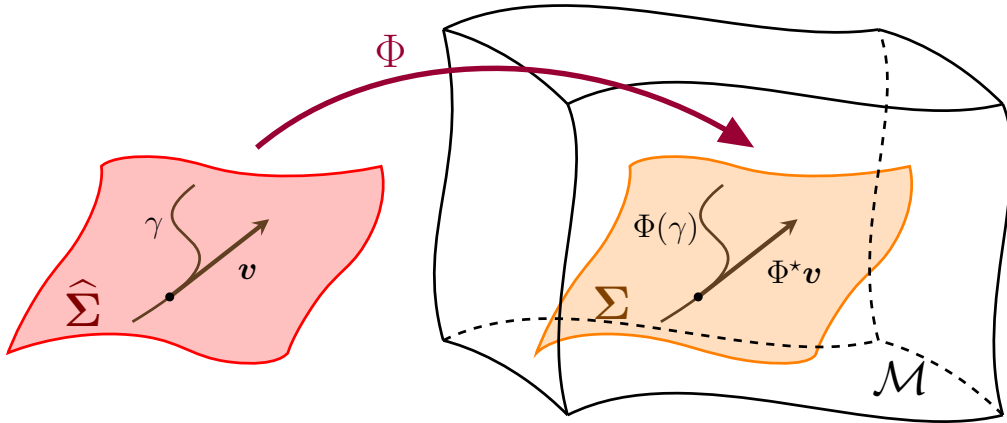


Figure 3.1. Embedding Φ of the 3-dimensional manifold $\widehat{\Sigma}$ into \mathcal{M} which defines the hypersurface $\Sigma = \Phi(\widehat{\Sigma})$. An element \mathbf{v} tangent to some curve γ in $\widehat{\Sigma}$ will be pushed forward into \mathcal{M} via $\Phi^*\mathbf{v}$ tangent to $\Phi(\gamma)$.

Since $(\Phi^*\mathbf{v})^\mu = (\Phi^*)^\mu_a v^a$, we have,

$$(\Phi^*)^\mu_a = \frac{\partial X^\mu}{\partial x^a} = X^\mu_{,a}.\tag{3.4}$$

The explicit representation of the push forward for a $(k, 0)$ tensor S (not necessarily parametrized by $t = 0$) is given by [59],

$$(\Phi^* S)^{\mu_1 \dots \mu_k} = X^{\mu_1}_{,a_1} \dots X^{\mu_k}_{,a_k} S^{a_1 \dots a_k},\tag{3.5}$$

and for the pull back we have $(\Phi_* \omega)_a = (\Phi_*)_a^\mu \omega_\mu$ with,

$$(\Phi_*)_a^\mu = \frac{\partial X^\mu}{\partial x^a} = X^\mu_{,a}. \quad (3.6)$$

As we can see, this is the same equation as 3.4; however, the indices that will be contracted are different. Then, we have the following action on a $(0, l)$ tensor T ,

$$(\Phi_* T)_{a_1 \dots a_l} = X^{\mu_1}_{,a_1} \dots X^{\mu_l}_{,a_l} T_{\mu_1 \dots \mu_l}. \quad (3.7)$$

Moving on to the 3+1 decomposition, we define t^μ as a vector field in \mathcal{M} satisfying $t^\mu \nabla_\mu t = 1$. We decompose t^μ into its tangential and normal components (see figure 3.2),

$$t^\mu = N n^\mu + N^\mu, \quad (3.8)$$

where n^μ is a unit normal vector to Σ_t , the tangent N^μ is the *shift vector* and N is the *lapse function*.

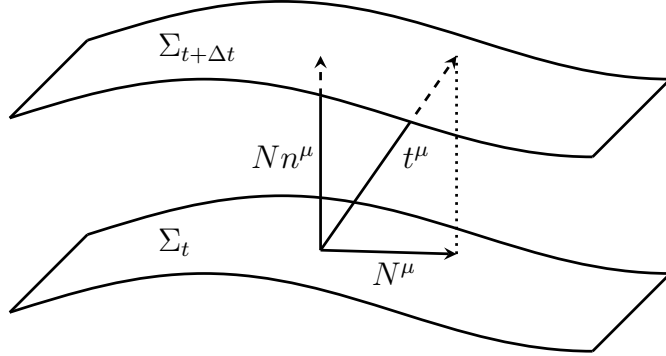


Figure 3.2. Schematic representation of the 3+1 decomposition of the vector field t^μ . N^μ is the shift tangent to the hypersurface Σ_t whereas the lapse N measures its flow of time.

Now, using the convention $(- +++)$ we consider the following tensor fields known as the first and second fundamental forms of Σ , respectively:

$$q_{\mu\nu} \equiv g_{\mu\nu} + n_\mu n_\nu, \quad (3.9)$$

$$K_{\mu\nu} \equiv q^\sigma_\mu \nabla_\sigma n_\nu, \quad (3.10)$$

with $n_\mu n^\mu = -1$, and where $q_{\mu\nu}$ is the induced metric on Σ , and $K_{\mu\nu}$ is the extrinsic curvature describing its embedding on \mathcal{M} . We can interpret the vector field t^μ as the time flow in the spacetime, providing us with a change of the 3-dimensional metric of the manifold Σ from $q_{\mu\nu}(t)$ to $q_{\mu\nu}(t + \Delta t)$. Therefore, it would suffice to have as initial data $q_{\mu\nu}$ and $K_{\mu\nu}$, since the first two are related to the spatial part, and the extrinsic curvature is related to its time evolution.

We can express the shift and lapse in Σ in terms of t^μ as,

$$N = -t^\mu n_\mu, \quad (3.11)$$

$$N_\mu = q_{\mu\nu} t^\nu. \quad (3.12)$$

Using equations 3.8 and 3.9, we can write the spacetime metric in terms of the shift N^μ and the lapse N ,

$$g^{\mu\nu} = q^{\mu\nu} - n^\mu n^\nu = q^{\mu\nu} - \frac{1}{N^2} (t^\mu - N^\mu) (t^\nu - N^\nu). \quad (3.13)$$

We can use equation 3.5 to express $g^{\mu\nu}$ (and $g_{\mu\nu}$) in terms of the pulled back quantities on $\widehat{\Sigma}$ [9],

$$g^{\mu\nu} = \begin{pmatrix} -1/N^2 & N_a/N^2 \\ N_a/N^2 & q^{ab} - N^a N^b / N^2 \end{pmatrix}, \quad g_{\mu\nu} = \begin{pmatrix} -N^2 + N^a N_a & N_a \\ -N_a & q_{ab} \end{pmatrix}. \quad (3.14)$$

As mentioned in chapter 2, the extrinsic curvature is related to the Lie derivative defined in equation 2.20. This curvature provides a well-defined notion of ‘time derivative’ of the spatial metric on Σ embedded in the spacetime. Using equation 3.9, we can reexpress the extrinsic curvature:

$$K_{\mu\nu} = \nabla_\mu n_\nu + n_\mu n^\sigma \nabla_\sigma n_\nu = \frac{1}{2} \mathcal{L}_n q_{\mu\nu}. \quad (3.15)$$

Recalling equation 3.8, it is direct to see that,

$$\dot{q}_{\mu\nu} \equiv \mathcal{L}_t q_{\mu\nu} = 2N K_{\mu\nu} + \mathcal{L}_{\vec{N}} q_{\mu\nu}, \quad (3.16)$$

which describes the evolution of the metric, and tells us that the extrinsic curvature is related to the evolution of the induced metric.

Previously, we defined certain functions living on the spacetime manifold \mathcal{M} , such as the covariant derivative or the Riemann curvature tensor. Now, we need to redefine these quantities to fit in the hypersurface Σ .

We define the covariant derivative in Σ acting on a tensor (k, l) as:

$$D_\sigma T^{\mu_1 \dots \mu_k}_{\nu_1 \dots \nu_l} = (q_{\rho_1}^{\mu_1} \dots q_{\rho_k}^{\mu_k} q_{\nu_1}^{\eta_1} \dots q_{\nu_l}^{\eta_l}) q_\sigma^\xi \nabla_\xi T^{\rho_1 \dots \rho_k}_{\eta_1 \dots \eta_l}, \quad (3.17)$$

where ∇_μ is the derivative associated to the spacetime metric $g_{\mu\nu}$. This derivative is also hypersurface-metric compatible, $D_\mu q_{\nu\sigma} = 0$. Consequently, the extrinsic curvature is given by:

$$\begin{aligned} K_{\mu\nu} &= \frac{1}{2} \mathcal{L}_t q_{\mu\nu} \\ &= \frac{1}{2} N^{-1} [\dot{q}_{\mu\nu} - D_\mu N_\nu - D_\nu N_\mu]. \end{aligned} \quad (3.18)$$

Now, we can obtain the curvature tensor ${}^{(3)}R_{\mu\nu\sigma}{}^\rho$ in Σ directly based on the commutator between two covariant derivatives, as we did in chapter 2:

$$[D_\mu, D_\nu] \omega_\sigma = {}^{(3)}R_{\mu\nu\sigma}{}^\rho \omega_\rho. \quad (3.19)$$

If we differentiate ω_σ twice, we get:

$$D_\mu D_\nu \omega_\sigma = K_{\mu\nu} n^\rho q_\sigma^\eta \nabla_\rho \omega_\eta + K_{\mu\sigma} q_\nu^\rho n^\eta \nabla_\rho \omega_\eta + q_\mu^\xi q_\nu^\rho q_\sigma^\eta \nabla_\xi \nabla_\rho \omega_\eta. \quad (3.20)$$

Here we have used that:

$$q_\mu^\nu q_\sigma^\rho \nabla_\nu q_\rho^\eta = K_{\mu\sigma} n^\eta, \quad (3.21)$$

$$q_\nu^\rho n^\eta \nabla_\rho \omega_\eta = -K_\nu^\eta \omega_\eta. \quad (3.22)$$

Finally, since $K_{\mu\nu}$ is symmetric, it is possible to obtain the following equation for the 3-dimensional Riemann curvature tensor:

$${}^{(3)}R_{\mu\nu\sigma}^\rho = q_\mu^\xi q_\nu^\gamma q_\sigma^\kappa q_\chi^\rho R_{\xi\gamma\kappa}^\chi - K_{\mu\sigma} K_\nu^\rho + K_{\nu\sigma} K_\mu^\rho. \quad (3.23)$$

Similarly, it can be shown that the following expression is also satisfied:

$$D_\mu K_\nu^\mu - D_\nu K_\mu^\mu = R_{\sigma\rho} n^\rho q_\nu^\sigma. \quad (3.24)$$

These last two equations are known as the *Gauss-Codacci equations* [61], relating the induced metric ($q_{\mu\nu}$) and the second fundamental form ($K_{\mu\nu}$) of a submanifold of a (pseudo-)Riemannian manifold. Contracting equation 3.23, we get,

$${}^{(3)}R = K^2 - K_{\mu\nu} K^{\mu\nu} + R, \quad (3.25)$$

which is the 3-dimensional Ricci scalar.

3.2 ADM Formalism

Making use of the mathematical tools presented in the previous section, we are now ready to develop the Hamiltonian formulation of General Relativity. This formulation facilitates the study of constraint and the subsequent attempt to canonical quantization.

At this point, we will work on the 3-dimensional Cauchy surface $\widehat{\Sigma}$. Therefore, we need to pull back various quantities,

$$q_{ab} = g_{\mu\nu} X_{,a}^\mu X_{,b}^\nu, \quad (3.26)$$

$$K_{ab} = X_{,a}^\mu X_{,b}^\nu \nabla_\mu n_\nu. \quad (3.27)$$

From these relations, we can see that,

$$K_{\mu\nu} K^{\mu\nu} = K_{\mu\nu} K_{\rho\sigma} g^{\rho\mu} g^{\sigma\nu} = K_{ab} K_{cd} q^{ac} q^{bd} = K_{ab} K^{ab}, \quad (3.28)$$

where for the second equality we have used the following relation,

$$K_{\mu\nu} n^\rho n^\mu = n^\rho n^\mu q_\mu^\sigma \nabla_\sigma n_\nu = 0. \quad (3.29)$$

Now, we use the Lagrangian of General Relativity (from which we could obtain Einstein's equations):

$$\mathcal{L}_G = \sqrt{-g} R, \quad (3.30)$$

where R is the curvature scalar and $g = \det(g_{\mu\nu})$ is the determinant of the metric, that can be expressed in terms of the induced metric as $\sqrt{-g} = N\sqrt{q}$. From expression 3.25, we can express the Lagrangian \mathcal{L}_G as:

$$\mathcal{L}_G = \sqrt{q}N[(^3)R + K_{ab}K^{ab} - K^2]. \quad (3.31)$$

As we can see, the Lagrangian does not depend on the time derivatives of N and N_a . Thus, we can not interpret them as dynamical variables; instead, they behave as Lagrange multipliers, and the terms multiplying them will be the constraints of the system.

To obtain an expression for the Hamiltonian, we need the canonically conjugate momenta:

$$\pi^{ab} = \frac{\partial \mathcal{L}_G}{\partial \dot{q}_{ab}} = \sqrt{q} (K^{ab} - K q^{ab}), \quad (3.32)$$

and using the Legendre transformation, the Hamiltonian reads:

$$\begin{aligned} \mathcal{H}_G &= \pi^{ab}\dot{q}_{ab} - \mathcal{L}_G \\ &= \sqrt{q} \left\{ N \left[-(^3)R + \frac{\pi^{ab}\pi_{ab}}{q} - \frac{\pi^2}{2q} \right] - 2N_b D_a \left(\frac{\pi^{ab}}{\sqrt{q}} \right) + D_a \left(2 \frac{N_b \pi^{ab}}{\sqrt{q}} \right) \right\}. \end{aligned} \quad (3.33)$$

When we integrate this Hamiltonian density the last term will vanish since it only contributes a boundary term.

From the Lagrange multipliers, we can obtain information about the constraints of the system. Varying \mathcal{H}_G with respect to N and N_a , we get:

$$H = \frac{\partial \mathcal{H}_G}{\partial N} = -(^3)R + \frac{\pi^{ab}\pi_{ab}}{q} - \frac{\pi^2}{2q} = 0, \quad (3.34)$$

$$C^a = \frac{\partial \mathcal{H}_G}{\partial N_a} = D_b \left(\frac{\pi^{ba}}{\sqrt{q}} \right) = 0, \quad (3.35)$$

where H is the Hamiltonian (or scalar) constraint and C^a is the diffeomorphism constraint. As we can see, the Hamiltonian is the sum of the 4 constraints, so it will also be a constraint.

The fact that we have constraints means that the phase space is ‘too large’, which is related to the gauge freedom of the configuration variables q_{ab} . For the moment, since the metric is a symmetric 3×3 tensor, it will have 6 degrees of freedom that, together with the 4 constraints of the system, results in a total of 2 degrees of freedom for General Relativity. A deeper explanation of these constraints will be given in forthcoming sections.

Finally, we obtain the differential equations describing the evolution of the coordinate variables and the conjugate momenta,

$$\dot{q}_{ab} = \frac{\delta H_G}{\delta \pi^{ab}} = 2 \frac{N}{\sqrt{q}} \left(\pi_{ab} - \frac{1}{2} q_{ab} \pi \right) + D_a N_b + D_b N_a, \quad (3.36)$$

$$\dot{\pi}^{ab} = -\frac{\delta H_G}{\delta q_{ab}} = -N\sqrt{q} \left((^3)R^{ab} - \frac{1}{2} (^3)R q^{ab} \right) + \frac{1}{2} \frac{N q^{ab}}{\sqrt{q}} q^{ab} \left(\pi_{cd} \pi^{cd} - \frac{1}{2} \pi^2 \right)$$

$$\begin{aligned}
& - 2 \frac{N}{\sqrt{q}} \left(\pi^{ac} \pi_c^b - \frac{1}{2} \pi \pi^{ab} \right) + \sqrt{q} (D^a D^b N - q^{ab} D^c D_c N) \quad (3.37) \\
& + \sqrt{q} D_c \left(\frac{N^c \pi^{ab}}{\sqrt{q}} \right) - 2 \pi^{ca} D_c N^b - 2 \pi^{cb} D_c N^a.
\end{aligned}$$

These two equations, together with the constraints, are equivalent to Einstein's equations in vacuum. Therefore, we have developed the Hamiltonian formulation of General Relativity, which is known as the ADM formalism, named after its authors R. Arnowitt, S. Deser, and C. W. Misner, who developed this description in 1959² [21].

3.2.1 Quantization

Historically, the first quantization of General Relativity came by the hands of B. DeWitt [23] in 1967 and was popularized by J. A. Wheeler [68] in the late 1960s. According to this proposal, we may quantize the canonical variables as multiplicative operator and the conjugate momenta as derivatives over q_{ab} :

$$\hat{q}_{ab} = q_{ab} \times, \quad \hat{p}^{ab} = -i\hbar \frac{\partial}{\partial q_{ab}}. \quad (3.38)$$

In terms of these variables, the wave functional $\psi[q_{ab}]$ will describe the probability of a given region to have a certain metric, so it contains all the information about the geometry of the Universe, and so its matter content. Constraints must annihilate physical states, and since the Hamiltonian of General Relativity is a linear combination of constraints, we have:

$$\hat{H}\psi[q_{ab}] = 0, \quad (3.39)$$

which is known as the Wheeler-DeWitt equation.

Nevertheless, this approach has remained as a theoretical development except for homogeneous cosmological models in Quantum Cosmology with just a few degrees of freedom [69, 70]. Defining an inner product in the space of all metrics constitutes one of the main problems of this development. Without an inner product, the theory loses its predictive power—we can no longer define expectation values, probabilities, or even normalized wave functions. Therefore, we will move to a different formalism where connections are used as canonical variables rather than the 3-dimensional metric.

3.3 Ashtekar Variables

In 1986 A. Ashtekar [24] introduced a new set of variables which facilitated the development of a Hamiltonian formulation to describe General Relativity. The Ashtekar configuration variables are SU(2) connections A_a^i , and their conjugate momenta are the densitized triads \tilde{E}_i^a . These elements will be defined in the following sections.

²A review of this formalism was published by the authors in [66] and a reprint in [67].

3.3.1 Triads

Let us introduce the triads E_i^a , which are a set of orthogonal vector fields relating a generic metric q_{ab} with *spatial indices* (a, b) and a flat space metric δ^{ij} with *internal indices* (i, j). The triads diagonalize the metric at each point,

$$q^{ab} = E_i^a E_j^b \delta^{ij}, \quad (3.40)$$

with $i = 1, 2, 3$. Since the internal indices are lowered and raised using δ^{ij} , we will treat the upper and lower indices indistinctively. This relationship is invariant under $\text{SO}(3)$ rotations $E_i^a \rightarrow O_i^j E_j^a$, $O_i^j \in \text{SO}(3)$. Although both sets of indices range from 1 to 3, we must treat them differently since they act on a different ‘space’. Accordingly, we will redefine the covariant derivative operators in order to consider these new indices [64],

$$\mathcal{D}_a T_j = \partial_a T_j + \Gamma_{ajk} T^k, \quad (3.41)$$

$$\mathcal{D}_a T^j = \partial_a T^j - \Gamma_{ajk} T^k, \quad (3.42)$$

where Γ_{ajk} is given by:

$$\Gamma_{ajk} = -E_k^b (\partial_a E_b^j - \Gamma_{ab}^c E_c^j), \quad (3.43)$$

in order to obtain the metric compatible derivative $\mathcal{D}_a E_b^j = 0$.

Now, we will introduce the concept of densitization, which consists of transforming an object by multiplying it with $\det(q)^{\omega/2}$, where ω denotes the *weight*. A densitized object, f , will be denoted as \tilde{f} if $\omega = +1$, and \underline{f} if $\omega = -1$:

$$\tilde{f} = \sqrt{\det(q)} f, \quad \underline{f} = \frac{1}{\sqrt{\det(q)}} f. \quad (3.44)$$

This will be useful to define integrals on a manifold with a generic set of coordinates.

In our case, we will work with triads of density weight $\omega = +1$:

$$\tilde{E}_i^a = \sqrt{\det(q)} E_i^a. \quad (3.45)$$

Consequently, the metric will be a weight $\omega = +2$ tensor:

$$\tilde{q}^{ab} = \det(q) q^{ab} = \tilde{E}_i^a \tilde{E}_j^b \delta^{ij}. \quad (3.46)$$

3.3.2 Connection

Even though a thorough analysis of the Yang-Mills theory is out of the scope of this work, it might be interesting to have a notion of its fundamental aspects. This theory was developed by C. N. Yang, and R. Mills in the 1950s aiming to unify the electromagnetic force with both the weak and strong nuclear forces by considering non-abelian Lie groups.

In Yang-Mills theory, we consider a vector potential in analogy with Maxwell’s theory. However, this vector potential is not a scalar number but a collection of matrices that are

members of an algebra. For the case of the $\mathfrak{su}(2)$ Lie algebra, the vector potential can be expanded in the following way [71]:

$$\mathbf{A}_\nu = A_\nu^i \sigma^i, \quad (3.47)$$

where σ^i are the Pauli matrices and A_ν^i are the components of the vector potential in such basis, by means of which we can construct a covariant derivative:

$$\mathbf{D}_\nu = \partial_\nu - i \frac{g}{2} \sigma^i A_\nu^i, \quad (3.48)$$

where g is known as the coupling constant. For a given basis of an algebra V^i , the structure constants f^{jkl} of such algebra will obey the following relation:

$$[V^j, V^k] = i f^{jkl} V^l. \quad (3.49)$$

In the basis given by the Pauli matrices, the structure constants are the 3-dimensional Levi-Civita symbols $f^{ijk} = 2\epsilon^{ijk}$. Finally, let us introduce the field strength, $F_{\mu\nu}^i$:

$$F_{\mu\nu}^i = \partial_\mu A_\nu^i - \partial_\nu A_\mu^i + g \epsilon^{ijk} A_\mu^j A_\nu^k. \quad (3.50)$$

Now that we have had a quick look at the fundamental aspects of the Yang-Mills theory, we are prepared to recover our analysis of the Hamiltonian formulation.

3.3.3 Hamiltonian Formulation

Let us introduce the Ashtekar connection,

$$A_a^i = \Gamma_a^i + \beta K_a^i, \quad (3.51)$$

where $K_a^i = K_{ab} \tilde{E}^{bi} / \sqrt{\det(q)}$ and β is known as the *Barbero-Immirzi parameter*, named after G. Immirzi [72] and F. Barbero [25]. This parameter is introduced to account for the invariance of the Poisson bracket $\{E_i^a, K_b^j\}$ under the reescaling $(E_i^a, K_b^j) \mapsto (E_i^a/\beta, \beta K_b^j)$, and it can take any value $\beta \in \mathbb{C} - \{0\}$. Nevertheless, to construct an inner product for the Hilbert space of LQG, we will only consider real values of β [25].

As we know from the Hamiltonian formulation, the Poisson bracket between the canonical variables and their conjugate momenta will be proportional to the Dirac delta. In the present case,

$$\{A_a^i(x), \tilde{E}_j^b(y)\} = 8\pi G \beta \delta_a^b \delta_j^i \delta^3(x - y). \quad (3.52)$$

where $\Gamma_a^i = \Gamma_{ajk} \epsilon^{jki}$ is the *spin connection*.

We can write the diffeomorphism constraint from equation 3.35 in terms of the Ashtekar variables as,

$$C_a = \tilde{E}_k^b F_{ba}^k - A_a^i \left(\mathbf{D}_b \tilde{E}_i^b \right) = 0, \quad (3.53)$$

where F_{ba}^k comes from equation 3.50. Then, the Hamiltonian constraint from equation 3.34 generating ‘time evolution’ reads,

$$H = \epsilon_{ijk} \tilde{E}_i^a \tilde{E}_j^b F_{ab}^k + 2 \frac{(\beta^2 + 1)}{\beta^2} \left(\tilde{E}_i^a \tilde{E}_j^b - \tilde{E}_j^a \tilde{E}_i^b \right) (A_a^i - \Gamma_a^i) (A_b^j - \Gamma_b^j) = 0. \quad (3.54)$$

Finally, we have a new set of constraints known as the Gauss’ law,

$$\mathcal{G}^i = D_a \tilde{E}_i^a = 0. \quad (3.55)$$

This is a direct consequence of the presence of the triads. When we introduce the triads, we gain an additional set of degrees of freedom due to the liberty of orientation of the coordinate basis at each point, which translates into a SU(2) gauge invariance of the formalism. Since we have two indices running from 1 to 3 in A_a^i , we will have 9 degrees of freedom. Considering the 7 constraints, we recover the 2 degrees of freedom for the complete theory, as we expected.

In the following chapter, we will mention the attempts to quantize the theory in terms of the Ashtekar variables, and we will introduce a new formulation, which will serve to overcome the difficulties presented by the quantization.

Chapter 4

Loop Representation for Quantum Gravity

Once we have the classical formulation of Hamiltonian mechanics, we can build its quantum version by following the procedure of canonical quantization, constructing an internal product, and promoting the canonical variables to quantum operators ($q_{ab} \rightarrow \hat{q}_{ab}$, $p_{ab} \rightarrow \hat{p}_{ab}$), as well as quantizing the constraints.

In terms of these variables, the natural path to follow would be to promote the connections to multiplication operators and the densitized triads to derivative operators:

$$\hat{A}_a^i \psi(A) = A_a^i \psi(A), \quad (4.1)$$

$$\hat{\tilde{E}}_i^a \psi(A) = -i\beta \frac{\delta \psi(A)}{\delta A_a^i}, \quad (4.2)$$

so the commutator would give:

$$\left[\hat{A}_b^j(y), \hat{\tilde{E}}_i^a(x) \right] = i\beta \delta_b^a \delta_i^j \delta^3(x - y). \quad (4.3)$$

However, the procedure of quantizing General Relativity in terms of the Ashtekar variables was found to be ill-defined (see [64] and [73] for a detailed explanation), since the Hamiltonian constraint from equation 3.54 presents several problems. The main difficulties when dealing with the Hamiltonian constraint are associated with its regularization and with the construction of a suitable inner product.

The next step is to look for an alternative representation, known as the *loop representation* of General Relativity, which uses SU(2) connections to build new observables, known as *holonomies*. This representation was introduced by C. Rovelli and L. Smolin in [27, 28], and it is based on the tools provided by Lattice Gauge Theories, widely used in other branches of physics such as Quantum Chromodynamics [74, 75].

4.1 Holonomies

In differential geometry, the concept of holonomy emerges as a consequence of the curvature of the connection in a smooth manifold. The holonomy measures how the geometrical data are affected when we transport them along closed curves. To construct these holonomies, we are going to calculate the parallel transport operator $\mathcal{U}_{||}$ along a curve $\gamma(t)$, which is obtained from a recursive relation:

$$\mathcal{U}_{||}(t) = \sum_{n=0}^{\infty} \left((-ig)^n \int_{t_1 \geq \dots \geq t_n \geq 0} \dot{\gamma}^{a_1}(t_1) \mathbf{A}_{a_1}(t_1) \dots \dot{\gamma}^{a_n}(t_n) \mathbf{A}_{a_n}(t_n) dt_1 \dots dt_n \right), \quad (4.4)$$

where g is the coupling constant from equation 3.48. Now, we introduce the *path ordered product*, widely used in Quantum Field Theories [74, 75]:

$$\mathcal{P}(\mathbf{A}_{a_1}(t_1) \dots \mathbf{A}_{a_n}(t_n)). \quad (4.5)$$

This product acting on a collection of functions $A_{a_i}(t_i)$ will arrange them by moving those terms with bigger t_i to the left. We can express equation 4.4 as a path ordered exponential [71]:

$$\mathcal{U}_{||} = \mathcal{P} \left[\exp \left(-ig \int_0^t \dot{\gamma}^a(s) \mathbf{A}_a(s) ds \right) \right]. \quad (4.6)$$

For the special case where the curve is closed, $\gamma(0) = \gamma(t)$, this is known as the *holonomy*, which is an element of the SU(2) Lie group (given that \mathbf{A}_a is an element of $\mathfrak{su}(2)$).

Due to the cyclical properties of the traces, the traces of holonomies will be gauge-invariant,

$$\text{Tr} (\Lambda M \Lambda^{-1}) = \text{Tr} (M), \quad \Lambda \in \text{SU}(2), \quad (4.7)$$

where M is a general matrix. Therefore, we take the trace of the holonomy,

$$W_\gamma[A] = \text{Tr} \left(P \left[\exp \left(-ig \oint_\gamma \dot{\gamma}^a(s) \mathbf{A}_a(s) ds \right) \right] \right), \quad (4.8)$$

which is known as the Wilson loop [76]: the trace of the path-ordered exponential of a gauge field \mathbf{A}_a along a closed curve.

To proceed, we would like to know whether these elements are suitable canonical variables to build a candidate theory of quantum gravity. According to Giles' Reconstruction theorem [77], all the gauge-invariant information of the connection can be obtained from the traces of the holonomies around all the possible loops of the manifold. Consequently, the Wilson loops constitute a basis for all the gauge-invariant functions, which will be a solution to Gauss' law (which restricts the possible states to those that are gauge-invariant functions of the connection.). Therefore, we can expand the states of A as,

$$\Psi[A] = \sum_\gamma \Psi[\gamma] W_\gamma[A], \quad (4.9)$$

where γ are all the possible closed loops. Working with functions that depend on the holonomies is known as the *loop representation* and the relation between the connection representation and this new loop representation is given by equation 4.9.

In the following section, we will generalize these holonomies to arbitrary curves, not necessarily closed curves. This will lead to a new representation for a candidate theory of quantum gravity.

4.2 Spin Networks

As we have mentioned in section 3.3.2, the Ashtekar connection is a $\mathfrak{su}(2)$ connection. According to equation 3.47, we can express it in terms of the Pauli matrices¹ σ_i (which are the fundamental representation of the algebra) as,

$$[\sigma_a, \sigma_b] = 2i\epsilon_{abc}\sigma_c. \quad (4.10)$$

The irreducible representations of $\mathfrak{su}(2)$ are labelled by half-integers j codified in $(2j+1)$ -dimensional square matrices. Nevertheless, the basis provided by the loop representation is overcomplete, meaning that not all the loops are independent of each other. The issues resulting from the overcompleteness of the basis were overcome by C. Rovelli and L. Smolin in [29] with the introduction of *spin networks*.

A spin network is a wave function that can be represented pictorially as a ‘dressed’ graph [78], i.e. a graph endowed with some objects at the edges and vertices. The edges will be associated with the holonomies, and will be labeled with a spin j that will tell us which $SU(2)$ irreducible representation is being used. Then, the vertices that join these edges together will be equipped with some objects known as *intertwiners*, which will link the different representations carried by the edges, ensuring the $SU(2)$ invariance of the construction². An example is shown in figure 4.1.

This way, we have constructed a representation of LQG that already accounts for the $SU(2)$ gauge symmetry formalized by Gauss’ law. Therefore, this constraint will already be included in our construction. Nevertheless, we can go one step further and incorporate also the diffeomorphism constraint. To do so, we will work with generalized spin networks via representatives of equivalence classes, where the equivalence relation will be spatial diffeomorphisms. Consequently, when working with a specific spin network, we will work simultaneously with all the spin networks related to this one by a diffeomorphism or a graph refinement. This way, the diffeomorphism constraint will also be implicitly included in the formalism.

¹In what follows, we will use the following normalization for the Pauli matrices,

$$\sigma_x = \begin{pmatrix} 0 & 1 \\ 1 & 0 \end{pmatrix}, \quad \sigma_y = \begin{pmatrix} 0 & -i \\ i & 0 \end{pmatrix}, \quad \sigma_z = \begin{pmatrix} 1 & 0 \\ 0 & -1 \end{pmatrix}.$$

²For a 2-valent and 3-valent vertex, these intertwiners will be given in terms of the Clebsch-Gordan coefficients and the 3j-symbols [79], respectively.

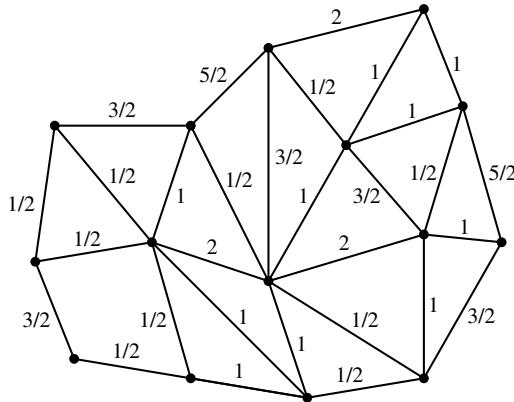


Figure 4.1. An example of a spin network. The numbers labeling the edges account for the irreducible representations of the holonomies (elements of the $SU(2)$ group). An edge with number j corresponds to a matrix of dimension $(2j + 1)$. For every vertex of the graph we have an intertwiner, which is a $SU(2)$ invariant tensor ensuring the gauge invariance of the theory.

Still, there remains the Hamiltonian constraint from equation 3.54. Classically, this constraint is related to time diffeomorphisms, so it is needed in order to account for the dynamics. However, imposing the Hamiltonian constraint is one of the biggest open problems of the theory; this is why we usually refer to the kinematical sector of LQG. Nevertheless, several mechanisms have been carried out to handle this situation, such as the spin foam models [41, 42] based on Feynman’s path integrals, the so-called ‘Thiemann’s trick’ and the master constraint [43–45]. Despite many advances have been carried out in this field, the implementation of the dynamics still remains as an important open problem.

4.2.1 Inner product

To calculate probabilities and expectation values, we need to endow the Hilbert space \mathcal{H}_{LQG} with a suitable inner product. This will be given by the Ashtekar-Lewandowski measure, $d\mu_{\text{AL}}$, developed in [80–83]. Now, the kinematical Hilbert space will be given by:

$$\mathcal{H}_{\text{LQG}} = L^2(\text{SU}(2), d\mu_{\text{AL}}). \quad (4.11)$$

This inner product has a discrete spectrum, so we will be working with connections that are not smooth functions but distributions. Consequently, the connection and the triads will not be suitable observables since they will not be promoted to well-defined quantum operators. Therefore, we will need to work with holonomies and triad fluxes obtained by integrating the triads along a surface, which will lead us to the holonomy-flux algebra.

The uniqueness theorem for the loop representation in quantum gravity (the LOST-F theorem) has been proven by J. Lewandowski, A. Okolow, H. Sahlmann, and T. Thiemann [84] and, in a slightly different version by C. Fleischhack [85]. Under some mild assumptions, this theorem states that the loop representation is the only possible way to quantize a diffeomorphism invariant theory [73].

4.3 Geometric Operators

When quantizing a theory, one expects to obtain operators that act on certain (eigen)states give us the discrete spectrum of a certain observable, such as the energy or velocity. When we quantize General Relativity, a theory that studies spacetime dynamics, we would expect to discretize geometrical operators like areas and volumes, giving us an idea of the discrete structure of spacetime at the quantum level. Following this idea, C. Rovelli and L. Smolin [12] and A. Ashtekar and J. Lewandowski [10, 11] proposed a quantum operator for the area and volume.

4.3.1 Area Operator

Given a surface Σ , we can calculate its area using:

$$A_\Sigma = \int_{\Sigma} dx^1 dx^2 \sqrt{\det q^{(2)}}, \quad (4.12)$$

where $q^{(2)}$ is the metric of the two-dimensional space where the surface is embedded. Writing this equation in terms of the Ashtekar variables and promoting it to a quantum operator, we get the following expression for the area operator acting on a spin network state ψ_s ,

$$\hat{A}_\Sigma \psi_s = 8\pi \ell_{\text{Planck}}^2 \beta \sum_i \sqrt{j_i(j_i + 1)} \psi_s, \quad (4.13)$$

where j_i is the spin of the edge i that pierces the surface Σ . Therefore, a surface Σ will acquire an area if it is pierced at least by one edge of the spin network. This equation tells us that the spin network state ψ_s is an eigenstate of the area operator, and will provide a quanta of area proportional to the Planck length square ℓ_{Planck}^2 [10, 12].

As we can see, the spectrum of the area is not linear. Nevertheless, there exists a different regularization with equidistant eigenvalues $\propto \sum_i j_i$, which is also mathematically consistent. Furthermore, this spectrum will be the total area, since it is the quantity that will be preserved in the $U(N)$ formalism, that we will introduce in section 5.2. Therefore, the equidistant spectrum will be a more natural choice within the spinorial and $U(N)$ formalisms [37].

Since the Barbero-Immirzi parameter is directly related to the area, we require the value of β to be positive. Using this area operator, in the late 1990s, an explicit formula for the entropy of a black hole was proposed, and some years later, alternative derivations were also computed [48–53]. Comparing these results with the Bekenstein-Hawking formula for the black hole entropy, an explicit value for β was obtained. Nevertheless, more results would be desirable in order to fix precisely the parameter in a consistent way.

4.3.2 Volume Operator

To proceed, we are going to discuss the volume operator, given by the following expression:

$$V(R) = \int_R d^3x \sqrt{\det q} = \frac{1}{6} \int_R d^3x \sqrt{\left| \varepsilon_{abc} \epsilon^{ijk} \tilde{E}_i^a \tilde{E}_j^b \tilde{E}_k^c \right|}. \quad (4.14)$$

The quantum version of the volume operator is complicated and highly dependent on the spin network under consideration (in [86] they calculate several eigenvalues explicitly), so we will omit it here. Nevertheless, it is interesting to understand its action and implications. This operator will act on the vertices of the spin network and will provide the region with quanta of volume, as long as there are at least four non-coplanar edges linked to that vertex. Therefore, just as the edges of the spin network will be in charge of providing quanta of area to a surface, the vertices will endow a region with quanta of volume. This description in terms of the area and volume operators provides an intuitive notion of the discreteness of space in LQG.

Chapter 5

Spinorial Techniques and $U(N)$ Formalism

In the loop representation, we can see the space of LQG as a collection of Hilbert spaces \mathcal{H}_Γ associated with each graph Γ , which can be expressed as the tensorial product of all the Hilbert spaces associated with each edge e of the graph¹, \mathcal{H}_e .

Working with a specific graph corresponds to a truncation of the theory since we restrict ourselves to a finite number of degrees of freedom instead of considering the infinitely many degrees of freedom of the whole Hilbert space \mathcal{H}_{LQG} [87].

In this chapter, we are going to introduce the classical spinorial framework [31], whose quantization will give us the kinematical Hilbert space of LQG.

5.1 Spinorial Classical Framework

Let us consider² a spinor $|z\rangle \in \mathbb{C}^2$ and its transposed complex conjugate $\langle z| \in \mathbb{C}^2$ [31]:

$$|z\rangle = \begin{pmatrix} z^0 \\ z^1 \end{pmatrix}, \quad \langle z| = \begin{pmatrix} \bar{z}^0 & \bar{z}^1 \end{pmatrix}. \quad (5.1)$$

We endow the \mathbb{C}^2 space with the following symplectic structure:

$$\{z^A, \bar{z}^B\} = -i\delta^{AB} \implies \{|z\rangle, \langle z|\} = -i\mathbb{I}. \quad (5.2)$$

Since spinors are elements of \mathbb{C}^2 , they transform in a natural way under the fundamental representation of the group $SU(2)$,

$$h : \mathbb{C}^2 \rightarrow \mathbb{C}^2; \quad |z\rangle \rightarrow h|z\rangle, \quad \forall h \in SU(2). \quad (5.3)$$

¹The Hilbert space of an edge is given by $\mathcal{H}_e = L^2(SU(2), d\mu)$, where $d\mu$ is the Haar measure which enables an appropriate integration for that space. For a detailed explanation see [64].

²This treatment is entirely classical even though we are using Dirac notation.

Furthermore, we define the internal product of these spinors as $\langle \omega | z \rangle = \bar{\omega}^0 z^0 + \bar{\omega}^1 z^1$, for which the norm will be given by $\|z\| = \sqrt{\langle z | z \rangle}$. It will be advantageous for future calculations to introduce the following shorthand:

$$[z] = -i\sigma_y |\bar{z}\rangle = \begin{pmatrix} -\bar{z}^1 \\ \bar{z}^0 \end{pmatrix}. \quad (5.4)$$

From expressions 5.1 and 5.4, we can verify the following relations:

$$[z | \omega\rangle = z^0 \omega^1 - \omega^0 z^1 \implies [z | z\rangle = 0, \quad (5.5)$$

$$[z | \omega] = \overline{\langle z | \omega \rangle} = \langle \omega | z \rangle \implies [z | z] = \langle z | z \rangle. \quad (5.6)$$

Since $|z\rangle \langle z|$ is a Hermitian 2×2 matrix, we can decompose it in terms of the Pauli matrices σ_i and the identity $\mathbb{I}_{2 \times 2}$:

$$|z\rangle \langle z| = \frac{1}{2} \left(\langle z | z \rangle \mathbb{I}_{2 \times 2} + \vec{N} \cdot \vec{\sigma} \right), \quad (5.7)$$

where the vector \vec{N} is given by,

$$\vec{N} = \frac{1}{2} \langle z | \vec{\sigma} | z \rangle \implies |\vec{N}| = \frac{1}{2} \langle z | z \rangle. \quad (5.8)$$

Therefore, we uniquely associate to each spinor a 3-dimensional vector \vec{N} , whose components can be expressed as:

$$N^1 = \text{Re}(z^0 \bar{z}^1), \quad N^2 = \text{Im}(z^0 \bar{z}^1), \quad N^3 = \frac{1}{2} \left(|z^0|^2 - |z^1|^2 \right), \quad (5.9)$$

with $N = \vec{N} \cdot \vec{\sigma}$ being a $\mathfrak{su}(2)$ Lie-algebra element.

To proceed, we are going to associate a spinor $|z_e^v\rangle$ to an edge e linked to the vertex v . Since every edge will be linked to a pair of vertices, we will have a *source* spinor $|z_e^s\rangle$ and a *target* spinor $|z_e^t\rangle$ for every outgoing and incoming edge e , respectively.

Let us construct a $SU(2)$ element from the source and target spinors $(|z_e^s\rangle, |z_e^t\rangle)$ of the edge e [88]:

$$g_e = \frac{|z_e^t| \langle z_e^s | - |z_e^s\rangle [z_e^t]}{\|z_e^t\| \|z_e^s\|} \in SU(2). \quad (5.10)$$

This element acts on the spinors in the following way:

$$g_e |z_e^s\rangle = |z_e^t\rangle, \quad g_e |z_e^t\rangle = -|z_e^s\rangle, \quad (5.11)$$

with,

$$g_e g_e^\dagger = g_e^\dagger g_e = \mathbb{I}. \quad (5.12)$$

The phase space of these Hilbert spaces \mathcal{H}_e is given by the cotangent bundle over $SU(2)$, which is $T^* SU(2)$. With the two elements defined above, we can parametrize the phase space as $T^* SU(2) \simeq SU(2) \times \mathfrak{su}(2) \ni (g, N)$ associated with each edge of the graph. This constitutes the classical spinorial representation of the holonomy-flux algebra.

Furthermore, we will require the following *closure constraint* at each vertex,

$$\vec{\mathcal{C}} = \sum_e \langle z_e | \vec{\sigma} | z_e \rangle = 0, \quad (5.13)$$

which is equivalent to imposing:

$$\sum_e |z_e\rangle \langle z_e| = \frac{1}{2} \sum_e \langle z_e | z_e \rangle \mathbb{I}, \quad (5.14)$$

and can be translated into the following relations:

$$\sum_e |z_e^0|^2 - |z_e^1|^2 = 0, \quad (5.15)$$

$$\sum_e \bar{z}_e^0 z_e^1 = 0. \quad (5.16)$$

This constraint generates $SU(2)$ gauge transformations on the spinors $|z_e\rangle \rightarrow h|z_e\rangle$ with $h \in SU(2)$,

$$\{\vec{\mathcal{C}}, |z_e\rangle\} = \vec{\sigma} |z_e\rangle. \quad (5.17)$$

Upon quantization, the closure constraint will account for the gauge invariance of the quantum theory.

Since we can uniquely assign to each spinor $|z\rangle$ a 3-dimensional vector \vec{N} , we will use a theorem from H. Minkowski [32] to associate a discrete notion of space with this classical framework:

Theorem 1 *Let $\vec{N}_1 \dots \vec{N}_F$ be non coplanar unit vectors and $\lambda_1 \dots \lambda_F$ positive numbers that obey the following relation:*

$$\sum_{e=1}^F \lambda_e \vec{N}_e = 0. \quad (5.18)$$

Then, there exist a unique convex polyhedron (up to translations) whose faces “e” have normal vectors \vec{N}_e and areas λ_e .

By means of this theorem, the classical spinorial representation provides a geometrical notion by assigning a closed polyhedron to each vertex of the graph (see figure 5.1). Since these polyhedrons will be joined together, we will consider an additional constraint that will restrict the possible “attachings” among them. This will be the *area matching constraint* \mathcal{M} , which imposes the matching of the areas on the joined faces. Since the normal vector to the face e of the polyhedron is \vec{N}_e , its norm $|\vec{N}_e|$ will give us the area of that face. Thus, we can express the area matching constraint in terms of the spinors as,

$$\mathcal{M} = \langle z_e^s | z_e^s \rangle - \langle z_e^t | z_e^t \rangle = 0, \quad (5.19)$$

which is equivalent to imposing $|\vec{N}_e^s| = |\vec{N}_e^t|$. This geometrical interpretation is known as *twisted geometries* [33–35].

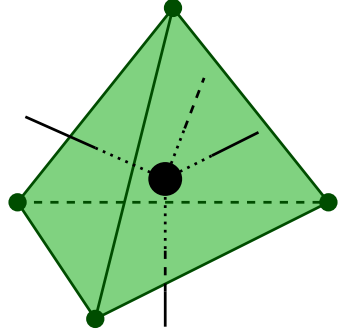


Figure 5.1. We can interpret each vertex of the spin network as a polyhedron, where the faces correspond to the edges.

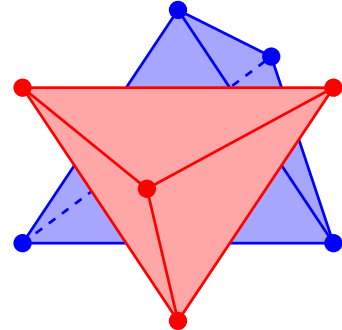
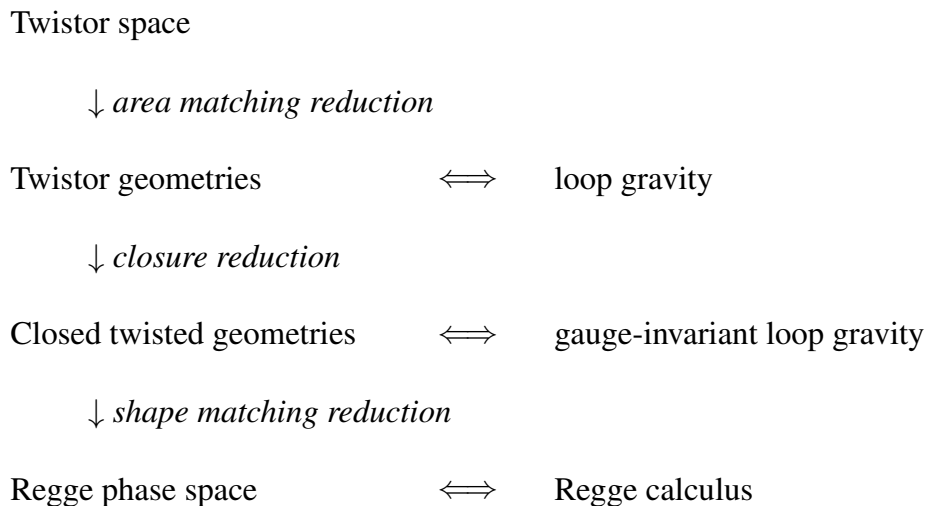


Figure 5.2. In the twisted geometries, the polyhedrons can be joined by faces of different shape (but not different area).

At this point, it might be interesting to relate the discretization of space presented by the twisted geometries with the one introduced by T. Regge in 1961 [89]. In the Regge calculus, the spacetime is triangulated into 4-simplices (the 4-dimensional concept of a tetrahedron), which are constrained to be closed via the closure constraint and connected by faces of equal shape via the *gluing* or *shape matching constraint*. However, in the twisted geometries, the faces are not constraint to have the same shape (see figure 5.2). This additional freedom on the shape of the faces is what gives the name “twisted” to the framework.

Since we have a pair of spinors (source and target) linked to every edge, we introduce the twistor space $\mathbb{T} = \mathbb{C}^2 \times \mathbb{C}^2$. From here, we can obtain the different phase spaces associated with a graph, depending on the restrictions we impose, as we can see from the following scheme [35]:



In this section, we have described a classical formalism where we have dressed a graph with a pair of spinors at every edge, which obeyed the closure and matching constraints.

Within this construction, we have provided a geometrical notion to these graphs via the twisted geometries. Now, we will present a new formalism that can be useful to move from this classical phase space to the kinematical Hilbert space of LQG. Moreover, we will use this formalism to propose dynamics in truncated models, as we will see in chapter 6.

5.2 $U(N)$ Formalism

This section will explore the $U(N)$ framework for LQG, which studies the Hilbert space associated with the intertwiners. These objects live at the vertices of the spin network and ensure the $SU(2)$ invariance of the theory. The $U(N)$ formalism is based on the Schwinger representation of the $\mathfrak{su}(2)$ Lie algebra, used in quantum mechanics (see, for example, [40]).

Let us introduce $2N$ uncoupled harmonic oscillators with the following commutation relations [38],

$$[\hat{a}_i, \hat{a}_j^\dagger] = [\hat{b}_i, \hat{b}_j^\dagger] = \delta_{ij}, \quad (5.20)$$

where $(\hat{a}_i^\dagger, \hat{b}_i^\dagger)$ and (\hat{a}_i, \hat{b}_i) are the creation and annihilation operators of the edge i , respectively. According to the Schwinger representation, we can express the generators of the $SU(2)$ group acting on each leg of the intertwiner in terms of creation and annihilation operators as,

$$\hat{J}_i^z = \frac{1}{2} (\hat{a}_i^\dagger \hat{a}_i - \hat{b}_i^\dagger \hat{b}_i), \quad \hat{J}_i^+ = \hat{a}_i^\dagger \hat{b}_i, \quad \hat{J}_i^- = \hat{a}_i \hat{b}_i^\dagger, \quad \hat{E}_i = (\hat{a}_i^\dagger \hat{a}_i + \hat{b}_i^\dagger \hat{b}_i), \quad (5.21)$$

where the J_i 's obey,

$$[\hat{J}_i^z, \hat{J}_i^\pm] = \pm \hat{J}_i^\pm, \quad [\hat{J}_i^+, \hat{J}_i^-] = 2 \hat{J}_i^z, \quad (5.22)$$

and \hat{E}_i is the Casimir operator $[\hat{E}_i, \hat{J}_i] = 0$. This Casimir operator will give twice the area of the edge i and therefore $\hat{E} = \sum_i \hat{E}_i$ will be twice the total area of the corresponding polyhedron. Now, we introduce a more general set of operators which act on a pair of spinors (i, j) as,

$$\hat{E}_{ij} = \hat{a}_i^\dagger \hat{a}_j + \hat{b}_i^\dagger \hat{b}_j, \quad \hat{E}_{ij}^\dagger = \hat{E}_{ji}, \quad (5.23)$$

$$\hat{F}_{ij} = \hat{a}_i \hat{b}_j - \hat{a}_j \hat{b}_i, \quad \hat{F}_{ji} = -\hat{F}_{ij}. \quad (5.24)$$

We recover the Casimir operator in equation 5.21 from the diagonal terms of \hat{E}_{ij} ; $\hat{E}_{ii} = \hat{E}_i$.

Now, we compute their commutation relations, which give [38],

$$\begin{aligned} [\hat{E}_{ij}, \hat{F}_{kl}] &= \delta_{il} \hat{F}_{jk} - \delta_{ik} \hat{F}_{jl}, & [\hat{E}_{ij}, \hat{F}_{kl}^\dagger] &= \delta_{jk} \hat{F}_{il}^\dagger - \delta_{jl} \hat{F}_{ik}^\dagger, \\ [\hat{F}_{ij}, \hat{F}_{kl}] &= 0, & [\hat{F}_{ij}^\dagger, \hat{F}_{kl}^\dagger] &= 0, \\ [\hat{E}_{ij}, \hat{E}_{kl}] &= \delta_{jk} \hat{E}_{il} - \delta_{il} \hat{E}_{kj}, \\ [\hat{F}_{ij}, \hat{F}_{kl}^\dagger] &= \delta_{ik} \hat{F}_{lj} - \delta_{il} \hat{F}_{kj} - \delta_{jk} \hat{F}_{li} + \delta_{jl} \hat{F}_{ki}. \end{aligned} \quad (5.25)$$

These relations define a closed algebra, known as $\mathfrak{so}^*(2N)$ [90, 91]. Moreover, their commutators with \widehat{E} give:

$$[\widehat{E}, \widehat{E}_{ij}] = 0, \quad [\widehat{E}, \widehat{F}_{ij}] = -2\widehat{F}_{ij}, \quad [\widehat{E}, \widehat{F}_{ij}^\dagger] = +2\widehat{F}_{ij}^\dagger. \quad (5.26)$$

On the one hand, the operator \widehat{E}_{ij} increases/decreases the area of each edge while keeping the total area of the polyhedron unchanged, since it commutes with \widehat{E} . Furthermore, these \widehat{E} -observables alone form a closed $u(N)$ algebra (giving the name to the formalism), which is a subalgebra of $\mathfrak{so}^*(2N)$ itself. On the other hand, \widehat{F}_{ij}^\dagger and \widehat{F}_{ij} act as creation and annihilation operators of the total area, respectively.

Looking for a classical-quantum correspondence, we promote the spinors (z_i^0, z_i^1) to annihilation operators (\hat{a}_i, \hat{b}_i) and their complex conjugates $(\bar{z}_i^0, \bar{z}_i^1)$ to creation operators $(\hat{a}_i^\dagger, \hat{b}_i^\dagger)$,

$$|z_i\rangle = \begin{pmatrix} z_i^0 \\ z_i^1 \end{pmatrix} \rightarrow \begin{pmatrix} \hat{a}_i \\ \hat{b}_i \end{pmatrix}, \quad \langle z_i| = \begin{pmatrix} \bar{z}_i^0 & \bar{z}_i^1 \end{pmatrix} \rightarrow \begin{pmatrix} \hat{a}_i^\dagger & \hat{b}_i^\dagger \end{pmatrix}. \quad (5.27)$$

This way, we get,

$$E_{ij} = \langle z_i | z_j \rangle, \quad F_{ij} = [z_i | z_j \rangle, \quad \bar{F}_{ij} = \langle z_j | z_i], \quad (5.28)$$

which are the classical observables associated with \widehat{E}_{ij} , \widehat{F}_{ij} and \widehat{F}_{ij}^\dagger , respectively. The matrix E_{ij} is Hermitian, while F_{ij} is anti-symmetric and holomorphic³ in the spinor variables.

These observables are $SU(2)$ invariant; that is, for any $h \in SU(2)$ [88]:

$$|z_i\rangle \xrightarrow{h \in SU(2)} h|z_i\rangle, \quad (5.30)$$

we have,

$$E_{kl} = \langle z_k | z_l \rangle \rightarrow \langle z_k | h^\dagger h | z_l \rangle = \langle z_k | z_l \rangle = E_{kl}, \quad (5.31)$$

$$F_{kl} = [z_k | z_l \rangle \rightarrow i \langle \bar{z}_k | h^t \sigma_y h | z_l \rangle = [z_k | z_l \rangle = F_{kl}. \quad (5.32)$$

To prove equation 5.32, we calculate the general expression of a $SU(2)$ group element and show that $h^t \sigma_y h = \sigma_y$, $\forall h \in SU(2)$. The Poisson brackets of E , F and \bar{F} can be directly obtained from their quantum version (equation 5.25) using the standard relation $\{\cdot, \cdot\} \rightarrow -i[\cdot, \cdot]$.

³A function $f(z)$ is holomorphic if it can be expanded in powers of z and does not depend on the complex conjugate \bar{z} ,

$$f(z) = \sum_{n=0}^{\infty} c_n z^n. \quad (5.29)$$

Chapter 6

Dynamics for 2-Vertex Models

In this chapter, we will study the dynamics for truncated 2-vertex models. To begin with, we will describe the current state of the 2-vertex models in the literature, which essentially consists of a symmetry reduction to the homogeneous and isotropic sector. Then, we will propose classical dynamics which are compatible with the symmetries of the system. Since we have freedom in choosing a renormalization, we will propose three different Hamiltonians.

Afterward, we will calculate the dynamics of various 2-vertex models. For that, we are going to get out of the reduced sector, and work with more general models.

6.1 Reduced Sector in 2-Vertex Models

As we have previously explained, a truncation of the theory consists of restricting ourselves to a particular graph with specific edges and vertices. Although we are leaving out infinitely many degrees of freedom, it can help us gain insight into the nature of the discrete structure of space favored by the twisted geometries. In this chapter, we will consider various 2-vertex models linked by an arbitrary number of edges (see figure 6.1), as done in [39].

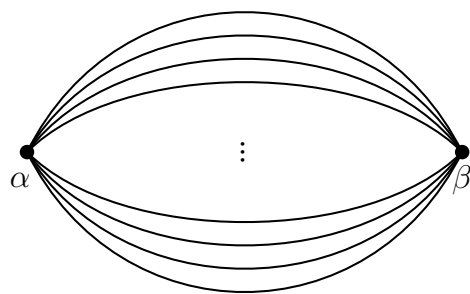


Figure 6.1. General 2-vertex graph. The vertices α and β are linked by an arbitrary number of edges.

In these models, we will have one intertwiner space associated with each vertex. Consequently, the operators will be denoted by a superscript, labeling the vertex where they belong, \widehat{E}_{ij}^α , \widehat{F}_{ij}^α and \widehat{E}_{ij}^β , \widehat{F}_{ij}^β .

Since we are working with a pair of vertices, it will be convenient to define the following symmetric operators acting on α and β [39],

$$\widehat{e}_{ij} \equiv \widehat{E}_{ij}^\alpha \widehat{E}_{ij}^\beta, \quad \widehat{f}_{ij} \equiv \widehat{F}_{ij}^\alpha \widehat{F}_{ij}^\beta, \quad \widehat{f}_{ij}^\dagger \equiv \widehat{F}_{ij}^{\alpha\dagger} \widehat{F}_{ij}^{\beta\dagger}, \quad (6.1)$$

which consistently deform the boundaries between both vertices. The operator \widehat{e}_{ij} increases the spin of the edge i and decreases the spin of j , thus keeping the total area invariant. Then, the operator \widehat{f}_{ij} decreases the spin of both i and j while \widehat{f}_{ij}^\dagger increases them.

In [38], it was considered a symmetry reduction of a 2-vertex model by imposing an addition constraint $\widehat{\mathcal{E}}_{ij}$,

$$\widehat{\mathcal{E}}_{ij} \equiv \widehat{E}_{ij}^\alpha - \widehat{E}_{ji}^\beta = \widehat{E}_{ij}^\alpha - \widehat{E}_{ij}^{\beta\dagger} = 0, \quad (6.2)$$

that can be seen as a generalization of the matching constraint, since $\widehat{\mathcal{E}}_{ii} \equiv \widehat{E}_{ii}^\alpha - \widehat{E}_{ii}^\beta = 0$. This constraint forms a new $u(N)$ algebra, which will act on the two intertwiner system¹. Furthermore, it was shown that the states invariant under this new $U(N)$ symmetry only depended on the total area. They labeled these states as homogeneous (for their independence concerning the vertex) and isotropic (invariant under changes of spins which keep the total area unchanged).

Constructing a homogeneous and isotropic model inside the formalism of LQG could help us find a relationship between LQG and LQC. In fact, a possible relation between these reduced models and cosmology was pointed out in [38] and [39]. We recall that LQC follows a separate path from LQG by first imposing symmetry reductions and then proceeding to the quantization. Generally, these two processes do not commute [57], so obtaining cosmological results from LQG alone is definitely an interesting aspect.

6.2 Proposal for the Dynamics

Now, we are going to propose various classical Hamiltonians which will respect the constraints of the system. Since in the quantized theory we have freedom in choosing a suitable regularization, in this classical sector we will introduce three Hamiltonians which differ by a renormalization factor.

6.2.1 Simplest non-Trivial Hamiltonian

To account for the dynamics on a 2-vertex model where the $2N$ spinors satisfy both the closure and matching constraints, we must consider all four possible actions given by the

¹In equation 5.25, we mentioned that the operators \widehat{E}_{ij} themselves formed a $u(N)$ algebra acting on the corresponding vertex. This new constraint $\widehat{\mathcal{E}}_{ij}$ relates both vertices via $\widehat{E}_{ij}^\alpha - \widehat{E}_{ji}^\beta$, so the corresponding algebra $u(N)$ will be inherit from previous 1-vertex case. This constraint is imposed in order to account for a global $u(N)$ symmetry involving both vertices.

observables $E_{ij}^\alpha E_{ij}^\beta$, $\bar{E}_{ij}^\alpha \bar{E}_{ij}^\beta$, $F_{ij}^\alpha F_{ij}^\beta$ and $\bar{F}_{ij}^\alpha \bar{F}_{ij}^\beta$. Then, the most general gauge invariant Hamiltonian at first order² is [38],

$$H = \sum_{ij} \lambda_{ij} E_{ij}^\alpha E_{ij}^\beta + \gamma_{ij}^+ F_{ij}^\alpha F_{ij}^\beta + \gamma_{ij}^- \bar{F}_{ij}^\alpha \bar{F}_{ij}^\beta, \quad (6.3)$$

where γ_{ij}^+ , γ_{ij}^- and λ_{ij} are the coupling constants. However, imposing the Hamiltonian to be real, they must restrict to $\gamma_{ij}^- = \overline{\gamma^+}_{ij}$ and $\lambda_{ij} \in \mathbb{R}$. Now, for simplicity, we will consider that the coupling constants are independent of the edges, i.e. $\gamma_{ij}^\pm = \gamma^\pm$ and $\lambda_{ij} = \lambda$. Therefore, the most general Hamiltonian reads,

$$H_{\text{LQG}} = \sum_{k,l} \lambda E_{kl}^\alpha E_{kl}^\beta + \gamma F_{kl}^\alpha F_{kl}^\beta + \bar{\gamma} \bar{F}_{kl}^\alpha \bar{F}_{kl}^\beta = \lambda e_0 + \gamma f_0 + \bar{\gamma} \bar{f}_0, \quad (6.4)$$

where $\gamma = \gamma^+$ and e_0, f_0, \bar{f}_0 are given by,

$$e_0 = \sum_{k,l} E_{kl}^\alpha E_{kl}^\beta, \quad f_0 = \sum_{k,l} F_{kl}^\alpha F_{kl}^\beta, \quad \bar{f}_0 = \sum_{k,l} \bar{F}_{kl}^\alpha \bar{F}_{kl}^\beta. \quad (6.5)$$

These elements satisfy the following Poisson brackets,

$$\{f_0, \bar{f}_0\} = -4iEe_0, \quad \{e_0, f_0\} = 2iEf_0, \quad \{e_0, \bar{f}_0\} = -2iE\bar{f}_0, \quad (6.6)$$

where $E = \sum_i E_{ii}$. Moreover, they form a $\mathfrak{sl}(2, \mathbb{R})$ algebra³, with great relevance in LQC [92]. Moreover, its complex analog, $\text{SL}(2, \mathbb{C})$, plays a crucial role in the spin foam framework [93, 94].

By construction, the Hamiltonian from equation 6.4 is invariant under global $\text{SU}(2)$ gauge transformations,

$$\{H_{\text{LQG}}, \vec{\mathcal{C}}^v\} = 0, \quad (6.7)$$

at each vertex v , and also commutes with the matching constraint at each vertex i :

$$\{H_{\text{LQG}}, \mathcal{M}_i\} = 0. \quad (6.8)$$

This ensures that both constraints will also be satisfied after the system has evolved. The Hamiltonian H_{LQG} is not unique since we can build other expressions (respecting the symmetries and constraints), which differ by a renormalization factor depending on the total boundary area [39].

²This is first order in the observables that consider both vertices, i.e. allowing non-trivial changes of area. However, in terms of the spinors this would be a fourth order Hamiltonian since $E_{ij}^\alpha E_{ij}^\beta \propto z^4$.

³This can be proven by making the change of variables $e_0 = 2iEe$, thus obtaining:

$$\{e, f_0\} = f_0, \quad \{\bar{f}_0, e\} = \bar{f}_0, \quad \{\bar{f}_0, f_0\} = 2e,$$

which is the usual commutator relation characterizing the algebra.

6.2.2 Generalized Lattice Gauge Hamiltonian

Equivalently, we can construct an alternative Hamiltonian by considering the SU(2) holonomy for a loop linking both vertices (α, β) by a pair of edges (k, l) ,

$$\begin{aligned}\chi_{kl} &= \text{Tr } g_k g_l^{-1} = \frac{\text{Tr}(|\omega_k| \langle z_k | - |\omega_k| [z_k]) (|z_l| [\omega_l] - |z_l| \langle \omega_l |)}{\sqrt{\langle z_k | z_k \rangle \langle \omega_k | \omega_k \rangle \langle z_l | z_l \rangle \langle \omega_l | \omega_l \rangle}} \\ &= \frac{E_{kl}^\alpha E_{kl}^\beta + E_{lk}^\alpha E_{lk}^\beta + F_{kl}^\alpha F_{kl}^\beta + \bar{F}_{kl}^\alpha \bar{F}_{kl}^\beta}{4\sqrt{N_k^\alpha N_l^\alpha N_k^\beta N_l^\beta}},\end{aligned}\quad (6.9)$$

where $N_k^\alpha = \langle z_k^\alpha | z_k^\alpha \rangle / 2$ and $N_k^\beta = \langle z_k^\beta | z_k^\beta \rangle / 2$. Thus, summing over all pairs of edges and adding the coupling constants to account for different weights, we have:

$$H_0 = \sum_{k,l} \frac{\lambda E_{kl}^\alpha E_{kl}^\beta + \gamma F_{kl}^\alpha F_{kl}^\beta + \bar{\gamma} \bar{F}_{kl}^\alpha \bar{F}_{kl}^\beta}{4\sqrt{N_k^\alpha N_l^\alpha N_k^\beta N_l^\beta}} = \lambda e + \gamma f + \bar{\gamma} \bar{f}. \quad (6.10)$$

In this case,

$$\begin{aligned}e &= \frac{1}{2} \sum_{k,l} \frac{E_{kl}^\alpha E_{kl}^\beta}{\sqrt{N_k^\alpha N_l^\alpha N_k^\beta N_l^\beta}}, \\ f &= \frac{1}{4} \sum_{k,l} \frac{F_{kl}^\alpha F_{kl}^\beta}{\sqrt{N_k^\alpha N_l^\alpha N_k^\beta N_l^\beta}}, \quad \bar{f} = \frac{1}{4} \sum_{k,l} \frac{\bar{F}_{kl}^\alpha \bar{F}_{kl}^\beta}{\sqrt{N_k^\alpha N_l^\alpha N_k^\beta N_l^\beta}}.\end{aligned}\quad (6.11)$$

Finding the algebra of a set of elements is interesting since we can use the properties of such algebra to reduce our calculations. Therefore, we have calculated the Poisson-brackets of these e, f, \bar{f} :

$$\begin{aligned}\{e, f\} &= + \frac{i}{4} \sum_{k,l,m} \left[- \frac{E_{kl}^\alpha F_{mk}^\alpha F_{lm}^\beta + E_{kl}^\beta F_{mk}^\beta F_{lm}^\alpha}{\sqrt{N_k^\alpha N_l^\beta} \sqrt{N_l^\alpha N_m^\beta N_m^\alpha N_k^\beta}} \right] \\ &\quad + \frac{i}{8} f \sum_{k,l} \frac{E_{kl}^\alpha E_{kl}^\beta + E_{lk}^\alpha E_{lk}^\beta}{\sqrt{N_k^\alpha N_l^\alpha N_k^\beta N_l^\beta}} \left(\frac{1}{N_k^\alpha} + \frac{1}{N_l^\beta} \right),\end{aligned}\quad (6.12)$$

$$\begin{aligned}\{e, \bar{f}\} &= - \frac{i}{4} \sum_{k,l,m} \left[- \frac{E_{lk}^\alpha \bar{F}_{mk}^\alpha \bar{F}_{lm}^\beta + E_{lk}^\beta \bar{F}_{mk}^\beta \bar{F}_{lm}^\alpha}{\sqrt{N_k^\alpha N_l^\beta} \sqrt{N_l^\alpha N_m^\beta N_m^\alpha N_k^\beta}} \right] \\ &\quad - \frac{i}{8} \bar{f} \sum_{k,l} \frac{E_{lk}^\alpha E_{lk}^\beta + E_{kl}^\alpha E_{kl}^\beta}{\sqrt{N_k^\alpha N_l^\alpha N_k^\beta N_l^\beta}} \left(\frac{1}{N_k^\alpha} + \frac{1}{N_l^\beta} \right),\end{aligned}\quad (6.13)$$

$$\begin{aligned}\{f, \bar{f}\} &= - \frac{i}{4} \sum_{k,l,n} \left[\frac{F_{kl}^\beta \bar{F}_{kn}^\beta E_{nl}^\alpha + F_{kl}^\alpha \bar{F}_{kn}^\alpha E_{nl}^\beta}{\sqrt{N_k^\alpha N_l^\beta} \sqrt{N_k^\alpha N_l^\alpha N_k^\beta N_l^\beta N_n^\alpha N_n^\beta}} \right] \\ &\quad + \frac{i}{8} \sum_{k,l,m,n} \left[\frac{F_{kl}^\alpha F_{kl}^\beta}{\sqrt{N_k^\alpha N_l^\alpha N_k^\beta N_l^\beta}} \frac{\bar{F}_{mn}^\alpha \bar{F}_{mn}^\beta}{\sqrt{N_m^\alpha N_n^\alpha N_m^\beta N_n^\beta}} \left(\frac{1}{N_n^\alpha} + \frac{1}{N_n^\beta} + \frac{1}{N_k^\alpha} + \frac{1}{N_k^\beta} \right) \right].\end{aligned}\quad (6.14)$$

However, we have not found a closed form of the algebra.

6.2.3 Intermediate Normalization Hamiltonian

Due to the complexity of the algebra of observables e , f , and \bar{f} , we can propose an alternative regularization for the Hamiltonian, where the normalization lies outside the sum of equation 6.10,

$$H_{\text{inter}} = \frac{1}{\sqrt{N^\alpha N^\beta}} \sum_{k,l} \left(\lambda E_{kl}^\alpha E_{kl}^\beta + \gamma F_{kl}^\alpha F_{kl}^\beta + \bar{\gamma} \bar{F}_{kl}^\alpha \bar{F}_{kl}^\beta \right), \quad (6.15)$$

with $N^v = \sum_i N_i^v$ and,

$$e_1 = \frac{1}{\sqrt{N^\alpha N^\beta}} e_0, \quad f_1 = \frac{1}{\sqrt{N^\alpha N^\beta}} f_0, \quad \bar{f}_1 = \frac{1}{\sqrt{N^\alpha N^\beta}} \bar{f}_0. \quad (6.16)$$

Their Poisson-brackets are,

$$\{e_1, f_1\} = 4i \left(1 - \frac{e_1}{4N} \right) f_1, \quad (6.17)$$

$$\{e_1, \bar{f}_1\} = -4i \left(1 - \frac{e_1}{4N} \right) \bar{f}_1, \quad (6.18)$$

$$\{f_1, \bar{f}_1\} = -4i \left(2e_1 - \frac{f_1 \bar{f}_1}{2N} \right). \quad (6.19)$$

These operators form a closed algebra with quadratic terms.

6.3 Dynamics for H_{LQG}

In what follows, we will calculate the dynamics of various truncated 2-vertex models using the Hamiltonian H_{LQG} from equation 6.4 (since we are only going to consider one Hamiltonian, we will call it H). The time evolution of the spinor i living at the vertex v will be calculated via the equations of motion provided by the Hamiltonian mechanics,

$$|\dot{z}_i^v\rangle = \{ |z_i^v\rangle, H \}. \quad (6.20)$$

After lengthy but straightforward computation, we obtain the following equation for a spinor $|\dot{z}_i^\alpha\rangle$ living at the vertex⁴ α ,

$$|\dot{z}_i^\alpha\rangle = \sum_l -i\lambda E_{il}^\beta |z_l^\alpha\rangle + 2i\bar{\gamma} \bar{F}_{il}^\beta |z_l^\alpha\rangle. \quad (6.21)$$

Now, using this equation, we will compute the dynamics of different models.

6.3.1 2 Edges

One of the simplest non-trivial models we can consider is a bivalent 2-vertex model, i.e. a pair of vertices linked by two edges. Each edge will have two spinors, one belonging to the vertex α and the other one corresponding to β .

This first model is,

⁴The corresponding equation for $|\dot{z}_i^\beta\rangle$ can be obtained directly from the change $\alpha \leftrightarrow \beta$.

$$\begin{aligned} |z_1\rangle &= |z\rangle, & |\omega_1\rangle &= |\omega\rangle, \\ |z_2\rangle &= e^{i\theta}|z\rangle, & |\omega_2\rangle &= e^{i\varphi}|\omega\rangle, \end{aligned}$$

where $|z\rangle$ is defined in expression 5.1. Both spinors ($|z\rangle, |\omega\rangle$) and phases (θ, φ) will be time-dependent. These relations will automatically satisfy the closure constraint from equations 5.15 and 5.16. Using equation 6.21, we obtain the following differential equations for the spinors,

$$|\dot{z}\rangle = -i E^\beta (\lambda + 2 \bar{\gamma} e^{-i(\theta+\varphi)}) |z\rangle, \quad (6.22)$$

$$|\dot{\omega}\rangle = -i E^\alpha (\lambda + 2 \bar{\gamma} e^{-i(\theta+\varphi)}) |\omega\rangle, \quad (6.23)$$

with $E^\alpha = \langle z|z\rangle$ and $E^\beta = \langle \omega|\omega\rangle$. For the phases, we have,

$$\dot{\theta} = -2 E^\beta [\lambda + \gamma e^{i(\theta+\varphi)} + \bar{\gamma} e^{-i(\theta+\varphi)}], \quad (6.24)$$

$$\dot{\varphi} = -2 E^\alpha [\lambda + \gamma e^{i(\theta+\varphi)} + \bar{\gamma} e^{-i(\theta+\varphi)}]. \quad (6.25)$$

On the other hand, the equations of motion for the E^α and E^β read:

$$\dot{E}^\alpha = 2i E^\alpha E^\beta [\gamma e^{i(\theta+\varphi)} - \bar{\gamma} e^{-i(\theta+\varphi)}], \quad (6.26)$$

$$\dot{E}^\beta = 2i E^\alpha E^\beta [\gamma e^{i(\theta+\varphi)} - \bar{\gamma} e^{-i(\theta+\varphi)}]. \quad (6.27)$$

As we can see, $\dot{E}^\alpha = \dot{E}^\beta$, and from the matching constraint, $E^\alpha = E^\beta$. Now, we define $\Theta = \theta + \varphi$:

$$\dot{\Theta} = -4E^\alpha (\lambda + \gamma e^{i\Theta} + \bar{\gamma} e^{-i\Theta}), \quad (6.28)$$

$$\dot{E}^\alpha = 2i E^{\alpha 2} (\gamma e^{i\Theta} - \bar{\gamma} e^{-i\Theta}). \quad (6.29)$$

Substituting the values of $E_{kl}, F_{kl}, \bar{F}_{kl}$ into equation 6.4, we can express the Hamiltonian as:

$$H = 2E^{\alpha 2} (\lambda + \gamma e^{i\Theta} + \bar{\gamma} e^{-i\Theta}). \quad (6.30)$$

Comparing this with equation 6.28, we see that:

$$\dot{\Theta} = -\frac{2H}{E^\alpha}. \quad (6.31)$$

Finally, manipulating equations 6.28 and 6.29, we obtain two independent expressions:

$$\frac{2}{E^{\alpha 3}} \dot{E}^{\alpha 2} - \frac{1}{E^{\alpha 2}} \ddot{E}^\alpha = -\frac{4H}{E^\alpha} \left(\frac{H}{2E^{\alpha 2}} - \lambda \right), \quad (6.32)$$

$$\ddot{\Theta} = 4iH (\gamma e^{i\Theta} - \bar{\gamma} e^{-i\Theta}). \quad (6.33)$$

In equations 6.28 and 6.29, we had two first-order differential equations, so we only needed a single initial value to specify the evolution of each variable. However, we

now have two second-order differential equations (6.32, 6.33), so we need to specify the initial value of the variables and their first derivatives. This arises from the differentiation processes we carried out to separate the coupled first-order differential equations. To fix this, we simply need to consider that the initial values of $\dot{\Theta}$ and \dot{E}^α must satisfy the first-order differential equations.

In particular, it is direct to calculate the special case of $H = 0$ analitically. In this case, we get that Θ must remain constant, $\dot{\Theta} = 0$, and for E^α we have:

$$E^\alpha(t) = \frac{1}{4t \operatorname{Im}(\gamma e^{i\Theta}) + 1/E^\alpha(0)}. \quad (6.34)$$

Apart from the initial values of the spinors and the phases, we have 3 additional free parameters; H , γ and λ . Nevertheless, these are not independent of each other since we can clear up λ from equation 6.4,

$$\lambda = \frac{H - \gamma f_0 - \bar{\gamma} \bar{f}_0}{e_0}. \quad (6.35)$$

In what follows, we will study the evolution of the spinors for different values of H and γ (λ will then be fixed by equation 6.35).

To avoid redundant arguments, we will restrict our analysis to the vertex α . All the explanations given will also apply to the vertex β . Let us then illustrate⁵ the evolution of the spinor $|z\rangle$ and (double) area E^α for different values of (H, γ) , and different initial values, which will be chosen conveniently to provide a general overview of the evolution.

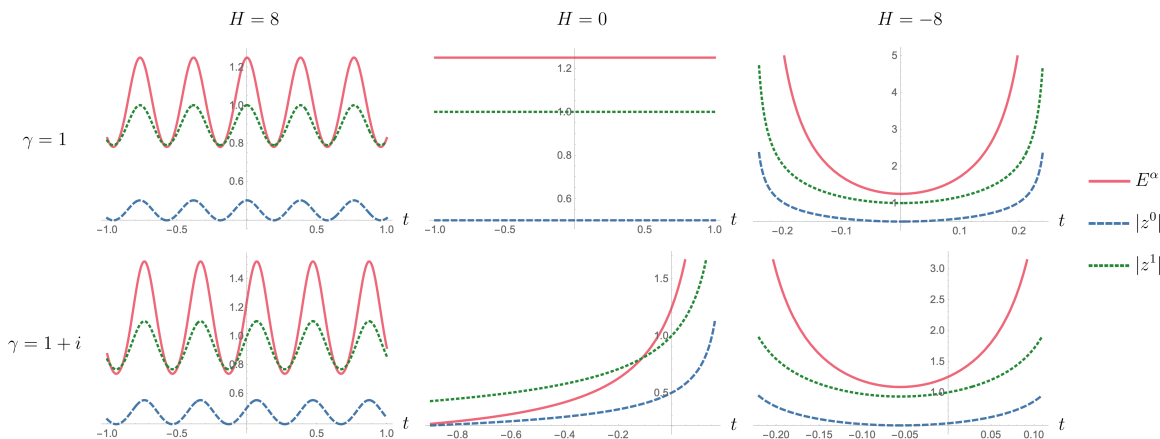


Figure 6.2. Evolution of $|z^0|$, $|z^1|$, and E^α with initial values $(z^0, z^1) = (0.5, 1)$, $(\omega^0, \omega^1) = (0.5, 1)$, $(\theta, \varphi) = (\pi/2, \pi/2)$.

From figure 6.2, we can appreciate three different behaviors; oscillatory (where the area decreases and increases periodically), divergent (where the area reaches a minimum value and then increases rapidly), and constant. These regimes depend strongly on the coupling constants and the initial values of the spinors and phases. To fully understand the relationship between this broad parameter spectrum and the different regimes, we would need to

⁵All the numerical results carried out in this project will be solved using [Wolfram Mathematica](#).

solve equation 6.33 and study the effect of each parameter on the evolution. Nevertheless, we have resorted to numerical procedures to provide an approximate description of the regimes.

To look for a relationship between the parameter spectrum and the different regimes, we have calculated a large number of plots (~ 80.000) and looked for different patterns in them. Systematically, we have changed the initial values of the spinors and phases, and we have chosen different values of the coupling constants λ , and γ , trying to span as many scenarios as possible. We have crossed real positive and real negative values, as well as imaginary numbers with positive and negative components. In our analysis, we have obtained the following results for the areas (that were satisfied in all of our cases):

Result 1. If $\lambda^2 > 4|\gamma|^2$, the evolution oscillates.

Result 2. If $\lambda^2 < 4|\gamma|^2$, the evolution diverges.

Result 3. If $\lambda^2 = 4|\gamma|^2$, we see three different behaviors. If $\gamma \in \mathbb{R} > 0$ with $\theta = \varphi = 0$, $\gamma = 0$, or $\gamma \in \mathbb{R} < 0$ with $\theta = \varphi = \pi/2$, the evolution will be constant. For the remaining values of γ , we have obtained a divergent regime.

Remarkably, these three main regimes were also found in [39] for the evolution of the quantum Hamiltonian, and for the classical reduced sector in [38], where mathematical analogies with cosmological models were explored.

Alternatively, we have also studied the dependence of the regimes on the Hamiltonian; we choose the value of H and using equation 6.35, we fix λ . In this case, we have also combined real and imaginary initial values, with positive and negative components. With this procedure, looking for a relationship between the parameters and the regimes is more complicated; however, we have still found interesting results.

Result 4. The number of oscillations depends on the value of $|H|$; for high values of $|H|$, the oscillatory regimes oscillate more.

Result 5. When we decrease the energy, oscillations tend to relax. In some cases, if we have a set of initial values with an oscillatory behavior and we lower the value of H , the oscillatory regime may evolve to a divergent regime. Nevertheless, the opposite has not been observed; we have not found a divergent regime that moved to an oscillatory one when we lowered the value of H (still maintaining the sign). Therefore, it appears that we can stimulate oscillations by increasing the absolute energy of the system.

Result 6. For $H = 0$, we have not found any oscillatory regime. In fact, since we have solved this case analitically in equation 6.34, we can see that it will always diverge, except for $\text{Im}(\gamma e^{i\Theta}) = 0$, where it will remain constant.

Result 7. We have studied these behaviors by first imposing $|z\rangle = |\omega\rangle$ and then $|z\rangle = 2|\omega\rangle$. In both cases, we have obtained the same regimes and behaviors (although not the same plots, since the former satisfies the matching constraint whereas the latter does

not).

As an example, in what follows we will focus on a single set of initial values and coupling constants:

$$\begin{aligned} z^0 &= 0.5, & z^1 &= \frac{1+i}{\sqrt{2}}, & \theta &= \frac{\pi}{2}, \\ \omega^0 &= 0.2i, & \omega^1 &= -1.1, & \varphi &= \frac{\pi}{3}. \end{aligned} \quad (6.36)$$

with $H = 1$ and $\gamma = 1$. From equation 6.35, we get that $\lambda \approx 2.05$, so $\lambda^2 > 4|\gamma|^2$ and thus, we would expect it to oscillate. To see this, we are going to plot the evolution of our variables. As we can see from figure 6.3, the spinors oscillate (as we expected), and the phase decreases while making small oscillations.

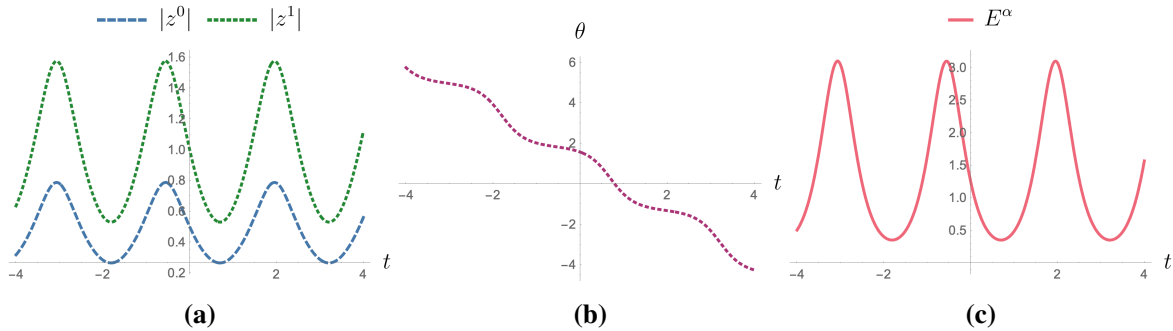
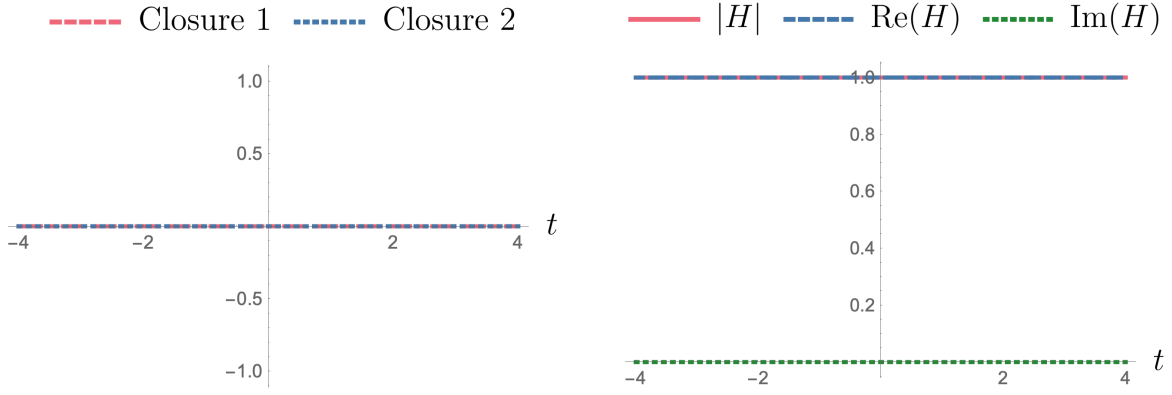


Figure 6.3. Time evolution of (a) the spinor components, (b) the phase and (c) E^α , providing twice the area of $|z_1\rangle$, which will be the total area carried by the vertex α since we only have two edges.

When pursuing any mathematical development, it is interesting to have some consistency checks to ensure that our calculations are following a correct path. In the present case, since the closure constraint Poisson-commutes with the Hamiltonian (equation 6.7), we can check that it will not evolve in time. Furthermore, since the Hamiltonian is a constant of motion, this should also remain constant (figure 6.4). We have employed these checks in all of our calculations to avoid erroneous results.



(a) Evolution of the closure constraint from equation 5.15 (Closure 1) and equation 5.16 (Closure 2).

(b) Evolution of the Hamiltonian. Since it is an observable of the theory, its value has to be real.

Figure 6.4. Consistency checks. Both the closure constraint and the Hamiltonian must be preserved in time.

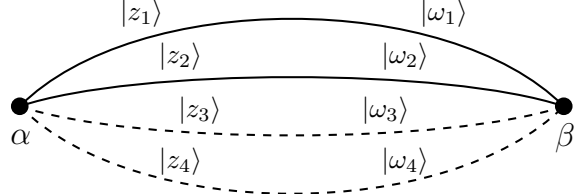
6.3.2 4 Edges

As we have said in chapter 4, the most elementary geometry into which space can be discretized is a tetrahedron (4-valent vertex). Therefore, we have proposed a couple of models with 4 edges linking both vertices.

6.3.2.1 Generalization of the Bivalent Model

Let us first introduce the following set of spinors,

$$\begin{aligned} |z_1\rangle &= |z\rangle, & |\omega_1\rangle &= |z\rangle, \\ |z_2\rangle &= e^{i\theta_2}|z\rangle, & |\omega_2\rangle &= e^{i\varphi_2}|z\rangle, \\ |z_3\rangle &= |\varepsilon\rangle, & |\omega_3\rangle &= |\varepsilon\rangle, \\ |z_4\rangle &= e^{i\theta_4}|\varepsilon\rangle, & |\omega_4\rangle &= e^{i\varphi_4}|\varepsilon\rangle, \end{aligned}$$



which automatically satisfy the closure constraint in α and β .

Solving carefully equation 6.21, we obtain the following differential equations describing the evolution of the spinors:

$$\begin{aligned} |\dot{z}\rangle &= -i\lambda \left[E_z |z\rangle + (\bar{z}^0 \varepsilon^0 + \bar{z}^1 \varepsilon^1) |\varepsilon\rangle + (\bar{z}^1 \bar{\varepsilon}^0 - \bar{z}^0 \bar{\varepsilon}^1) e^{i(\theta_4 + \varphi_4)} |\varepsilon\rangle \right] \\ &\quad - 2i\bar{\gamma} \left[E_z e^{-i(\bar{\theta}_2 + \bar{\varphi}_2)} |z\rangle + (\bar{z}^1 \bar{\varepsilon}^0 - \bar{z}^0 \bar{\varepsilon}^1) |\varepsilon\rangle + (\bar{z}^1 \varepsilon^1 + \bar{z}^0 \varepsilon^0) e^{-i(\bar{\theta}_4 + \bar{\varphi}_4)} |\varepsilon\rangle \right], \end{aligned} \quad (6.37)$$

$$\begin{aligned} |\dot{\varepsilon}\rangle &= -i\lambda \left[E_\varepsilon |\varepsilon\rangle + (\bar{\varepsilon}^0 z^0 + \bar{\varepsilon}^1 z^1) |z\rangle + (\bar{\varepsilon}^1 \bar{z}^0 - \bar{\varepsilon}^0 \bar{z}^1) e^{i(\theta_2 + \varphi_2)} |z\rangle \right] \\ &\quad - 2i\bar{\gamma} \left[E_\varepsilon e^{-i(\bar{\theta}_4 + \bar{\varphi}_4)} |\varepsilon\rangle + (\bar{\varepsilon}^1 \bar{z}^0 - \bar{\varepsilon}^0 \bar{z}^1) |z\rangle + (\bar{\varepsilon}^1 z^1 + \bar{\varepsilon}^0 z^0) e^{-i(\bar{\theta}_2 + \bar{\varphi}_2)} |z\rangle \right], \end{aligned} \quad (6.38)$$

and the following equations for the phases:

$$\dot{\theta}_2 = -\frac{\lambda}{\bar{z}^1} \left[E_z \bar{z}^1 (1 + e^{i(\varphi_2 - \bar{\varphi}_2)}) \right]$$

$$\begin{aligned}
& + z^0 \left(\bar{\varepsilon}^0 \bar{\varepsilon}^1 (1 + e^{-i(\bar{\varphi}_2 - \varphi_4)} e^{i(\theta_4 - \theta_2)}) - \varepsilon^1 \varepsilon^0 (e^{-i(\bar{\varphi}_4 + \bar{\theta}_4)} + e^{-i(\bar{\varphi}_2 + \theta_2)}) \right) \\
& + z^1 \left(\bar{\varepsilon}^1 \bar{\varepsilon}^1 (1 + e^{-i(\bar{\varphi}_2 - \varphi_4)} e^{i(\theta_4 - \theta_2)}) + \varepsilon^0 \varepsilon^0 (e^{-i(\bar{\theta}_4 + \bar{\varphi}_4)} + e^{-i(\bar{\varphi}_2 + \theta_2)}) \right) \quad (6.39) \\
& - \frac{2\gamma}{\bar{z}^1} \left[E_z \bar{z}^1 e^{i(\varphi_2 + \theta_2)} + z^0 (\bar{\varepsilon}^0 \bar{\varepsilon}^1 e^{i(\varphi_4 + \theta_4)} - \varepsilon^0 \varepsilon^1) + z^1 (\varepsilon^0 \varepsilon^0 + \bar{\varepsilon}^1 \bar{\varepsilon}^1 e^{i(\theta_4 + \varphi_4)}) \right] \\
& - \frac{2\bar{\gamma}}{\bar{z}^1} \left[E_z \bar{z}^1 + z^0 (\bar{\varepsilon}^0 \bar{\varepsilon}^1 - \varepsilon^1 \varepsilon^0 e^{-i(\bar{\theta}_4 + \bar{\varphi}_4)}) + z^1 (\bar{\varepsilon}^1 \bar{\varepsilon}^1 + \varepsilon^0 \varepsilon^0 e^{-i(\bar{\theta}_4 + \bar{\varphi}_4)}) \right] e^{-i(\bar{\varphi}_2 + \theta_2)},
\end{aligned}$$

$$\begin{aligned}
\dot{\theta}_4 = & -\frac{\lambda}{\bar{\varepsilon}^1} \left[E_\varepsilon \bar{\varepsilon}^1 (1 + e^{i(\varphi_4 - \bar{\varphi}_4)}) \right. \\
& + \varepsilon^0 \left(\bar{z}^0 \bar{z}^1 (1 + e^{-i(\bar{\varphi}_4 - \varphi_2)} e^{i(\theta_2 - \theta_4)}) - z^1 z^0 (e^{-i(\bar{\varphi}_2 + \bar{\theta}_2)} + e^{-i(\bar{\varphi}_4 + \theta_4)}) \right) \\
& \left. + \varepsilon^1 \left(\bar{z}^1 \bar{z}^1 (1 + e^{-i(\bar{\varphi}_4 - \varphi_2)} e^{i(\theta_2 - \theta_4)}) + z^0 z^0 (e^{-i(\bar{\theta}_2 + \bar{\varphi}_2)} + e^{-i(\bar{\varphi}_4 + \theta_4)}) \right) \right] \quad (6.40) \\
& - \frac{2\gamma}{\bar{\varepsilon}^1} \left[E_\varepsilon \bar{\varepsilon}^1 e^{i(\varphi_4 + \theta_4)} + \varepsilon^0 (\bar{z}^0 \bar{z}^1 e^{i(\varphi_2 + \theta_2)} - z^0 z^1) + \varepsilon^1 (z^0 z^0 + \bar{z}^1 \bar{z}^1 e^{i(\theta_2 + \varphi_2)}) \right] \\
& - \frac{2\bar{\gamma}}{\bar{\varepsilon}^1} \left[E_\varepsilon \bar{\varepsilon}^1 + \varepsilon^0 (\bar{z}^0 \bar{z}^1 - z^1 z^0 e^{-i(\bar{\theta}_2 + \bar{\varphi}_2)}) + \varepsilon^1 (\bar{z}^1 \bar{z}^1 + z^0 z^0 e^{-i(\bar{\theta}_2 + \bar{\varphi}_2)}) \right] e^{-i(\bar{\varphi}_4 + \theta_4)},
\end{aligned}$$

$$\begin{aligned}
\dot{\varphi}_2 = & -\frac{\lambda}{\bar{z}^1} \left[E_z \bar{z}^1 (1 + e^{i(\theta_2 - \bar{\theta}_2)}) \right. \\
& + z^0 (\bar{\varepsilon}^0 \bar{\varepsilon}^1 (1 + e^{-i(\bar{\theta}_2 - \theta_4)} e^{i(\varphi_4 - \varphi_2)}) - \varepsilon^1 \varepsilon^0 (e^{-i(\bar{\theta}_4 + \bar{\varphi}_4)} + e^{-i(\bar{\theta}_2 + \varphi_2)})) \\
& \left. + z^1 (\bar{\varepsilon}^1 \bar{\varepsilon}^1 (1 + e^{-i(\bar{\theta}_2 - \theta_4)} e^{i(\varphi_4 - \varphi_2)}) + \varepsilon^0 \varepsilon^0 (e^{-i(\bar{\varphi}_4 + \bar{\theta}_4)} + e^{-i(\bar{\theta}_2 + \varphi_2)})) \right] \quad (6.41) \\
& - \frac{2\gamma}{\bar{z}^1} \left[E_z \bar{z}^1 e^{i(\theta_2 + \varphi_2)} + z^0 (\bar{\varepsilon}^0 \bar{\varepsilon}^1 e^{i(\theta_4 + \varphi_4)} - \varepsilon^0 \varepsilon^1) + z^1 (\varepsilon^0 \varepsilon^0 + \bar{\varepsilon}^1 \bar{\varepsilon}^1 e^{i(\varphi_4 + \theta_4)}) \right] \\
& - \frac{2\bar{\gamma}}{\bar{z}^1} \left[E_z \bar{z}^1 + z^0 (\bar{\varepsilon}^0 \bar{\varepsilon}^1 - \varepsilon^1 \varepsilon^0 e^{-i(\bar{\varphi}_4 + \bar{\theta}_4)}) + z^1 (\bar{\varepsilon}^1 \bar{\varepsilon}^1 + \varepsilon^0 \varepsilon^0 e^{-i(\bar{\varphi}_4 + \bar{\theta}_4)}) \right] e^{-i(\bar{\theta}_2 + \varphi_2)},
\end{aligned}$$

$$\begin{aligned}
\dot{\varphi}_4 = & -\frac{\lambda}{\bar{\varepsilon}^1} \left[E_\varepsilon \bar{\varepsilon}^1 (1 + e^{i(\theta_4 - \bar{\theta}_4)}) \right. \\
& + \varepsilon^0 (\bar{z}^0 \bar{z}^1 (1 + e^{-i(\bar{\theta}_4 - \theta_2)} e^{i(\varphi_2 - \varphi_4)}) - z^1 z^0 (e^{-i(\bar{\theta}_2 + \bar{\varphi}_2)} + e^{-i(\bar{\theta}_4 + \varphi_4)})) \\
& \left. + \varepsilon^1 (\bar{z}^1 \bar{z}^1 (1 + e^{-i(\bar{\theta}_4 - \theta_2)} e^{i(\varphi_2 - \varphi_4)}) + z^0 z^0 (e^{-i(\bar{\varphi}_2 + \bar{\theta}_2)} + e^{-i(\bar{\theta}_4 + \varphi_4)})) \right] \quad (6.42) \\
& - \frac{2\gamma}{\bar{\varepsilon}^1} \left[E_\varepsilon \bar{\varepsilon}^1 e^{i(\theta_4 + \varphi_4)} + \varepsilon^0 (\bar{z}^0 \bar{z}^1 e^{i(\theta_2 + \varphi_2)} - z^0 z^1) + \varepsilon^1 (z^0 z^0 + \bar{z}^1 \bar{z}^1 e^{i(\varphi_2 + \theta_2)}) \right] \\
& - \frac{2\bar{\gamma}}{\bar{\varepsilon}^1} \left[E_\varepsilon \bar{\varepsilon}^1 + \varepsilon^0 (\bar{z}^0 \bar{z}^1 - z^1 z^0 e^{-i(\bar{\varphi}_2 + \bar{\theta}_2)}) + \varepsilon^1 (\bar{z}^1 \bar{z}^1 + z^0 z^0 e^{-i(\bar{\varphi}_2 + \bar{\theta}_2)}) \right] e^{-i(\bar{\theta}_4 + \varphi_4)}.
\end{aligned}$$

Although this is a set of 8 highly non-linear complex differential equations, they can be

solved numerically. While developing equation 6.21, we find a new constraint, \mathcal{K} :

$$\begin{aligned} \mathcal{K} = & -\lambda(-z^1\varepsilon^0 + z^0\varepsilon^1)(\varepsilon^0\bar{z}^0 + \varepsilon^1\bar{z}^1) \left(e^{-i(\bar{\varphi}_2+\theta_2)} + e^{-i(\bar{\varphi}_4+\bar{\theta}_4)} \right) \\ & + \lambda e^{-i(\bar{\varphi}_2+\theta_2)} e^{i(\varphi_4+\theta_4)} (z^1\bar{\varepsilon}^1 + z^0\bar{\varepsilon}^0) (\bar{\varepsilon}^1\bar{z}^0 - \bar{\varepsilon}^0\bar{z}^1) \\ & + \lambda(z^0\bar{\varepsilon}^0 + z^1\bar{\varepsilon}^1)(\bar{\varepsilon}^1\bar{z}^0 - \bar{\varepsilon}^0\bar{z}^1) \\ & + 2i(z^1\bar{\varepsilon}^1 + z^0\bar{\varepsilon}^0)(\bar{\varepsilon}^1\bar{z}^0 - \bar{\varepsilon}^0\bar{z}^1) (\bar{\gamma}e^{-i\bar{\varphi}_2} - \gamma e^{i(\varphi_4+\theta_4)}) \\ & + 2i(-\varepsilon^1z^0 + \varepsilon^0z^1)(\varepsilon^0\bar{z}^0 + \varepsilon^1\bar{z}^1) (\bar{\gamma}e^{-i\bar{\varphi}_2} e^{-i(\bar{\varphi}_4+\bar{\theta}_4)} - \gamma) = 0. \end{aligned} \quad (6.43)$$

This constraint arises due to the highly restrictive model we have constructed; we have linked our 4 edges by pairs ($|z_1\rangle$ with $|z_2\rangle$ and $|z_3\rangle$ with $|z_4\rangle$), where both vertices α and β have the same spinors up to a phase factor. Therefore, unless we ensure that our initial conditions satisfy equation 6.43, this system will not provide consistent results. Although we have not been capable of proving that \mathcal{K} will be preserved in time by checking whether $\{\mathcal{K}, H\} = 0$, we have seen that for all the initial values we have considered, this constraint was conserved in time. For instance, the equation 6.43 will be automatically satisfied if we take $(z^0, \varepsilon^0) = (z^1, \varepsilon^1)$, or either $|z\rangle \rightarrow 0$ or $|\varepsilon\rangle \rightarrow 0$. In our case, we will restrict to $(\theta_2, \theta_4) = (\varphi_2, \varphi_4) = 0$ and $|z\rangle, |\varepsilon\rangle \in \mathbb{R}$, which also satisfies the constraint \mathcal{K} .

Apart from the usual checks of figure 6.4, we can also take $|\varepsilon\rangle \rightarrow 0$ and see that we recover the results from figure 6.2 (see figure 6.5).

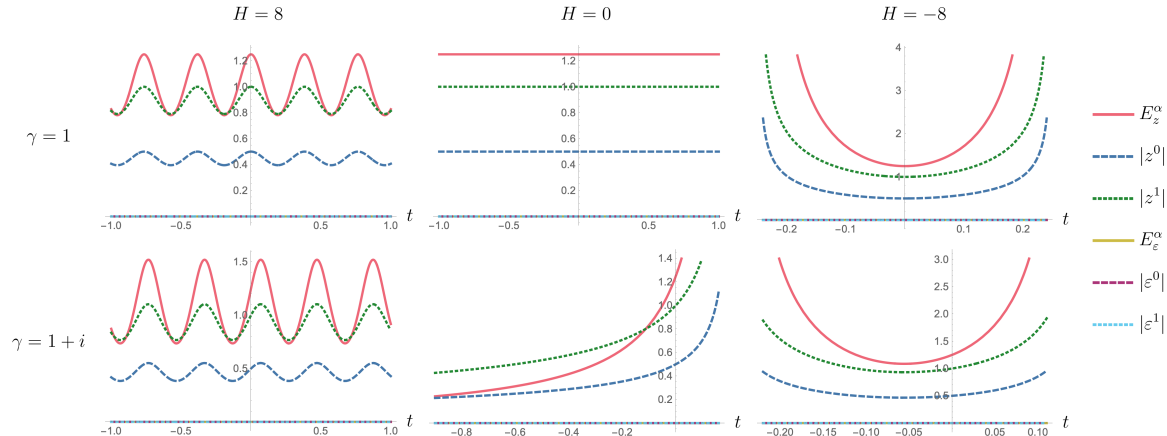


Figure 6.5. Time evolution of the spinor components and double areas with initial values $(z^0, z^1) = (0.5, 1)$, $(\varepsilon^0, \varepsilon^1) = (10^{-4}, 10^{-4})$, $(\theta_2, \theta_4) = (\pi/2, 0)$, $(\varphi_2, \varphi_4) = (\pi/2, 0)$. Since we are taking $|\varepsilon\rangle \ll 1$ this configuration will automatically satisfy the constraint \mathcal{K} .

As an example, let us take the following initial values:

$$\begin{aligned} z^0 &= 0.5, & z^1 &= 1, \\ \varepsilon^0 &= -0.7, & \varepsilon^1 &= 0.6. \end{aligned} \quad (6.44)$$

with $H = 10$, $\gamma = 0.5i$ and null phases. Now, we proceed to study the dynamics of the corresponding tetrahedron. In figure 6.6, we illustrate the evolution of the different variables associated with α . The initial values and coupling constants that we have chosen provide an oscillatory regime for the dynamics of the system.

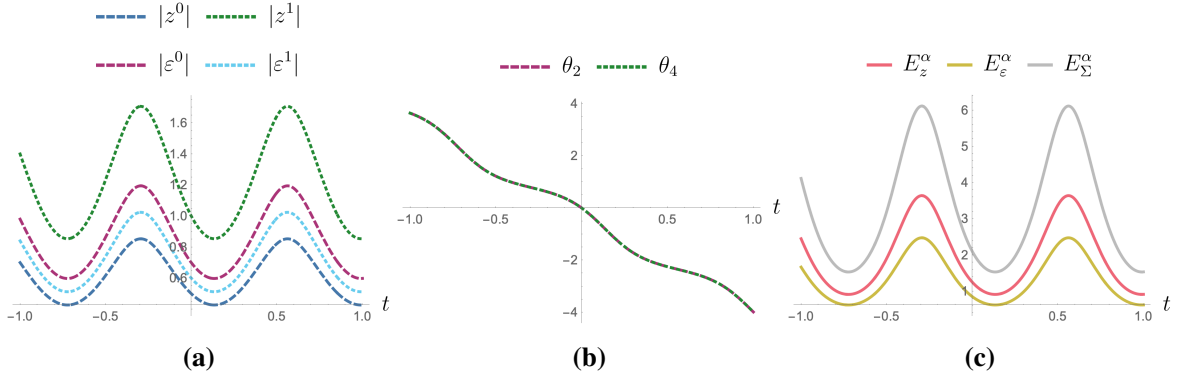


Figure 6.6. Time evolution of (a) the spinor components, (b) the phases and (c) twice the area carried by each spinor, where $E_\Sigma^\alpha = E_z^\alpha + E_\varepsilon^\alpha$.

In order to study the evolution of the tetrahedron, it is interesting to calculate the quadrupole of the area T^{ab} as studied in [95], which is a symmetric matrix that describes how the area is distributed along the polyhedron, giving us a notion of its deformation. Therefore, we will follow this idea and calculate T^{ab} using the following expression:

$$T^{ab} = \frac{1}{2} \sum_{i=1}^n \frac{\vec{N}_i^a \vec{N}_i^b}{|\vec{N}_i|}, \quad \text{Tr } T = \sum_i N_i = \mathcal{A}. \quad (6.45)$$

where n is the number of edges, \vec{N}_i is the normal vector to the face i and \mathcal{A} is the total area of the tetrahedron. Recalling the geometrical interpretation provided by the spinorial formalism, we can express these normal vectors in terms of the spinors as $\vec{N}_i = \langle z_i | \vec{\sigma} | z_i \rangle / 2$.

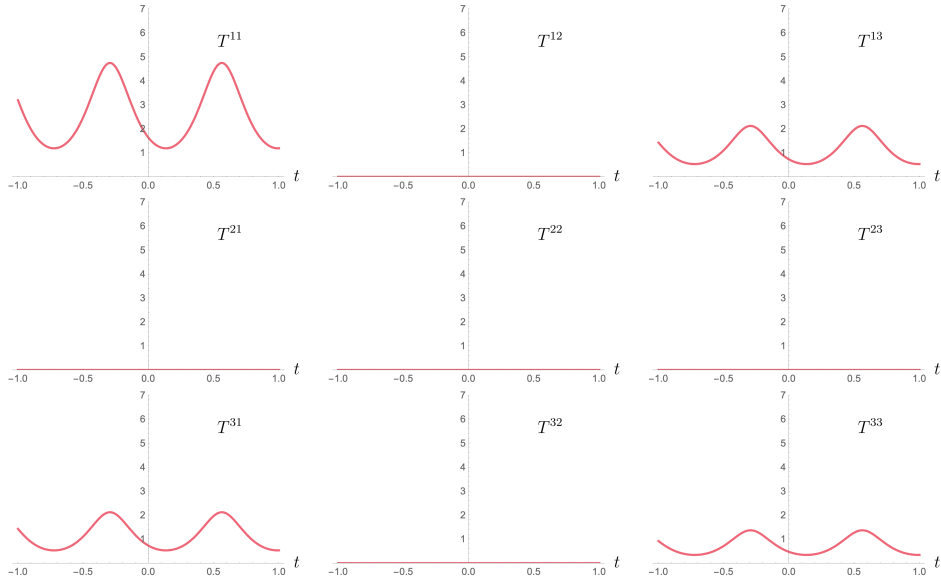


Figure 6.7. Time evolution of each component of the quadrupole T^{ab} from equation 6.45.

As we can see from figure 6.7, the distribution of the area will be highly unbalanced; all the area will be distributed in the directions x and z . To better appreciate it, we can

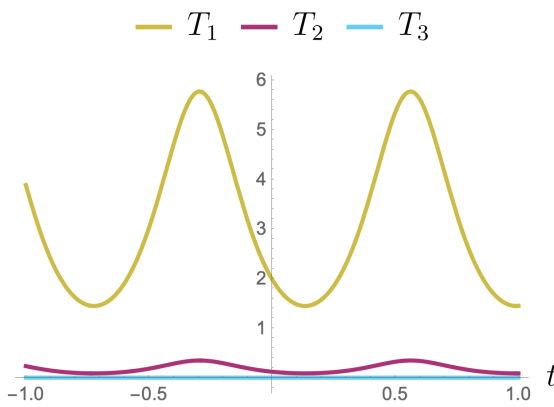


Figure 6.8. Evolution of the eigenvalues of T^{ab} . There will not be area in the y direction (the eigenvector of T_3) and most of the area will be distributed in one direction (the eigenvector of T_1).

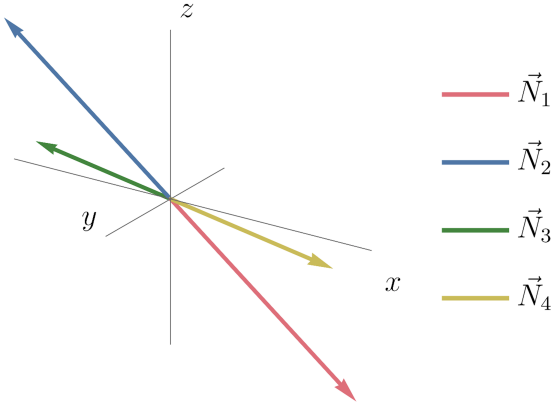


Figure 6.9. Normal vectors to the faces at $t = 0$. The evolution of the spinors will make these vectors increase and decrease (periodically), but their direction will remain unchanged, so they will always remain (anti-)parallel by pairs.

illustrate the evolution of the eigenvalues, which will provide a clearer notion of the deformation (figure 6.8).

In agreement with figure 6.6c, the area will oscillate periodically. Furthermore, it will oscillate consistently in both (eigen-)directions—the minimum values of the eigenvalue T_1 coincide with those of the eigenvalue T_2 . If we illustrate the normal vectors (figure 6.9), we see that \vec{N}_1 and \vec{N}_2 are pointing in the same direction, and so are \vec{N}_3 and \vec{N}_4 . Geometrically, this would correspond to a tetrahedron with parallel faces. To understand this, we can go one step further and calculate the volume V , [95]:

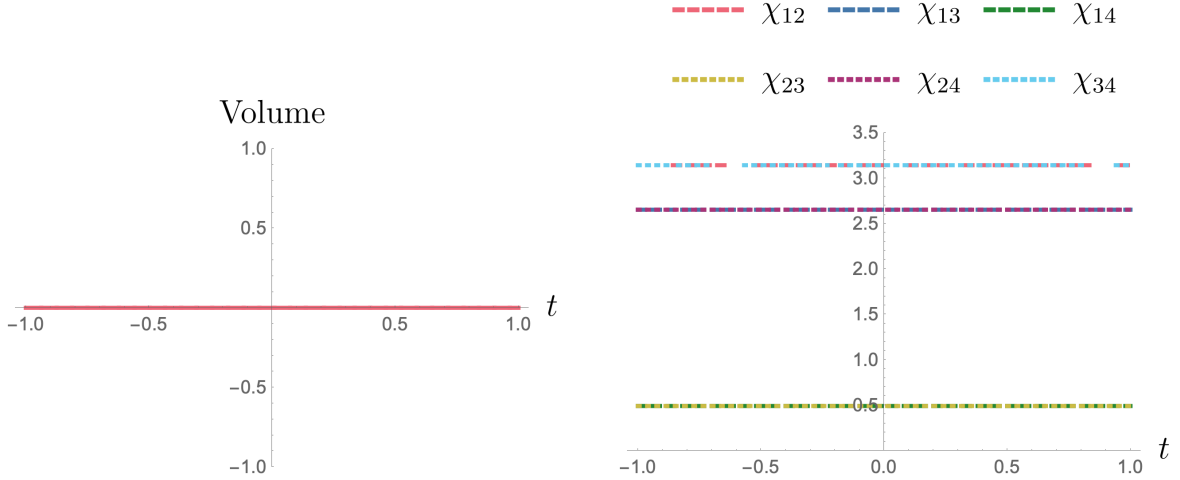
$$V^2 = \frac{2}{9} |\vec{N}_1 \cdot (\vec{N}_2 \wedge \vec{N}_3)|. \quad (6.46)$$

Moreover, the angle χ_{ij} between the faces of the tetrahedron labeled by the edges i and j will be given by,

$$\chi_{ij} = \arccos \left(\frac{N_{ij}^2 - N_i^2 - N_j^2}{2N_i N_j} \right), \quad (6.47)$$

where $\vec{N}_{ij} = \vec{N}_i + \vec{N}_j$. The volume V and the angles χ_{ij} are represented in figures 6.10 and 6.11, respectively. As we can see, the volume of our tetrahedron will be zero. Furthermore, since each $\hat{n}_i = \vec{N}_i/N_i$ is constant, their evolution will not change the direction of the normals, so the tetrahedron will always remain volumeless.

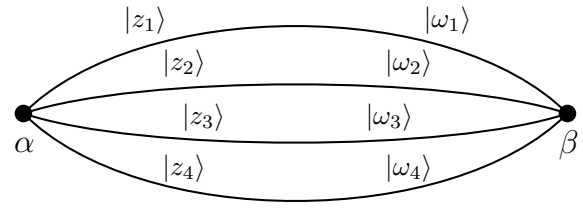
To study the behavior of the elementary ‘atoms’ of space, we will look for a tetrahedron with a non-vanishing volume. Therefore, we will introduce a new 4-edged graph.

**Figure 6.10.** Evolution of the volume.**Figure 6.11.** Evolution of the angles between the faces.

6.3.2.2 Non-Zero Volume Tetrahedron

This model will be defined as:

$$\begin{aligned} |z_1\rangle &= \begin{pmatrix} \alpha \\ \beta \end{pmatrix}, & |\omega_1\rangle &= \begin{pmatrix} \alpha \\ \beta \end{pmatrix}, \\ |z_2\rangle &= \begin{pmatrix} \alpha \\ -\beta \end{pmatrix}, & |\omega_2\rangle &= \begin{pmatrix} \alpha \\ -\beta \end{pmatrix}, \\ |z_3\rangle &= \begin{pmatrix} \xi \\ \delta e^{i\theta} \end{pmatrix}, & |\omega_3\rangle &= \begin{pmatrix} \xi \\ \delta e^{i\varphi} \end{pmatrix}, \\ |z_4\rangle &= \begin{pmatrix} \xi \\ -\delta e^{i\theta} \end{pmatrix}, & |\omega_4\rangle &= \begin{pmatrix} \xi \\ -\delta e^{i\varphi} \end{pmatrix}, \end{aligned}$$



where θ and φ are constants. Imposing the closure constraint we can determine the value of one parameter, say δ :

$$|\delta| = \sqrt{|\alpha|^2 + |\xi|^2 - |\beta|^2}. \quad (6.48)$$

The evolution of the spinors will be given by,

$$\dot{\alpha} = -2i\lambda\bar{\alpha}(\alpha^2 + \xi^2) - 4i\bar{\gamma}\bar{\alpha}(\bar{\beta}^2 + \bar{\delta}^2 e^{-i(\theta+\varphi)}), \quad (6.49)$$

$$\dot{\beta} = -2i\lambda\bar{\beta}(\beta^2 + \delta^2 e^{i(\theta+\varphi)}) - 4i\bar{\gamma}\bar{\beta}(\bar{\alpha}^2 + \bar{\xi}^2), \quad (6.50)$$

$$\dot{\xi} = -2i\lambda\bar{\xi}(\alpha^2 + \xi^2) - 4i\bar{\gamma}\bar{\xi}(\bar{\beta}^2 + \bar{\delta}^2 e^{-i(\theta+\varphi)}), \quad (6.51)$$

$$\dot{\delta} = -2i\lambda\bar{\delta}e^{-i(\varphi+\theta)}(\beta^2 + \delta^2 e^{i(\theta+\varphi)}) - 4i\bar{\gamma}\bar{\delta}e^{-i(\varphi+\theta)}(\bar{\alpha}^2 + \bar{\xi}^2). \quad (6.52)$$

As we can see, their evolution will not depend on the phases independently, but on

$\theta + \varphi$. Nevertheless, the spinors $|z_i\rangle$ do depend on the individual phases. Therefore, the quadrupole will change for different values of θ and φ , even if $\theta + \varphi$ is the same.

In the present case, we have also proceeded with a systematic strategy by calculating numerous plots (~ 15.000) and studying the evolution of the total area for different initial values and coupling constants, as done in the bivalent vertex model. Again, we have obtained the three regimes; oscillatory, divergent, and constant.

After computing several plots, we have found the following:

Result 1. If $|\lambda|^2 > 4|\gamma|^2$, the evolution oscillates, except for $\gamma = 0$, where it remains constant.

Result 2. If $|\lambda|^2 < 4|\gamma|^2$, the evolution diverges.

Result 3. If $|\lambda|^2 = 4|\gamma|^2$, the evolution will in general diverge. However, we have found some exceptions where it remained constant; for example, when $\lambda = 4$, $\gamma = -2$ and $\theta = \varphi = 0$.

Result 4. If we change $H \rightarrow -H$ and $\gamma \rightarrow -\gamma$, the evolution will be inverted $t \rightarrow -t$.

Result 5. We have not seen oscillatory regimes in $H = 0$.

Result 6. The evolution is invariant under changes in the sign of any variable; $z^m \rightarrow -z^m$ (even all of them), regardless if they are real or complex. We can directly check this from equations 6.49 - 6.52.

To study the dynamics, we choose, as an example, the following initial values:

$$\alpha = -0.314, \quad \beta = 0.122, \quad \xi = 0.62, \quad \theta = \pi, \quad \varphi = \frac{\pi}{3}, \quad (6.53)$$

with $H = 20$ and $\gamma = i$. The initial value of δ will be determined by equation 6.48. For these values, the spinors will oscillate “irregularly” (see figure 6.12); nevertheless, they will still be periodic. Even if the individual components of the spinors have an irregular behavior, $E_\Sigma = E_{\alpha\beta} + E_{\xi\delta}$ will be regular. We have seen this tendency in all the oscillatory regimes we have studied within this model.

As we already know, the quadrupole T^{ab} gives us an idea of how the area is distributed along the polyhedron. In this case, T^{ab} will not be very deformed (figure 6.13), in contrast to the previous model. Furthermore, from its eigenvalues (figure 6.14), we see that the distribution of the area will evolve irregularly along the three main directions. Nevertheless, the three directions carry a non-zero projection of the area, so we expect the volume to be non-zero.

Then, let us check whether this actually occurs. In figures 6.15 and 6.16, we have plotted the evolution of the volume and the angles between the faces, respectively. As we can see, both the volume and the angles will increase and decrease non-periodically. The volume will be determined by the modulus of the spinors and their relative direction; so it will vanish when one spinor is zero or two normal vectors point in the same direction.

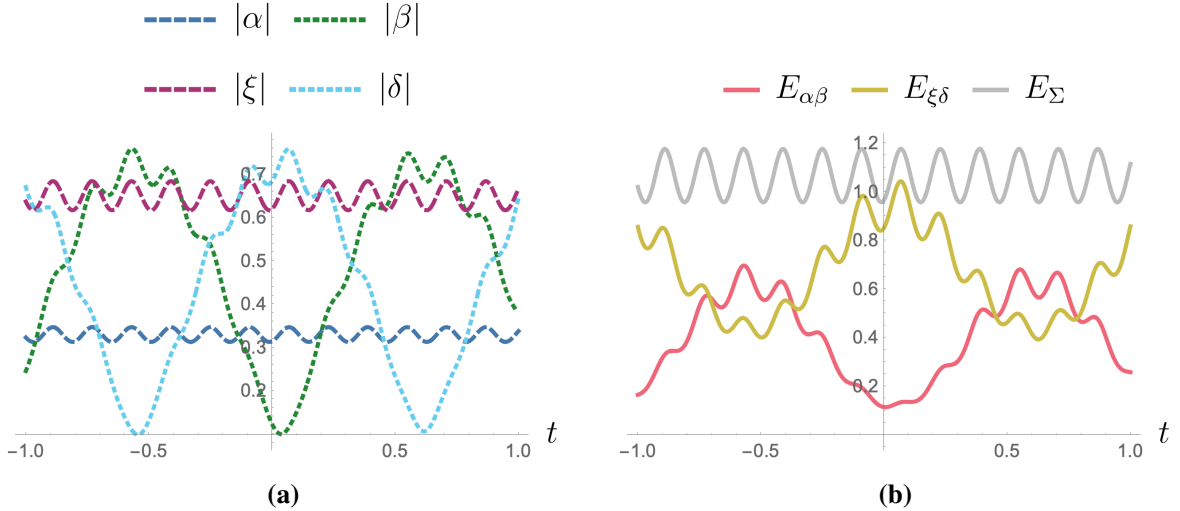


Figure 6.12. Evolution of (a) the spinor components and (b) twice their area. $E_{\alpha\beta}$ corresponds to the spinors $|z_1\rangle$ and $|z_2\rangle$, since they carry the same area. Equivalently, $E_{\xi\delta}$ correspond to $|z_3\rangle$ and $|z_4\rangle$.

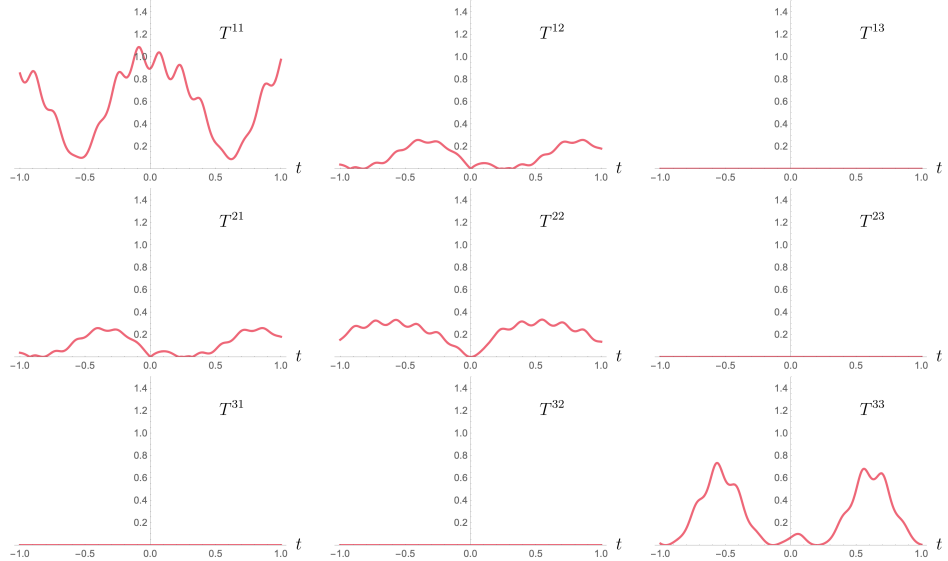


Figure 6.13. Time evolution of the quadrupole T^{ab} .

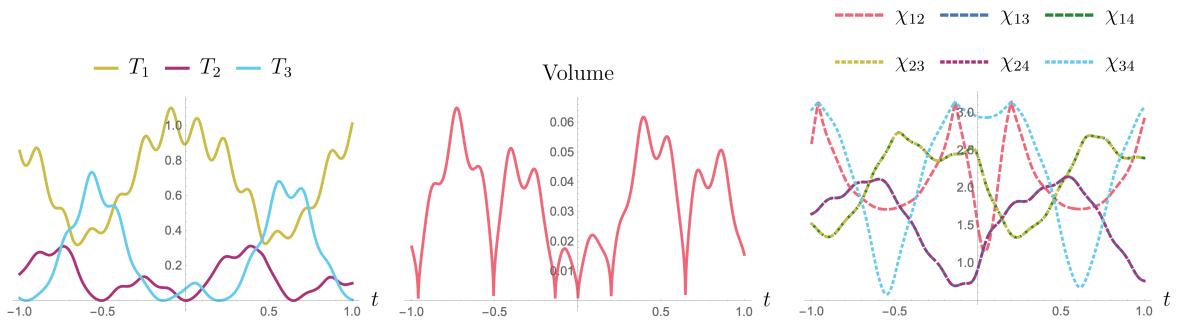


Figure 6.14. Evolution of the eigenvalues of T^{ab} .

Figure 6.15. Evolution of the volume.

Figure 6.16. Evolution of the angles between the faces.

In order to gain intuition about the evolution of the tetrahedron and to see how all these features merge (area, quadrupole, volume and angles between the faces), we will construct the tetrahedron from the normal vectors \vec{N} . First, we need to locate its vertices, which will be labeled by the normal vectors at the opposite face. To ease the notation, we call $\vec{N}_a \equiv \vec{N}_1$, $\vec{N}_b \equiv \vec{N}_2$, $\vec{N}_c \equiv \vec{N}_3$ and $\vec{N}_d \equiv \vec{N}_4$. Naming the vertices a , b , c and d , the normal \vec{N}_c will belong to the face opposed to the vertex c , as shown in figure 6.17.

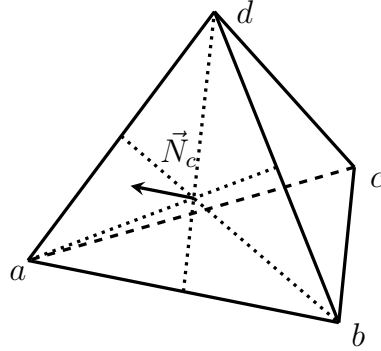


Figure 6.17. An example of a tetrahedron. The normal vector to the face opposed to c will be \vec{N}_c .

Now, the relationship between the edges of the tetrahedron and its normals will be given by [96]:

$$\vec{ad} = \sqrt{\frac{2}{U}} \vec{N}_b \times \vec{N}_c, \quad \vec{ab} = \sqrt{\frac{2}{U}} \vec{N}_c \times \vec{N}_d, \quad \vec{ac} = \sqrt{\frac{2}{U}} \vec{N}_d \times \vec{N}_b, \quad (6.54)$$

where $U = 9V^2/2$. This will uniquely characterize the tetrahedron. Therefore, if we fix the vertex a , the other vertices will be fixed by the relations 6.54. For visual clarity, we will locate the vertex a so that the centroid⁶ G of the tetrahedron is fixed at the origin $O = (0, 0, 0)$ at any time. The centroid is given by:

$$G = \frac{\vec{a} + \vec{b} + \vec{c} + \vec{d}}{4}. \quad (6.55)$$

If we solve for a and set $G = (0, 0, 0)$, we obtain the position of each vertex in terms of \vec{ad} , \vec{ab} and \vec{ac} :

$$\vec{d} = -\frac{1}{12}\vec{ab} - \frac{7}{12}\vec{ac} + \frac{10}{12}\vec{ad}, \quad (6.56)$$

$$\vec{c} = -\frac{3}{5}\vec{d} + \frac{1}{5}\vec{ab} + \frac{2}{5}\vec{ac}, \quad (6.57)$$

$$\vec{b} = \frac{1}{2}(-\vec{c} - \vec{d} + \vec{ab}), \quad (6.58)$$

$$\vec{a} = -\vec{b} - \vec{c} - \vec{d}. \quad (6.59)$$

Once we have the vertices, we can illustrate our model with 3-dimensional images. As we can see in figure 6.18, our tetrahedron will rotate, its faces will change their area and shape, and thus, the volume will also evolve.

⁶We can see the centroid of a 3-dimensional body as its geometric center; if the mass of the volume is distributed homogeneously, then the centroid will be the center of mass.

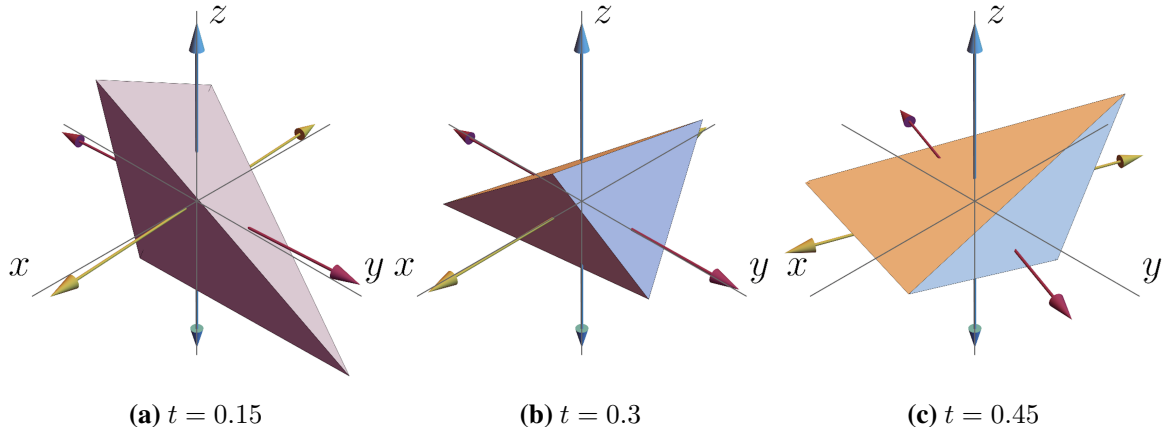


Figure 6.18. Images of the tetrahedron corresponding to three different time snaps. The yellow, purple and cyan arrows represent the normalized eigenvectors of T_1 , T_2 and T_3 , respectively.

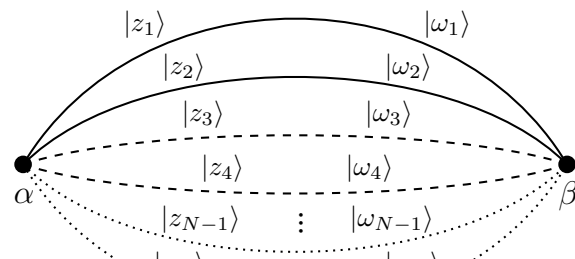
6.3.3 Arbitrary Number of Edges

In what follows, we will propose two generalized N-edged models that provide us with more freedom in choosing the number of variables.

6.3.3.1 2N Edges

Let us consider the following set of spinors satisfying the closure and matching constraints:

$$\begin{aligned} |z_1\rangle &= |\nu_1\rangle, & |\omega_1\rangle &= |\nu_1\rangle, \\ |z_2\rangle &= e^{i\theta_1}|\nu_1], & |\omega_2\rangle &= e^{i\varphi_1}|\nu_1], \\ |z_3\rangle &= |\nu_2\rangle, & |\omega_3\rangle &= |\nu_2\rangle, \\ |z_4\rangle &= e^{i\theta_2}|\nu_2], & |\omega_4\rangle &= e^{i\varphi_2}|\nu_2], \\ &\dots &&\dots \\ |z_{2N-1}\rangle &= |\nu_N\rangle, & |\omega_{2N-1}\rangle &= |\nu_N\rangle, \\ |z_{2N}\rangle &= e^{i\theta_N}|\nu_N], & |\omega_{2N}\rangle &= e^{i\varphi_N}|\nu_N]. \end{aligned}$$



The differential equations characterizing the evolution of the spinors are,

$$\dot{|\nu_k\rangle} = \sum_{n=1}^N \left\{ -i\lambda \left[(\bar{\nu}_k^0 \nu_n^0 + \bar{\nu}_k^1 \nu_n^1) |\nu_n\rangle + (\bar{\nu}_k^1 \bar{\nu}_n^0 - \bar{\nu}_k^0 \bar{\nu}_n^1) e^{i(\theta_n + \varphi_n)} |\nu_n\rangle \right] - 2i\bar{\gamma} \left[(\bar{\nu}_k^1 \bar{\nu}_n^0 - \bar{\nu}_k^0 \bar{\nu}_n^1) |\nu_n\rangle + (\bar{\nu}_k^1 \nu_n^1 + \bar{\nu}_k^0 \nu_n^0) e^{-i(\bar{\theta}_n + \bar{\varphi}_n)} |\nu_n\rangle \right] \right\}, \quad (6.60)$$

and for the phases we have,

$$\begin{aligned} \dot{\theta}_k &= \frac{1}{\bar{\nu}_k^1} \sum_{n=1}^N \left\{ (\nu_k^0 \nu_n^1 - \nu_k^1 \nu_n^0) \left[\lambda \left(e^{-i(\theta_k + \bar{\varphi}_k)} + e^{-i(\bar{\theta}_n + \bar{\varphi}_n)} \right) \right. \right. \\ &\quad \left. \left. + 2\bar{\gamma} e^{-i(\theta_k + \bar{\varphi}_k)} e^{-i(\bar{\theta}_n + \bar{\varphi}_n)} + 2\gamma \right] \nu_n^0 \right. \\ &\quad \left. - (\nu_k^1 \bar{\nu}_n^1 + \nu_k^0 \bar{\nu}_n^0) \left[\lambda \left(1 + e^{-i(\theta_k + \bar{\varphi}_k)} e^{i(\theta_n + \varphi_n)} \right) \right. \right. \\ &\quad \left. \left. + 2\bar{\gamma} e^{-i(\theta_k + \bar{\varphi}_k)} + 2\gamma e^{i(\theta_n + \varphi_n)} \right] \bar{\nu}_n^1 \right\}, \end{aligned} \quad (6.61)$$

$$\begin{aligned} \dot{\varphi}_k &= \frac{1}{\bar{\nu}_k^1} \sum_{n=1}^N \left\{ (\nu_k^0 \nu_n^1 - \nu_k^1 \nu_n^0) \left[\lambda \left(e^{-i(\varphi_k + \bar{\theta}_k)} + e^{-i(\bar{\varphi}_n + \bar{\theta}_n)} \right) \right. \right. \\ &\quad \left. \left. + 2\bar{\gamma} e^{-i(\varphi_k + \bar{\theta}_k)} e^{-i(\bar{\varphi}_n + \bar{\theta}_n)} + 2\gamma \right] \nu_n^0 \right. \\ &\quad \left. - (\nu_k^1 \bar{\nu}_n^1 + \nu_k^0 \bar{\nu}_n^0) \left[\lambda \left(1 + e^{-i(\varphi_k + \bar{\theta}_k)} e^{i(\varphi_n + \theta_n)} \right) \right. \right. \\ &\quad \left. \left. + 2\bar{\gamma} e^{-i(\varphi_k + \bar{\theta}_k)} + 2\gamma e^{i(\varphi_n + \theta_n)} \right] \bar{\nu}_n^1 \right\}. \end{aligned} \quad (6.62)$$

As with the first 4-edged model, we find a constraint from solving the equations of motion that arises to maintain the consistency of our model. This constraint \mathcal{K} now reads as,

$$\begin{aligned} \mathcal{K} &= \sum_{n=1}^N \left\{ \left(\frac{\nu_n^0}{\bar{\nu}_k^1} + \frac{\nu_n^1}{\bar{\nu}_k^0} \right) (\nu_k^0 \nu_n^1 - \nu_k^1 \nu_n^0) \left[\lambda \left(e^{-i(\theta_k + \bar{\varphi}_k)} + e^{-i(\bar{\theta}_n + \bar{\varphi}_n)} \right) \right. \right. \\ &\quad \left. \left. + 2\bar{\gamma} e^{-i(\theta_k + \bar{\varphi}_k)} e^{-i(\bar{\theta}_n + \bar{\varphi}_n)} + 2\gamma \right] \right. \\ &\quad \left. \left(\frac{\bar{\nu}_n^0}{\bar{\nu}_k^0} - \frac{\bar{\nu}_n^1}{\bar{\nu}_k^1} \right) (\nu_k^1 \bar{\nu}_n^1 + \nu_k^0 \bar{\nu}_n^0) \left[\lambda \left(1 + e^{-i(\theta_k + \bar{\varphi}_k)} e^{i(\theta_n + \varphi_n)} \right) \right. \right. \\ &\quad \left. \left. + 2\bar{\gamma} e^{-i(\theta_k + \bar{\varphi}_k)} + 2\gamma e^{i(\theta_n + \varphi_n)} \right] \right\} = 0. \end{aligned} \quad (6.63)$$

Again, we will restrict to null phases and real spinors, which obey equation 6.63. Now, we will study the dynamics for $N = 3$ pairs of edges (hexahedron). For instance, we take the following initial values,

$$\begin{aligned} \nu_1^0 &= 1.2, & \nu_2^0 &= -1.64, & \nu_3^0 &= 1.5, \\ \nu_1^1 &= -1.8, & \nu_2^1 &= 1.58, & \nu_3^1 &= -1.6, \end{aligned} \quad (6.64)$$

with $H = 10$, $\gamma = i$, and null phases. This initial configuration provides a divergent evolution of the spinors (see figure 6.19).

Again, the quadrupole will tell us that the distribution of area along the polyhedron will be highly unbalanced, as we can notice from the eigenvalues (figure 6.20). Illustrating the

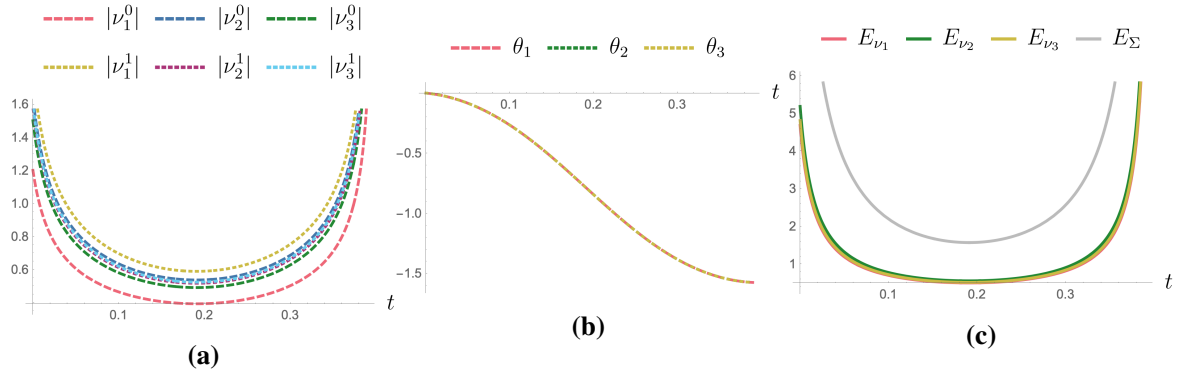


Figure 6.19. Evolution of (a) the spinors (b) the phases and (c) twice the area carried by each spinor.

normal vectors (figure 6.21), we see that this polyhedron will have null volume, as we expected, since this model can be seen as a generalization of the 4-valent one from section 6.3.2.1.

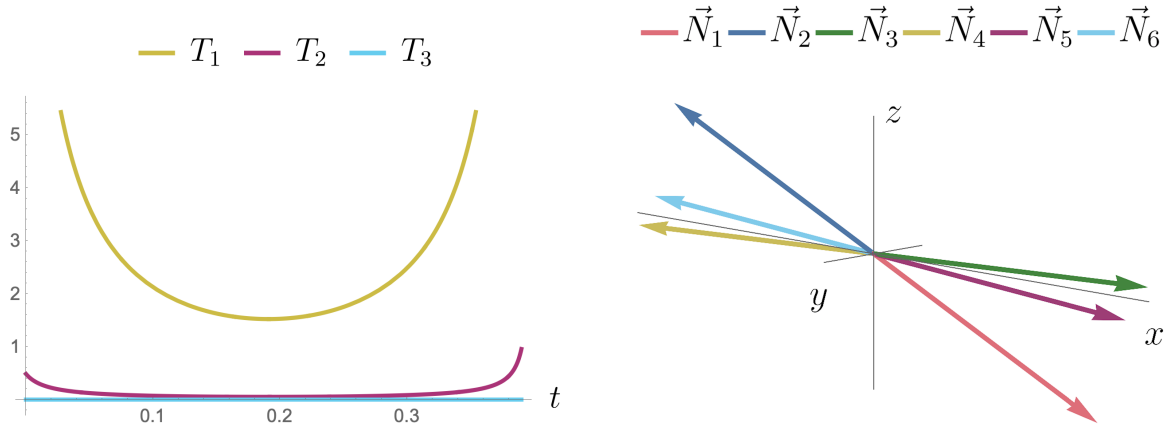


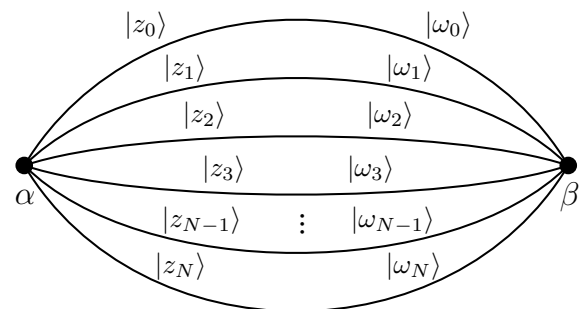
Figure 6.20. Evolution of the eigenvalues of T^{ab} .

Figure 6.21. Normal vectors to the faces at $t = 0$.

6.3.3.2 N+1 Edges

Finally, we have constructed a different N-edged model with the following configuration:

$$\begin{aligned} |z_0\rangle &= |z\rangle, & |\omega_0\rangle &= |\omega\rangle, \\ \dots & & \dots & \\ |z_j\rangle &= \frac{e^{i\theta_j}}{\sqrt{N}}|z\rangle, & |\omega_j\rangle &= \frac{e^{i\varphi_j}}{\sqrt{N}}|\omega\rangle, \end{aligned}$$



By simply looking at the configuration, we can infer that the spinor $|z_0\rangle$ will carry the

same area as the sum of the remaining N spinors.

The evolution of the spinor variables is:

$$|\dot{z}\rangle = -iE_{\omega_0}^\beta \left[\lambda + 2\bar{\gamma} \frac{1}{N} \sum_{j=1}^N e^{-i(\bar{\varphi}_j + \bar{\theta}_j)} \right] |z\rangle, \quad (6.65)$$

$$|\dot{\omega}\rangle = -iE_{z_0}^\alpha \left[\lambda + 2\bar{\gamma} \frac{1}{N} \sum_{j=1}^N e^{-i(\bar{\varphi}_j + \bar{\theta}_j)} \right] |\omega\rangle, \quad (6.66)$$

where $E_{z_i}^\alpha = \langle z_i | z_i \rangle$ and $E_{\omega_i}^\beta = \langle \omega_i | \omega_i \rangle$. The phases will evolve as:

$$\begin{aligned} \dot{\theta}_i &= \\ &- E_{\omega_0}^\beta \left[\lambda \left(1 + \frac{1}{N} \sum_{j=1}^N e^{-i(\bar{\varphi}_i - \bar{\varphi}_j)} e^{-i(\theta_i - \theta_j)} \right) + 2\bar{\gamma} e^{-i(\bar{\varphi}_i + \theta_i)} + \frac{2\gamma}{N} \sum_{j=1}^N e^{i(\varphi_j + \theta_j)} \right], \end{aligned} \quad (6.67)$$

$$\begin{aligned} \dot{\varphi}_i &= \\ &- E_{z_0}^\alpha \left[\lambda \left(1 + \frac{1}{N} \sum_{j=1}^N e^{-i(\bar{\theta}_i - \bar{\theta}_j)} e^{-i(\varphi_i - \varphi_j)} \right) + 2\bar{\gamma} e^{-i(\bar{\theta}_i + \varphi_i)} + \frac{2\gamma}{N} \sum_{j=1}^N e^{i(\theta_j + \varphi_j)} \right]. \end{aligned} \quad (6.68)$$

We choose, for instance, the following initial conditions:

$$\begin{aligned} z^0 &= -0.6, & z^1 &= 0.9i, & \omega^0 &= 0.9, & \omega^1 &= -0.6i, \\ \theta_1 &= \frac{\pi}{6}, & \theta_2 &= \frac{\pi}{5}, & \theta_3 &= \frac{\pi}{4}, & \theta_4 &= \frac{\pi}{3}, & \theta_5 &= \frac{\pi}{2}, & \theta_6 &= \pi, \\ \varphi_1 &= \frac{7\pi}{6}, & \varphi_2 &= \frac{4\pi}{3}, & \varphi_3 &= \frac{3\pi}{2}, & \varphi_4 &= \frac{5\pi}{3}, & \varphi_5 &= \frac{11\pi}{6}, & \varphi_6 &= 2\pi. \end{aligned} \quad (6.69)$$

with $H = 10$ and $\gamma = 1 + i$. Using these initial values, the evolution of the spinors will be oscillatory (see figure 6.22).

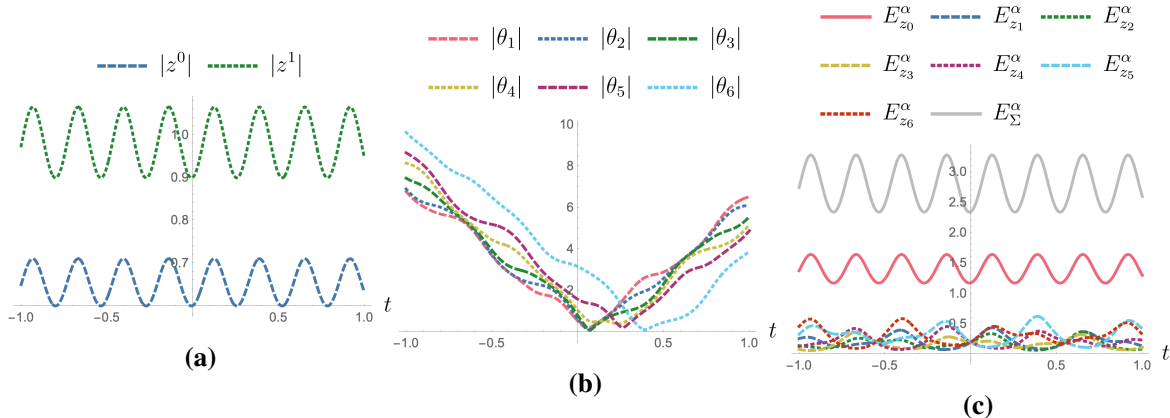


Figure 6.22. Evolution of (a) the spinor components, (b) the absolute value of the phases and (c) twice the areas, with $E_\Sigma^\alpha = \sum_{i=0}^N E_{z_i}^\alpha$. As we expected, the spinor $|z_0\rangle$ carries the same area as $|z_1\rangle + \dots + |z_N\rangle$.

From figure 6.23, we know that the area will also be centered in one direction. Moreover, from figure 6.24, we see that the normal vector corresponding to the spinor $|z_0\rangle$ will point

in one direction, whereas the rest of them will point in the opposite one, with a magnitude N times smaller than that of $|z_0\rangle$.

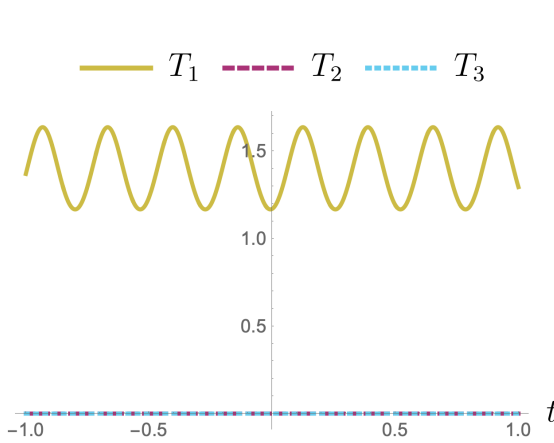


Figure 6.23. Evolution of the eigenvalues of T^{ab} .

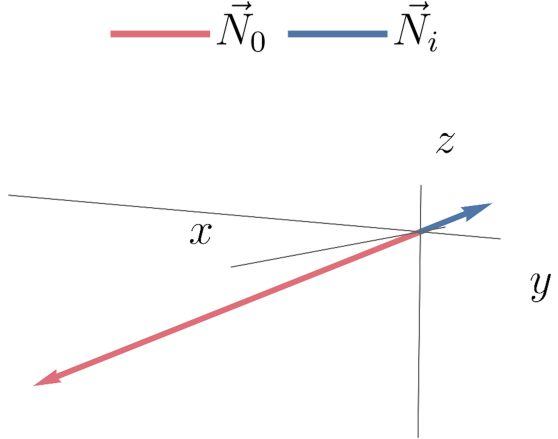


Figure 6.24. Normal vectors to the faces at $t = 0$.

6.4 Quantization

In this section we will propose a quantization for a 2-valent pair of vertices whose evolution is given by H_{LQG} . At each vertex, we attach a bivalent intertwiner state:

$$|j\rangle \equiv \frac{1}{\sqrt{2j+1}} \sum_{m=-j}^{+j} (-1)^{(j-m)} |j, m\rangle \otimes |j, -m\rangle, \quad (6.70)$$

which link the spins $|j, m\rangle$ and $|j, -m\rangle$ carried by both edges. These spins must be equal to ensure the $SU(2)$ invariance of the theory. Therefore, this intertwiner will be given by the Clebsch-Gordan coefficients with $J = 0$ and $M = 0$, so if we know the spin carried by the edges, then the intertwiner will also be known.

In the harmonic oscillator basis, given by the Schwinger representation, this state reads as,

$$|j\rangle = \frac{1}{\sqrt{2j+1}} \sum_{n+\tilde{n}=2j} (-1)^n |\tilde{n}, n\rangle \otimes |n, \tilde{n}\rangle. \quad (6.71)$$

The spin network basis state will consist on the tensorial product of two such bivalent intertwiner states, $|j_\alpha, j_\beta\rangle$. Imposing the matching constraint, both spins will match $j_\alpha = j_\beta$. The action of the operators \hat{E} , \hat{F} will then be,

$$\begin{aligned} \hat{E}_{11} |j\rangle &= 2j |j\rangle, & \hat{E}_{22} |j\rangle &= 2j |j\rangle, & \hat{E}_{12} |j\rangle &= 0, \\ \hat{F}_{12} |j\rangle &= \sqrt{(2j)(2j+1)} |j-1/2\rangle, & \hat{F}_{12}^\dagger |j\rangle &= \sqrt{(2j+1)(2j+2)} |j+1/2\rangle. \end{aligned} \quad (6.72)$$

Now, to promote H_{LQG} to a quantum operator, we express it in terms of these \hat{E} , \hat{F} and \hat{F}^\dagger . Therefore, its action on a pair of intertwiner states $|j, j\rangle$:

$$\begin{aligned}\hat{H} |j, j\rangle &= 2\lambda(2j)^2 |j, j\rangle \\ &\quad + 2\gamma(2j)(2j+1) |j - 1/2, j - 1/2\rangle \\ &\quad + 2\bar{\gamma}(2j+1)(2j+2) |j + 1/2, j + 1/2\rangle.\end{aligned}\tag{6.73}$$

Once we have an operator for the Hamiltonian, it would be interesting to look for the evolution operator. For an infinitesimal evolution of a state $|j, j\rangle$, it would be a good approximation to cut the expansion at second order:

$$|\psi(\tau)\rangle = e^{-i\frac{\tau}{2}\hat{H}} |j, j\rangle \sim \left(\mathbb{I} + i\frac{\tau}{2}\hat{H} - \frac{\tau^2}{8}\hat{H}^2 \right) |j, j\rangle.\tag{6.74}$$

This quantization of the bivalent 2-vertex model is the starting point to study numerous physical phenomenon, such as the entanglement of the system.

Chapter 7

Conclusion

In this project, we have introduced the general basis of LQG, a non-perturbative theory aiming to provide a quantum description of gravity. Such description has helped us gain insight into the complexity lying behind the mathematical construction of the theory. Afterward, we have presented the spinorial and $U(N)$ formalisms, in order to generalize the work done in [38, 39].

In the first place, we have followed a historical thread by introducing the early attempts to develop a Hamiltonian formulation of General Relativity. After describing the difficulties encountered in the quantization of these constructions, we have moved towards the description of the loop representation, introduced in [27, 28], where the basis elements of the kinematical Hilbert space of the theory are given by the spin networks [29]. These elements are wave-functions that can be represented pictorially as graphs whose edges carry a spin j labeling the irreducible representation of the $SU(2)$ Lie group, and whose vertices are associated with intertwiners, which link the different representations ensuring the gauge invariance of the theory.

Within the theory, it is possible to construct geometrical operators, such as the area and volume operators [10–12], whose eigenstates are the spin networks themselves. This description provides a discrete notion of space, where the edges generate quanta of area and the vertices are associated with chunks of volume. Due to the tininess of the area and volume eigenvalues, which are proportional to the Planck length, we will require extreme scenarios to appreciate the effects of the space discretization. This discreteness of space is considered one of the most outstanding achievements of LQG since we expect the quantization of a theory of gravity to exhibit a granular structure of space.

Later, we have reviewed the spinorial formalism [31], a classical framework whose quantization gives us the kinematical Hilbert space of LQG. Dressing a simple graph (not a spin network yet) with a pair of spinors attached to the vertices at the beginning and the end of each edge, we have reviewed the construction of the classical phase space in terms of $SU(2)$ group elements and $\mathfrak{su}(2)$ Lie algebra elements following the procedure carried out in [31]. If we impose a closure constraint on the spinors (equation 5.13), taking into

account that it is possible to associate a 3-dimensional vector to each spinor (equation 5.8), we can use an old theorem by H. Minkowski [32], to uniquely associate (up to translations) a polyhedron to each vertex. Therefore, we can see the graph as a collection of polyhedrons joined together. Then, the area matching constraint imposes the neighboring polyhedrons to be attached by faces sharing the same area but not necessarily the same shape. This freedom in the shape of the faces provides the name of twisted geometries to the formalism [33–35].

On the other hand, using the development carried out within the $U(N)$ formalism presented in [36–39], which is based on the Schwinger representation of the $\mathfrak{su}(2)$ algebra in terms of two uncoupled harmonic oscillators [40], we reviewed the construction of $SU(2)$ invariant operators acting on the vertices of the graph. This framework is useful to link the classical spinorial formalism and LQG, since it provides a suitable way of relating the spinor variables and the harmonic oscillator operators. Moreover, it was shown that the spinor formalism and the $U(N)$ framework may help explore the problem of the implementation of the dynamics in LQG [38], which is one of the main open problems of the theory.

In this sense, to make some progress in the resolution of the dynamics, we have considered some truncated classical models consisting of 2-vertices linked by arbitrary number of edges. The analysis of the 2-vertex model introduced in [38, 39] is restricted to the homogeneous and isotropic sector by imposing an additional constraint $\hat{\mathcal{E}}_{ij}$. Based on this idea, we have proposed various generalized 2-vertex models which remain out of the homogeneous and isotropic sector. In order to study the evolution of these truncated models, we have introduced three different Hamiltonians, which differ by renormalization factors. These Hamiltonians respect the $SU(2)$ invariance of the theory and commute with the closure and matching constraints. Furthermore, we have calculated the Poisson-brackets of the building blocks of these classical Hamiltonians, which were based on the operators developed in the $U(N)$ formalism. Even if all these Hamiltonians respect the symmetries of the theory and are suitable candidates to study the dynamics, we have considered H_{LQG} —since it is the simplest Hamiltonian acting on a pair of vertices—and we have obtained analytically a closed expression for the evolution of the spinors for general 2-vertex models.

After constructing a suitable general Hamiltonian, we have studied specific systems with different number of edges and parametrized by different spinors. In the first place, we have proposed a bivalent 2-vertex model and applied the equations of motion for its variables, which we have solved numerically. Nevertheless, in the special case of $H = 0$, we have obtained an analytical expression for the dynamics. Then, after plotting the evolution of the system, we have observed three different regimes; oscillatory, divergent, and constant. The evolution of the spinors show a periodic behavior in the oscillatory regime, whereas in the divergent regime, the area decreases up to a minimum value and then increases rapidly. These two behaviors depend strongly on the coupling constants, and given the difficulties of solving the equations, we have found that these regimes are hard to categorize analytically. Nevertheless, by plotting a large number of graphics (~ 80.000), we have

pursued a systematical analysis and found interesting tendencies. Remarkably, even though we have worked in the general case (out of the homogeneous and isotropic sector), we have recovered the same regimes obtained for the more restricted sector considered in [38].

In this sense, it was shown that the quantized Hamiltonian of the reduced 2-vertex model showed certain relations with the Hamiltonian in LQC [39]. Additionally, in the subsequent work [38], it was discussed the possible relation between this reduced sector in the 2-vertex model and the cosmological variant. According to this idea, the oscillatory and divergent regimes could describe the increasing and decreasing behavior of a Universe ruled by a Big Bounce. Nevertheless, we must be cautious with these interpretations since fully understanding the relationship (if any) between our results and the LQC framework requires further research.

Afterward, we have considered new models with a higher number of edges. In particular, we have studied two 4-valent and two N-valent models. The equations of motion for these proposals become highly non-linear, and thus, we have not been capable of finding an independent set of the differential equations analytically (as it was done in the case of two vertices). Nevertheless, we have found interesting results from the numerical calculations.

In the first 4-valent model, we have studied the oscillatory evolution of the spinors, the phases, and the total area of the associated tetrahedron. We have further computed the quadrupole of the area following the procedure presented in [95], which gave us an idea the deformation of the polyhedron under consideration. In particular, looking at the eigenvalues of the quadrupole, we saw the area of this tetrahedron was not evenly distributed; and indeed, the tetrahedron turned out to be volumeless. In an attempt to obtain a generalized 2-vertex model, we have followed the idea behind the construction of this 4-valent model to propose a pair of generalized systems, which, as expected, resulted in having zero volume as well.

Even though most of the models we have proposed have zero volume, they still behave consistently according to the symmetries of the system and present non-trivial evolutions of the variables. Therefore, even if the study of general models with non-zero volume will be interesting, the analysis performed here is still important and may shed light on the dynamics of reduced models in LQG, from which we can extract insightful results.

Finally, in section 6.3.2.2, we have constructed a new model trying to understand the geometrical discreteness of space. This model has the advantage of having a non-trivial volume, which allows us to get deep into the actual evolution of the ‘atoms’ of space. Here, we have also calculated the evolution of the spinors, the areas, and the quadrupole. Furthermore, we have constructed the 3-dimensional tetrahedron from the geometrical relations given in [96] and studied graphically their evolution. Interestingly, in this case we have also obtained three regimes. The dependence of these regimes with the coupling constant was inferred by a systematical procedure as done in the bivalent model.

In a certain way, we have constructed our models imposing some relations on the spinors. For example, in the bivalent model, the second spinor is completely determined from the

first one (up to a phase factor) through $|z_2\rangle \propto \sigma_y |\bar{z}_1\rangle$. Choosing convenient relations may be useful since the closure constraint will automatically be satisfied. Nevertheless, one interesting way to extend this work would be to explore N-valent models with random spinors.

In this sense, we could generate N arbitrary spinors with a statistical distribution on its normals following [97], and impose the closure constraint using the algorithm presented in [98]. On the other hand, it would be enlightening to represent the 3-dimensional N-faced polyhedron and study its evolution, just as we did for the 4-valent vertex. Nevertheless, constructing a polyhedron with more than four faces is a complex task since the relations between the face normals and the vertices are not given by explicit equations, such as those of the tetrahedron. Instead, we would need to implement reconstruction algorithms to compute the lengths and coordinates of the polyhedron, as done in [99].

To summarize, after giving a general overview of LQG and introducing the spinorial and $U(N)$ formalisms, which are useful to tackle the problem with the implementation of the dynamics, we have generalized the reduced 2-vertex models proposed in [38, 39] by considering states out of the homogeneous and isotropic sector. Remarkably, we have obtained the same regimes for the evolution of the spinors within this generalized problem, so the possible relations with cosmological models discussed there could also be applied in this more general case. Among the different models we have proposed, which all have non-trivial evolutions and are thus interesting in their own right, we pay special attention to the tetrahedron with non-zero volume. Within the spinorial framework of LQG, this model represents the simplest non-trivial building block of space, so the study of its evolution out of the restricted sector could represent an interesting step to advance in the study of the implementation of the dynamics.

Bibliography

- [1] B. Schutz, “Gravity from the Ground Up: An Introductory Guide to Gravity and General Relativity”, Cambridge University Press (2003).
- [2] J. Polchinski, “String Theory to the Rescue”, (2015). [arXiv:1512.02477](https://arxiv.org/abs/1512.02477)
- [3] Hugh Everett, ““Relative State” Formulation of Quantum Mechanics”, *Rev. Mod. Phys.* **29**, 454 (1957).
- [4] C. M. Hull, P. K. Townsend, “Unity of superstring dualities”, *Nuclear Physics B* **438**, 109 (1995). [arXiv:hep-th/9410167](https://arxiv.org/abs/hep-th/9410167)
- [5] E. Alvarez, “Quantum Gravity”, *Lecture Notes in Physics* **669**, 31 (2004). [arXiv:gr-qc/0405107](https://arxiv.org/abs/gr-qc/0405107)
- [6] J. Bedford, “An Introduction to String Theory”, (2011). [arXiv:1107.3967](https://arxiv.org/abs/1107.3967)
- [7] T. Thiemann, “Lectures on Loop Quantum Gravity”, *Lecture Notes in Physics* **631**, 41 (2003). [arXiv:gr-qc/0210094](https://arxiv.org/abs/gr-qc/0210094)
- [8] A. Ashtekar, E. Bianchi, “A Short Review of Loop Quantum Gravity”, *Reports on Progress in Physics* **84**, 042001 (2021). [arXiv:2104.04394](https://arxiv.org/abs/2104.04394)
- [9] N. Bodendorfer, “An Elementary Introduction to Loop Quantum Gravity”, (2016). [arXiv:1607.05129](https://arxiv.org/abs/1607.05129)
- [10] A. Ashtekar, J. Lewandowski, “Quantum Theory of Geometry: I. Area operators”, *Classical and Quantum Gravity* **14**, A55 (1997). [arXiv:gr-qc/9602046](https://arxiv.org/abs/gr-qc/9602046)
- [11] A. Ashtekar, J. Lewandowski, “Quantum Theory of Geometry II: Volume operators”, *Adv. Theor. Math. Phys.* **1**, 388 (1998). [arXiv:gr-qc/9711031](https://arxiv.org/abs/gr-qc/9711031)
- [12] C. Rovelli, L. Smolin, “Discreteness of Area and Volume in Quantum Gravity”, *Nuclear Physics B* **442**, 593 (1995). [arXiv:gr-qc/9411005](https://arxiv.org/abs/gr-qc/9411005)
- [13] M. E. Agishtein, A. A. Migdal, “Critical Behavior of Dynamically Triangulated Quantum Gravity in Four Dimensions”, *Nuclear Physics B* **385**, 395 (1992). [arXiv:hep-lat/9204004](https://arxiv.org/abs/hep-lat/9204004)
- [14] J. Ambjorn, M. Carfora, A. Marzuoli, “The Geometry of Dynamical Triangulations”, *Lecture Notes in Physics* **50**, 197 (1997). [arXiv:hep-th/9612069](https://arxiv.org/abs/hep-th/9612069)

- [15] S. Frittelli, C. Kozameh, and E. T. Newman, “GR via Characteristic Surfaces”, *Journal of Mathematical Physics* **36**, 4984 (1995). [arXiv:gr-qc/9502028](https://arxiv.org/abs/gr-qc/9502028)
- [16] S. Frittelli, C. N. Kozameh, E. T. Newman, C. Rovelli, R. S. Tate, “Fuzzy Spacetime from a Null-Surface Version of General Relativity”, *Classical and Quantum Gravity* **14**, A143 (1997). [arXiv:gr-qc/9502028](https://arxiv.org/abs/gr-qc/9502028)
- [17] S. Frittelli, C. N. Kozameh, E. T. Newman, C. Rovelli, R. S. Tate, “Quantization of the Null-Surface Formulation of General Relativity”, *Phys. Rev. D* **56**, 889 (1997). [arXiv:gr-qc/9612010](https://arxiv.org/abs/gr-qc/9612010)
- [18] C. Rovelli, “Loop Quantum Gravity”, *Living Reviews in Relativity* **1**, 1 (1998). [arXiv:gr-qc/9710008](https://arxiv.org/abs/gr-qc/9710008)
- [19] C. Rovelli, “Notes for a Brief History of Quantum Gravity”, (2000). [arXiv:gr-qc/0006061](https://arxiv.org/abs/gr-qc/0006061)
- [20] L. Rosenfeld, “Zur Quantelung der Wellenfelder”, *Annalen der Physik* **397**, 113 (2006).
- [21] R. Arnowitt, S. Deser, C. W. Misner, “Dynamical Structure and Definition of Energy in General Relativity”, *Phys. Rev.* **116**, 1322 (1959).
- [22] J. A. Wheeler, “Geometrodynamics”, New York: Academic Press (1962).
- [23] B. S. DeWitt, “Quantum Theory of Gravity. I. The Canonical Theory”, *Phys. Rev.* **160**, 1113 (1967).
- [24] A. Ashtekar, “New Variables for Classical and Quantum Gravity”, *Phys. Rev. Lett.* **57**, 2244 (1986).
- [25] J. F. Barbero, “Real Ashtekar Variables for Lorentzian Signature Space-Times”, *Phys. Rev. D* **51**, 5507 (1995). [arXiv:gr-qc/9410014](https://arxiv.org/abs/gr-qc/9410014)
- [26] T. Jacobson, L. Smolin, “Nonperturbative Quantum Geometries”, *Nucl. Phys. B* **299**, 295 (1988).
- [27] C. Rovelli, L. Smolin, “Knot Theory and Quantum Gravity”, *Phys. Rev. Lett.* **61**, 1155 (1988).
- [28] C. Rovelli, L. Smolin, “Loop Space Representation of Quantum General Relativity”, *Nuclear Physics B* **331**, 80 (1990).
- [29] C. Rovelli, L. Smolin, “Spin Networks and Quantum Gravity”, *Phys. Rev. D* **52**, 5743 (1995). [arXiv:gr-qc/9505006](https://arxiv.org/abs/gr-qc/9505006)
- [30] C. Rovelli and L. Smolin, “Quantum Theory and Beyond”, Cambridge University Press (1971).
- [31] E. Livine, J. Tambornino, “Spinor Representation for Loop Quantum Gravity”, *Journal of Mathematical Physics* **53**, 012503 (2012). [arXiv:1105.3385](https://arxiv.org/abs/1105.3385)

- [32] H. Minkowski, “Allgemeine Lehrsätze über die Convexen Polyeder”, *Nachrichten von der Gesellschaft der Wissenschaften zu Göttingen, Mathematisch-Physikalische Klasse* **1897**, 198 (1897).
- [33] L. Freidel, S. Speziale, “Twisted Geometries: A Geometric Parametrization of SU(2) Phase Space”, *Phys. Rev. D* **82**, 084040 (2010). [arXiv:1001.2748](https://arxiv.org/abs/1001.2748)
- [34] E. R. Livine, S. Speziale, and J. Tambornino, “Twistor Networks and Covariant Twisted Geometries”, *Phys. Rev. D* **85**, 064002 (2012). [arXiv:1108.0369](https://arxiv.org/abs/1108.0369)
- [35] L. Freidel, S. Speziale, “From Twistors to Twisted Geometries”, *Phys. Rev. D* **82**, 084041 (2010). [arXiv:1006.0199](https://arxiv.org/abs/1006.0199)
- [36] F. Girelli, E. R. Livine, “Reconstructing Quantum Geometry from Quantum Information: Spin Networks as Harmonic Oscillators”, *Classical and Quantum Gravity* **22**, 3295 (2005). [arXiv:gr-qc/0501075](https://arxiv.org/abs/gr-qc/0501075)
- [37] L. Freidel, E. R. Livine, “The Fine Structure of SU(2) Intertwiners from U(N) Representations”, *Journal of Mathematical Physics* **51**, 082502 (2010). [arXiv:0911.3553](https://arxiv.org/abs/0911.3553)
- [38] E. F. Borja, L. Freidel, I. Garay, E. R. Livine, “U(N) Tools for Loop Quantum Gravity: the Return of the Spinor”, *Classical and Quantum Gravity* **28**, 055005 (2011). [arXiv:1010.5451](https://arxiv.org/abs/1010.5451)
- [39] E. F. Borja, J. Díaz-Polo, I. Garay, E. R. Livine, “Dynamics for a 2-Vertex Quantum Gravity Model”, *Classical and Quantum Gravity* **27**, 235010 (2010). [arXiv:1006.2451](https://arxiv.org/abs/1006.2451)
- [40] J. J. Sakurai, “Modern quantum mechanics; rev. ed.”, Addison-Wesley (1994).
- [41] M. P. Reisenberger, C. Rovelli, ““Sum over Surfaces” Form of Loop Quantum Gravity”, *Phys. Rev. D* **56**, 3490 (1997). [arXiv:gr-qc/9612035](https://arxiv.org/abs/gr-qc/9612035)
- [42] C. Rovelli, “Quantum Gravity as a “Sum over Surfaces””, *Nuclear Physics B Proceedings Supplements* **57**, 28 (1997).
- [43] T. Thiemann, “The Phoenix Project: Master Constraint Programme for Loop Quantum Gravity”, *Classical and Quantum Gravity* **23**, 2211 (2006). [arXiv:gr-qc/0305080](https://arxiv.org/abs/gr-qc/0305080)
- [44] T. Thiemann, “Quantum Spin Dynamics: VIII. The Master Constraint”, *Classical and Quantum Gravity* **23**, 2249 (2006). [arXiv:gr-qc/0510011](https://arxiv.org/abs/gr-qc/0510011)
- [45] M. Han, Y. Ma, “Master Constraint Operators in Loop Quantum Gravity”, *Physics Letters B* **635**, 225 (2006). [arXiv:gr-qc/0510014](https://arxiv.org/abs/gr-qc/0510014)
- [46] B. Dittrich, “The Continuum Limit of Loop Quantum Gravity - a Framework for Solving the Theory”, (2014). [arXiv:1409.1450](https://arxiv.org/abs/1409.1450)

- [47] S. Gielen, “Emergence of a Low Spin Phase in Group Field Theory Condensates”, *Classical and Quantum Gravity* **33**, 224002 (2016). [arXiv:1604.06023](https://arxiv.org/abs/1604.06023)
- [48] C. Rovelli, “Black Hole Entropy from Loop Quantum Gravity”, *Phys. Rev. Lett.* **77**, 3288 (1996). [arXiv:gr-qc/9603063](https://arxiv.org/abs/gr-qc/9603063)
- [49] K. V. Krasnov, “Geometrical Entropy from Loop Quantum Gravity”, *Phys. Rev. D*, **55**, 3505 (1997).
- [50] A. Ashtekar, J. Baez, A. Corichi, K. Krasnov, “Quantum Geometry and Black Hole Entropy”, *Phys. Rev. Lett.* **80**, 904 (1998). [arXiv:gr-qc/9710007](https://arxiv.org/abs/gr-qc/9710007)
- [51] A. Ashtekar, J. Baez, K. Krasnov, “Quantum Geometry of Isolated Horizons and Black Hole Entropy”, (2000). [arXiv:gr-qc/0005126](https://arxiv.org/abs/gr-qc/0005126)
- [52] I. Agullo, J. F. Barbero, E. F. Borja, J. Diaz-Polo, E. J. S. Villaseñor, “Black Hole State Counting in Loop Quantum Gravity: A Number-Theoretical Approach”, *Phys. Rev. Lett.* **100**, 211301 (2008). [arXiv:0802.4077](https://arxiv.org/abs/0802.4077)
- [53] I. Agullo, J. F. Barbero, E. F. Borja, J. Diaz-Polo, E. J. S. Villaseñor, “Detailed Black Hole State Counting in Loop Quantum Gravity”, *Phys. Rev. D* **82**, 084029 (2010). [arXiv:1101.3660](https://arxiv.org/abs/1101.3660)
- [54] A. Ashtekar, P. Singh, “Loop Quantum Cosmology: a Status Report”, *Classical and Quantum Gravity* **28**, 213001 (2011). [arXiv:1108.0893](https://arxiv.org/abs/1108.0893)
- [55] M. Bojowald, R. Tavakol, “Loop Quantum Cosmology: Effective Theories and Oscillating Universes”, (2008). [arXiv:0802.4274](https://arxiv.org/abs/0802.4274)
- [56] M. Bojowald, “Loop Quantum Cosmology”, *Living Reviews in Relativity* **8**, 11 (2005). [arXiv:gr-qc/0601085](https://arxiv.org/abs/gr-qc/0601085)
- [57] J. Bilski, A. Marcianò, “Critical Insight into the Cosmological Sector of Loop Quantum Gravity”, *Phys. Rev. D* **101**, 066026 (2020). [arXiv:1905.00001](https://arxiv.org/abs/1905.00001)
- [58] A. Ashtekar, T. Pawłowski, P. Singh, “Quantum Nature of the Big Bang”, *Phys. Rev. Lett.* **96**, 141301 (2006). [arXiv:gr-qc/0602086](https://arxiv.org/abs/gr-qc/0602086)
- [59] S. M. Carroll, “Spacetime and Geometry”, Cambridge University Press (2019).
- [60] H. C. Ohanian, R. Ruffini, “Gravitation and Spacetime”, Cambridge University Press (2013).
- [61] R. M. Wald, “General relativity”, Chicago Univ. Press (1984).
- [62] R. D’Inverno. “Introducing Einstein’s Relativity”, Clarendon Press (1992).
- [63] T. Miramontes, D. Sudarsky, “El Formalismo 3+1 en Relatividad General y la Descomposición Tensorial Completa”, *Rev. Mex. de Fis. E* **64** (2018).
- [64] T. Thiemann, “Modern Canonical Quantum General Relativity”, Cambridge University Press (2007).

- [65] E. Gourgoulhon, “3+1 Formalism and Bases of Numerical Relativity”, (2007). [arXiv:gr-qc/0703035](https://arxiv.org/abs/gr-qc/0703035)
- [66] R. Arnowitt, S. Deser, C. W. Misner, “Gravitation: An introduction to current research”, Wiley (1962).
- [67] R. Arnowitt, S. Deser, C. W. Misner, “Republication of: The Dynamics of General Relativity”, *General Relativity and Gravitation* **40**, 1997 (2008). [arXiv:gr-qc/0405109](https://arxiv.org/abs/gr-qc/0405109)
- [68] D. Giulini, “The Superspace of Geometrodynamics”, *General Relativity and Gravitation* **41**, 785 (2009). [arXiv:0902.3923](https://arxiv.org/abs/0902.3923)
- [69] A. Tronconi, G. P. Vacca, G. Venturi, “Inflaton and Time in the Matter-Gravity System”, *Phys. Rev. D* **67**, 063517 (2003). [arXiv:gr-qc/0302030](https://arxiv.org/abs/gr-qc/0302030)
- [70] A. Y. Kamenshchik, A. Tronconi, G. Venturi, “The Born-Oppenheimer Approach to Quantum Cosmology”, *Classical and Quantum Gravity* (2020). [arXiv:2010.15628](https://arxiv.org/abs/2010.15628)
- [71] R. Gambini, J. Pullin, “A First Course in Loop Quantum Gravity”, Oxford University Press (2011).
- [72] G. Immirzi, “Quantum Gravity and Regge Calculus”, *Nuclear Physics B Proceedings Supplements* **57**, 65 (1997). [arXiv:gr-qc/9701052](https://arxiv.org/abs/gr-qc/9701052)
- [73] C. Rovelli, “Quantum Gravity”, Cambridge University Press (2004).
- [74] M. E. Peskin, D. V. Schroeder, “An Introduction to Quantum Field Theory”, Westview (1995).
- [75] M. D. Schwartz, “Quantum Field Theory and the Standard Model”, Cambridge University Press (2014).
- [76] J. C. Baez and J. P. Muniain, “Gauge Fields, Knots and Gravity”, World Scientific Publishing Company (1994).
- [77] R. Giles, “Reconstruction of Gauge Potentials from Wilson Loops”, *Phys. Rev. D* **24**, 2160 (1981).
- [78] E. R. Livine, “A Short and Subjective Introduction to the Spinfoam Framework for Quantum Gravity”, (2011). [arXiv:1101.5061](https://arxiv.org/abs/1101.5061)
- [79] I. Mäkinen, “Introduction to SU(2) Recoupling Theory and Graphical Methods for Loop Quantum Gravity”, (2019). [arXiv:1910.06821](https://arxiv.org/abs/1910.06821)
- [80] A. Ashtekar, J. Lewandowski, “Representation Theory of Analytic Holonomy C*-algebras”, *Knots and Quantum Gravity* 21 (1994). [arXiv:gr-qc/9311010](https://arxiv.org/abs/gr-qc/9311010)
- [81] A. Ashtekar, J. Lewandowski, “Projective Techniques and Functional Integration for Gauge Theories”, *Journal of Mathematical Physics* **36**, 2170 (1995). [arXiv:gr-qc/9411046](https://arxiv.org/abs/gr-qc/9411046)

- [82] J. Lewandowski, “Topological Measure and Graph-Differential Geometry on the Quotient Space of Connections”, *International Journal of Modern Physics D* **3**, 207 (1994). [arXiv:gr-qc/9406025](https://arxiv.org/abs/gr-qc/9406025)
- [83] A. Ashtekar, J. Lewandowski, “Differential Geometry on the Space of Connections Via Graphs and Projective Limits”, *Journal of Geometry and Physics* **17**, 191 (1995). [arXiv:hep-th/9412073](https://arxiv.org/abs/hep-th/9412073)
- [84] J. Lewandowski, A. Okołów, H. Sahlmann, T. Thiemann, “Uniqueness of Diffeomorphism Invariant States on Holonomy Flux Algebras”, *Communications in Mathematical Physics* **267**, 703 (2006). [arXiv:gr-qc/0504147](https://arxiv.org/abs/gr-qc/0504147)
- [85] C. Fleischhack, “Representations of the Weyl Algebra in Quantum Geometry”, *Communications in Mathematical Physics* **285**, 67 (2009). [arXiv:math-ph/0407006](https://arxiv.org/abs/math-ph/0407006)
- [86] R. de Pietri, C. Rovelli, “Geometry Eigenvalues and the Scalar Product from Recoupling Theory in Loop Quantum Gravity”, *Phys. Rev. D* **54**, 2664 (1996). [arXiv:gr-qc/9602023](https://arxiv.org/abs/gr-qc/9602023)
- [87] E. F. Borja, I. Garay, F. Vidotto, “Learning about Quantum Gravity with a Couple of Nodes”, *SIGMA* **8**, 015 (2012). [arXiv:1110.3020](https://arxiv.org/abs/1110.3020)
- [88] E. R. Livine, M. Martín-Benito, “Classical Setting and Effective Dynamics for Spinfoam Cosmology”, *Classical and Quantum Gravity* **30**, 035006 (2013). [arXiv:1111.2867](https://arxiv.org/abs/1111.2867)
- [89] T. Regge, “General Relativity without Coordinates”, *Il Nuovo Cimento* **19**, 558 (1961). [arXiv:1105.3385](https://arxiv.org/abs/1105.3385)
- [90] F. Girelli, G. Sellaroli, “SO*(2N) Coherent States for Loop Quantum Gravity”, *Journal of Mathematical Physics* **58**, 071708 (2017). [arXiv:1701.07519](https://arxiv.org/abs/1701.07519)
- [91] A. O. Barut, A. J. Bracken, “The Remarkable Algebra $so^*(2n)$, its Representations, its Clifford Algebra and Potential Applications”, *Journal of Physics A: Mathematical and General* **23**, 641 (1990).
- [92] J. Ben Achour, E. R. Livine, “The Cosmological Spinor”, *Phys. Rev. D* **101**, 103523 (2020). [arXiv:2004.06387](https://arxiv.org/abs/2004.06387)
- [93] E. R. Livine, “Projected Spin Networks for Lorentz Connection: Linking Spin Foams and Loop Gravity”, *Classical and Quantum Gravity* **19**, 5525 (2002). [arXiv:gr-qc/0207084](https://arxiv.org/abs/gr-qc/0207084)
- [94] M. Dupuis, E. R. Livine, “Lifting SU(2) Spin Networks to Projected Spin Networks”, *Phys. Rev. D* **82**, 064044 (2010). [arXiv:1008.4093](https://arxiv.org/abs/1008.4093)
- [95] C. Goeller, E. R. Livine, “Probing the Shape of Quantum Surfaces: the Quadrupole Moment Operator”, *Classical and Quantum Gravity* **35**, 215004 (2018). [arXiv:1805.08257](https://arxiv.org/abs/1805.08257)

- [96] C. Charles, E. R. Livine, “Closure Constraints for Hyperbolic Tetrahedra”, *Classical and Quantum Gravity* **32**, 135003 (2015). [arXiv:1501.00855](https://arxiv.org/abs/1501.00855)
- [97] E. R. Livine, D. R. Terno, “Entropy in the Classical and Quantum Polymer Black Hole Models”, *Classical and Quantum Gravity* **29**, 224012 (2012). [arXiv:1205.5733](https://arxiv.org/abs/1205.5733)
- [98] E. R. Livine, “Deformations of Polyhedra and Polygons by the Unitary Group”, *Journal of Mathematical Physics* **54**, 123504 (2013). [arXiv:1307.2719](https://arxiv.org/abs/1307.2719)
- [99] E. Bianchi, P. Doná, S. Speziale, “Polyhedra in Loop Quantum Gravity”, *Phys. Rev. D* **83**, 044035 (2011). [arXiv:1009.3402](https://arxiv.org/abs/1009.3402)